

AD-A092 303

NAVAL POSTGRADUATE SCHOOL MONTEREY CA
AN APPLICATION OF KALMAN FILTERING TO TORPEDO TRACKING.(U)

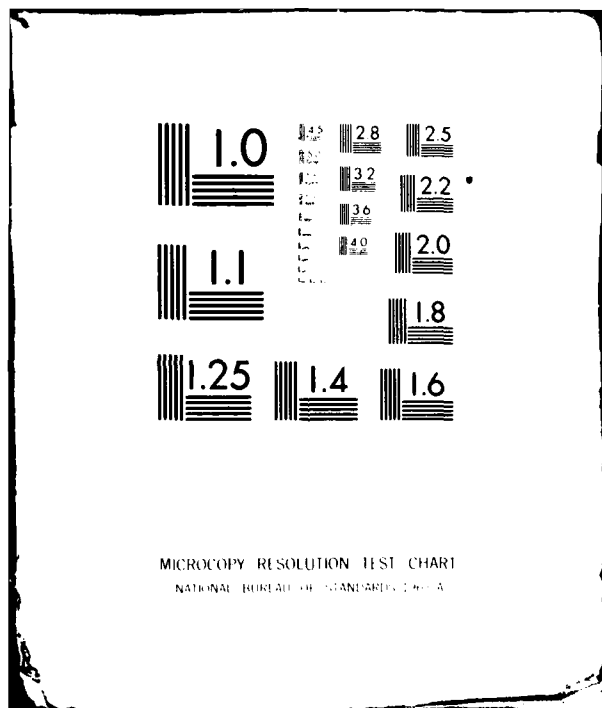
F/G 17/1

SEP 80 P A O'BRIEN

UNCLASSIFIED

Line 2
AD
A092303

NL



AD A 092303

LEVEL II
NAVAL POSTGRADUATE SCHOOL
Monterey, California

2
P. S.



DTIC
SELECTED
DEC 02 1980
S E D
E

THESIS

AN APPLICATION OF KALMAN FILTERING
TO TORPEDO TRACKING

by

Paul A. O'Brien

September 1980

Thesis Advisor:

H. A. Titus

Approved for public release; distribution unlimited

DDC FILE COPY

80 12 01 101

SECURITY CLASSIFICATION OF THIS PAGE (When Data Entered)

REPORT DOCUMENTATION PAGE		READ INSTRUCTIONS BEFORE COMPLETING FORM
1. REPORT NUMBER	2. GOVT ACCESSION NO.	3. RECIPIENT'S CATALOG NUMBER
	AD-A092 303	
4. TITLE (and Subtitle) AN APPLICATION OF KALMAN FILTERING TO TORPEDO TRACKING.	5. TYPE OF REPORT & PERIOD COVERED Master's Thesis September 1980	
6. AUTHOR(s) Paul A. O'Brien	7. CONTRACT OR GRANT NUMBER(s)	
8. PERFORMING ORGANIZATION NAME AND ADDRESS Naval Postgraduate School Monterey, California 93940	10. PROGRAM ELEMENT, PROJECT, TASK AREA & WORK UNIT NUMBERS	
11. CONTROLLING OFFICE NAME AND ADDRESS Naval Postgraduate School Monterey, California 93940	12. REPORT DATE September 1980	
14. MONITORING AGENCY NAME & ADDRESS (if different from Controlling Office) Naval Postgraduate School Monterey, California 93940	13. NUMBER OF PAGES 127	
16. DISTRIBUTION STATEMENT (of this Report) Approved for public release; distribution unlimited	15. SECURITY CLASS. (of this report) Unclassified	
17. DISTRIBUTION STATEMENT (of the abstract entered in Block 20, if different from Report)		
18. SUPPLEMENTARY NOTES		
19. KEY WORDS (Continue on reverse side if necessary and identify by block number) Kalman Filtering Torpedo Tracking		
20. ABSTRACT (Continue on reverse side if necessary and identify by block number) A sequential Extended Kalman filter routine was developed to provide real time estimates of torpedo position and depth on the three dimensional underwater tracking range at the Naval Torpedo Station, Keyport, Washington. Filter measurements consisted of acoustic pulse transit times from the torpedo to a receiving hydrophone array. These measurements, which are nonlinear functions of the position and depth coordinates, were linearized and		

20. (continued)

and the filter gains calculated on-line. Tests were conducted using simulated torpedo trajectories that traversed both single and multiple hydrophone arrays. It was found that filter performance was dependent on system noise and the distance the torpedo was from the hydrophone array. Position and depth errors ranged between 0 and 10 feet.

Accession For	
NTIS GRA&I	<input checked="" type="checkbox"/>
DDC TAB	<input type="checkbox"/>
Unannounced	<input type="checkbox"/>
Justification _____	
By _____	
Distribution _____	
Availability Codes	
Dist.	Available and/or special
A	

Approved for public release; distribution unlimited

An Application of Kalman Filtering
To Torpedo Tracking

by

Paul A. O'Brien
B.S., University of Maryland, 1972

Submitted in partial fulfillment of the
requirements for the degree of

MASTER OF SCIENCE IN ELECTRICAL ENGINEERING

from the

NAVAL POSTGRADUATE SCHOOL
September 1980

Author

Paul A. O'Brien

Approved by:

J.A. Titzer Thesis Advisor

Alex Gerba Jr. Second Reader

P.Kirk
Chairman, Department of Electrical Engineering

William M. Tolles
Dean of Science and Engineering

ABSTRACT

A sequential Extended Kalman filter routine was developed to provide real time estimates of torpedo position and depth on the three dimensional underwater tracking range at the Naval Torpedo Station, Keyport, Washington. Filter measurements consisted of acoustic pulse transit times from the torpedo to a receiving hydrophone array. These measurements, which are nonlinear functions of the position and depth coordinates, were linearized and the filter gains calculated on-line. Tests were conducted using simulated torpedo trajectories that traversed both single and multiple hydrophone arrays. It was found that filter performance was dependent on system noise and the distance the torpedo was from the hydrophone array. Position and depth errors ranged between 0 and 10 feet.

TABLE OF CONTENTS

	Page
I. INTRODUCTION	7
II. DESCRIPTION OF RANGE TRACKING GEOMETRY	9
III. THEORY--EXTENDED KALMAN FILTER	11
IV. PROBLEM DEFINITION--TORPEDO TRACKING WITH THE EXTENDED KALMAN FILTER	15
A. FILTER EQUATIONS	15
B. THE SEQUENTIAL EXTENDED KALMAN FILTER	23
V. TESTING AND SIMULATION	28
A. DESCRIPTION	28
B. EDITING ERRONEOUS TRANSIT TIME MEASUREMENTS . . .	29
C. BOUNDING RESIDUAL BIAS ERRORS	30
D. MULTIPLE ARRAY TRACKING	32
VI. TEST RESULTS AND DISCUSSION	36
A. SERIES ONE--STRAIGHT RUNS	36
B. SERIES TWO--MANEUVERING RUNS	39
C. SERIES THREE--MULTIPLE ARRAY TRACKING	44
VII. CONCLUSIONS	45
FIGURES	47
APPENDIX A: PROGRAM DESCRIPTION AND FIGURES	98
A. PROGRAM SUBROUTINES	100
B. UTILITY PROGRAMS	102
APPENDIX B: SEQUENTIAL EXTENDED KALMAN FILTER PROGRAM LISTING	103
LIST OF REFERENCES	126
INITIAL DISTRIBUTION LIST	127

ACKNOWLEDGEMENT

The author is deeply indebted to Professor Hal Titus for his counsel and professional guidance during this project.

I. INTRODUCTION

The Naval Torpedo Station (NAVTORPSTA) Keyport, Washington currently operates two three-dimensional (3-D) underwater tracking ranges with acoustical capability. The underwater tracking range utilizes a sonar transmitter installed in the torpedo to be tracked. The transmitter is synchronized with a master clock. Timed acoustic pulses are received by bottom mounted hydrophone arrays and then relayed via cable to a computer at the observation site. The computer calculates the positional coordinates of the torpedo and plots its trajectory through the water.

The measured data, which consists of the elapsed time from transmission of a pulse until its receipt at the hydrophone array, is corrupted with noise due to the combined effects of environmental factors and measurement instruments.

In order to achieve a more accurate plot of the torpedo path, editing and smoothing techniques have been applied to the data during post run analyses.

To improve the real-time capability of the 3-D tracking ranges, Kalman filtering theory has been applied to the computer generated X, Y, and Z positional coordinates but is not operational [1].

In the near future an updated computer system composed of three MODCOMPIV computers will be in operation. The

majority of the software development requires interfacing current tracking programs and other related programs to the new computer system.

An opportunity exists for expanding the capability of the tracking system by applying a Kalman filter routine which processes measurements of the transit times of the acoustic pulses and provides an estimate of the position of the tracked object in real time. Prior research in this area [2], revealed that a Kalman filter utilizing a sequential estimation approach was desirable.

The intention is to develop and test a sequential Kalman filter tracking algorithm that can be interfaced with the current underwater range system.

II. DESCRIPTION OF RANGE TRACKING GEOMETRY

The hydrophone array, consisting of four independent elements, defines an orthogonal coordinate system in which transit time measurements are made. As shown in Figure 1, four hydrophones X, Y, Z, and C are on four adjacent vertices separated by a distance d , along the edge of the cube. The origin of the array coordinates is at the center of the cube with the orthogonal coordinates parallel to its edge. Positional information is computed from the transit times of a periodic synchronous acoustic signal travelling from the torpedo to the four hydrophones on the array. The range measures the tracked torpedo's position every 1.31 seconds to an accuracy that is typically within 3 to 30 feet. A more detailed description of the range tracking capability is described in [3].

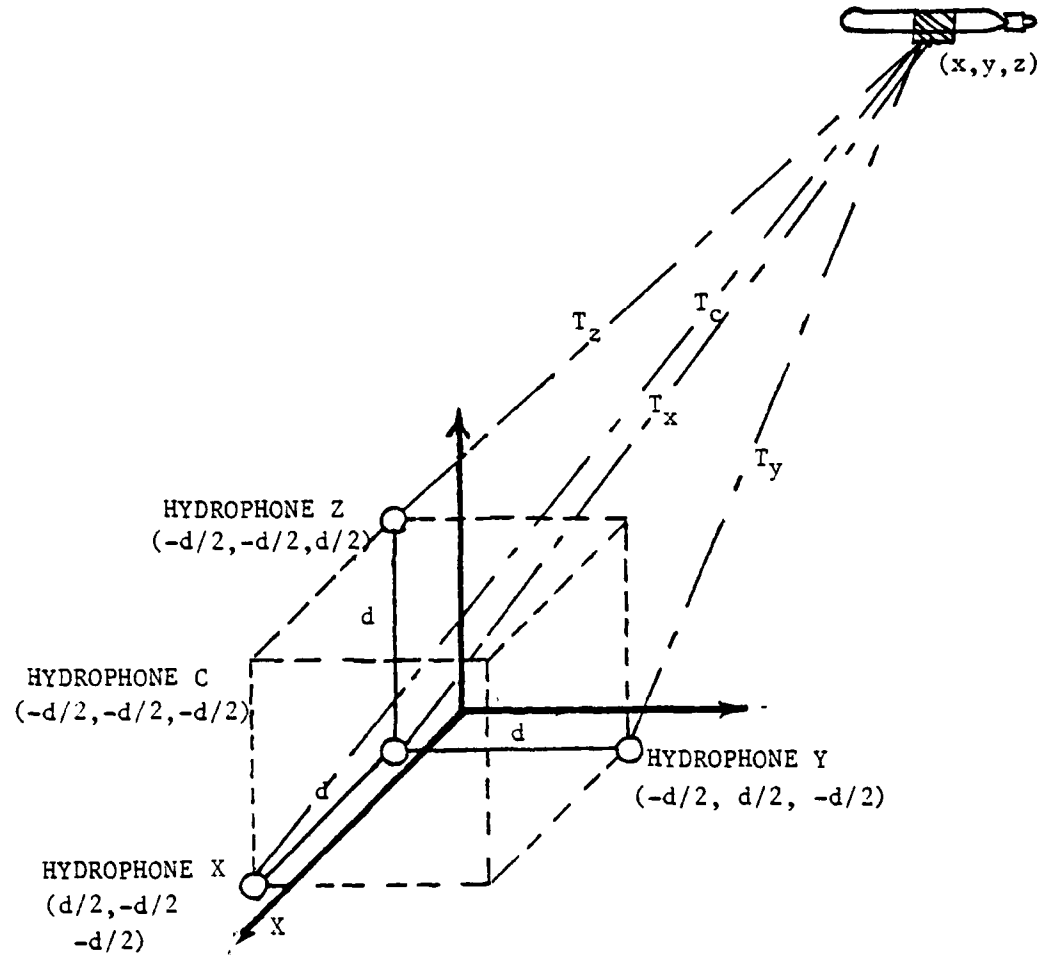


Figure 1. Geometry of a Tracking Array

III. THEORY--EXTENDED KALMAN FILTER

The equations describing the nonlinear relationship between transit times T_C , T_X , T_Y , T_Z and the position of the tracked torpedo are given by [3]

$$T_C = \frac{1}{VEL} [(x + \frac{d}{2})^2 + (y + \frac{d}{2})^2 + (z + \frac{d}{2})^2]^{\frac{1}{2}}, \quad (3.1)$$

$$T_X = \frac{1}{VEL} [(x - \frac{d}{2})^2 + (y + \frac{d}{2})^2 + (z + \frac{d}{2})^2]^{\frac{1}{2}}, \quad (3.2)$$

$$T_Y = \frac{1}{VEL} [(x + \frac{d}{2})^2 + (y - \frac{d}{2})^2 + (z + \frac{d}{2})^2]^{\frac{1}{2}}, \quad (3.3)$$

$$T_Z = \frac{1}{VEL} [(x + \frac{d}{2})^2 + (y + \frac{d}{2})^2 + (z - \frac{d}{2})^2]^{\frac{1}{2}}, \quad (3.4)$$

where $d = 30$ feet and $VEL \approx 4860$, which is approximately the average velocity of propagation of sound in water at Dabob Bay.* Since the transit times were readily available and are nonlinear functions of position, these equations can be linearized and Kalman Filter theory applied using the Extended Kalman Filter [2]. This procedure produces a real time measurement, with filtering on the corrupted transit times T_C , T_X , T_Y , and T_Z without the necessity of converting these times to positions.

*Sound velocity in water varies as a function of temperature, salinity, and depth.

For the three-dimensional location problem three position states (x , y , z) and two velocity states (v_x , v_y) specify target motion. The discrete linear and nonlinear observation equations are given by

$$\underline{x}(k+1) = \Phi \cdot \underline{x}(k) + \Gamma \cdot \underline{w}(k) \quad (3.5)$$

and

$$z(k) = h(\underline{x}(k), k) + \underline{v}(k) \quad (3.6)$$

In these equations Φ and Γ are constant matrices and h is a nonlinear function of the state variable \underline{x} . $\underline{w}(k)$ is plant excitation noise and $\underline{v}(k)$ is measurement noise. The plant noise and measurement noise are assumed uncorrelated (white) with zero mean.

That is,

$$E[\underline{w}(k) \cdot \underline{w}^T(j)] = Q'(k)\delta_{kj}$$

and

$$E[\underline{v}(k) \cdot \underline{v}^T(j)] = R(k)\delta_{kj}$$

with

$$\delta_{kj} = 1, k = j$$

$$= 0, k \neq j$$

In order to apply the linear filter equation (3.6) is expanded in a Taylor series about the best estimate of the

the state at that time and only the first-order terms are kept.

Equation (3.6) gives

$$z(k) = H(k) \cdot \underline{x}(k) + \underline{v}(k) \quad (3.7)$$

where

$$H(k) = \frac{\partial h}{\partial \underline{x}} \Big|_{x'(k)} = \hat{\underline{x}}(k/k-1) \quad (3.7a)$$

$\hat{\underline{x}}(k/k-1)$ is the predicted value of the state before the k^{th} measurement.

A state error vector is defined by

$$\tilde{\underline{x}} = \hat{\underline{x}}(k) - \underline{x}(k),$$

and a predicted state error vector is defined by

$$\tilde{\underline{x}}(k/k-1) = \hat{\underline{x}}(k/k-1) - \underline{x}(k).$$

The covariance of state error matrix is defined by

$$P(k) = E[\tilde{\underline{x}}(k) \cdot \tilde{\underline{x}}^T(k)],$$

and the predicted covariance of state error matrix is given by

$$P(k/k-1) = E[\tilde{\underline{x}}(k/k-1) \cdot \tilde{\underline{x}}^T(k/k-1)].$$

The state excitation matrix is given by

$$Q(k) = \Gamma(k)E[\underline{w}(k) \cdot \underline{w}^T(k)] \cdot \Gamma^T(k)$$

and the measurement noise covariance matrix is

$$R(k) = E[\underline{v}(k) \cdot \underline{v}^T(k)] .$$

The Kalman filter equations are given by [4,5]:

$$P(k+1/k) = \Phi P(k/k) \Phi^T + Q(k) \quad (3.8a)$$

$$G(k) = P(k/k-1) H^T(k) [H(k) \cdot P(k/k-1) H^T(k) + R(k)]^{-1} \quad (3.8b)$$

$$P(k) = [I - G(k) H(k)] P(k/k-1) \quad (3.8c)$$

$$\hat{x}(k+1/k) = \Phi \underline{x}(k/k) \quad (3.8d)$$

$$z(k/k-1) = h(\underline{x}(k/k-1), k) \quad (3.8e)$$

$$\hat{x}(k) = \hat{x}(k/k-1) + G(k) [z(k) - z(k/k-1)] \quad (3.8f)$$

The Q matrix serves not only to allow for maneuvering but also to account for any model inaccuracies, that is, any discrepancies between the true action of the torpedo and its characterization by Equation (3.5). The Q also serves to prevent the gain matrix $G(k)$ from approaching zero by always insuring uncertainty in the predicted covariance of error matrix $P(k+1/k)$.

IV. PROBLEM DEFINITION--TORPEDO TRACKING WITH THE EXTENDED KALMAN FILTER

A. FILTER EQUATIONS

Figure 2 illustrates the geometry of the states used for the filter. For a constant course, constant-speed torpedo, the plant state equations can be described as two second order systems, one for X and one for Y. The depth (Z) of the torpedo is maintained constant and any velocity in the Z direction is assumed to be random, uncorrelated with zero mean. Z is therefore described as a first order system.

The plant state equations are

$$\begin{bmatrix} x(k+1) \\ v_x(k+1) \\ y(k+1) \\ v_y(k+1) \\ z(k+1) \end{bmatrix} = \begin{bmatrix} x(k) + T v_x(k) + g_1(\gamma_{\dot{\theta}_t}, \gamma_{\dot{v}_t}, k) \\ v_x(k) + g_2(\gamma_{\dot{\theta}_t}, \gamma_{\dot{v}_t}, k) \\ y(k) + T v_y(k) + g_3(\gamma_{\dot{\theta}_t}, \gamma_{\dot{v}_t}, k) \\ v_y(k) + g_4(\gamma_{\dot{\theta}_t}, \gamma_{\dot{v}_t}, k) \\ z(k) + g_5(\gamma_z) \end{bmatrix} \quad (4.1)$$

where $x(k)$, and $y(k)$ are the position coordinates at time $t(k)$, $v_x(k)$ and $v_y(k)$ are the X and Y components of velocity. T is the time between observations, i.e. $t(k+1)-t(k)$ and $z(k)$ is the depth of the torpedo.

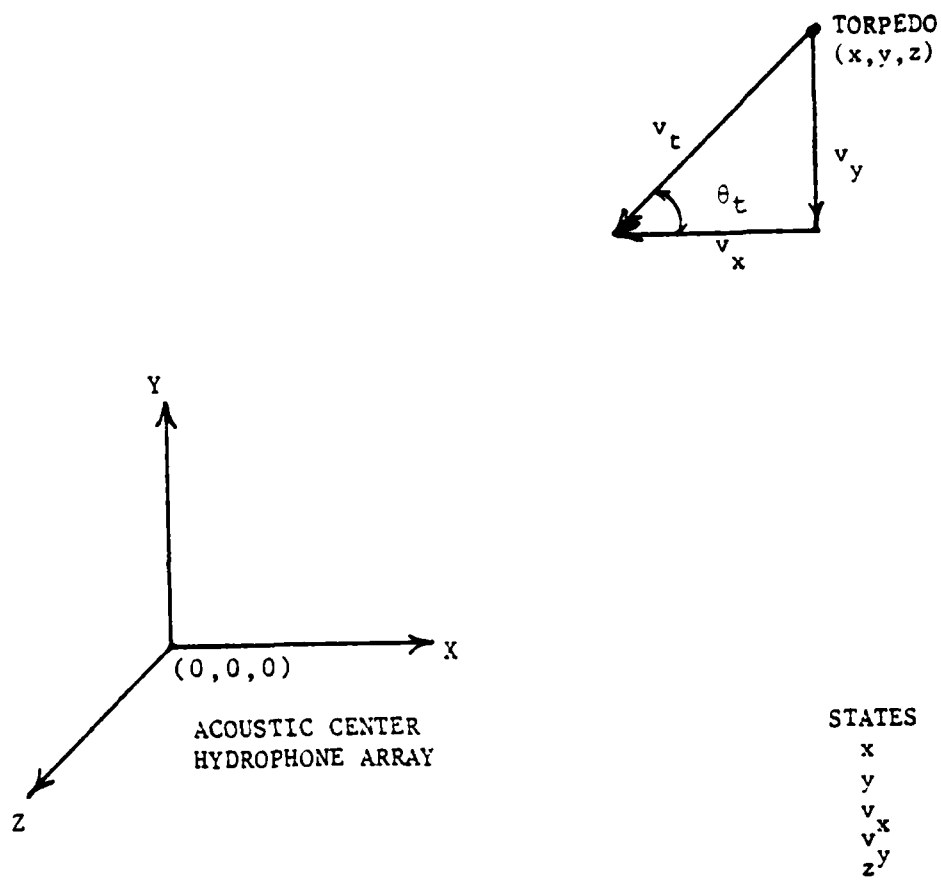


Figure 2. Filter Geometry

The excitation terms g_1 through g_5 are included to account for the random changes in speed, heading, and depth which can occur in a maneuvering torpedo. The quantities γ_{v_t} , γ_{θ_t} , and γ_z are the random changes of the torpedo which are assumed to be independent, zero mean, rates of change. They have variances defined by

$$\sigma_{\dot{v}_t}^2 = E[\gamma_{v_t}^2]$$

$$\sigma_{\dot{\theta}_t}^2 = E[\gamma_{\theta_t}^2]$$

$$\sigma_{\dot{z}}^2 = E[\gamma_z^2]$$

The values of the standard deviations are taken from typical maneuvering parameters for the torpedo;

$$\sigma_{\dot{\theta}_t} = 22^\circ/\text{sec}$$

$$\sigma_{\dot{v}_t} = 36 \text{ ft/sec}^2$$

$$\sigma_{\dot{z}} = 1 \text{ ft/sec}$$

The effect of this excitation is to increase the predicted value of the covariance of the state error matrix.

Writing the equations in state form results in

$$x(k+1) = \Phi x(k) + \Gamma w(k) \quad (4.2)$$

where

$$\phi = \begin{bmatrix} 1 & T & 0 & 0 & 0 \\ 0 & 1 & 0 & 0 & 0 \\ 0 & 0 & 1 & T & 0 \\ 0 & 0 & 0 & 1 & 0 \\ 0 & 0 & 0 & 0 & 1 \end{bmatrix}$$

and

$$\Gamma = \begin{bmatrix} T^2/2 & 0 & 0 \\ T & 0 & 0 \\ 0 & T^2/2 & 0 \\ 0 & T & 0 \\ 0 & 0 & T \end{bmatrix}$$

The vector $w(k)$ represents the effect on the states of the random excitations. Reference 5 has shown that the vector may be calculated from the equations relating torpedo X and Y velocity to the torpedo heading and velocity. The X velocity is

$$\dot{x} = v_x = v_t \cos \theta_t$$

which when differentiated gives

$$\ddot{x} = -v_t \dot{\theta}_t \sin \theta_t + \dot{v}_t \cos \theta_t \quad (4.4)$$

where

$$\dot{\theta}_t = \gamma \dot{\theta}_t$$

$$\dot{v}_t = \gamma \dot{v}_t$$

$$\sin \theta_t = \frac{v_y}{v_t}$$

$$\cos \theta_t = \frac{v_x}{v_t}$$

and upon substitution of the above relationship in equation (4.4),

$$\ddot{x} = -v_y \gamma \dot{\theta}_t + \gamma \dot{v}_t \frac{v_x}{v_t} \quad (4.5)$$

Similarly

$$\dot{y} = v_y = v_t \sin \theta_t \quad (4.6)$$

$$\ddot{y} = v_t \dot{\theta}_t \cos \theta_t + \dot{v}_t \sin \theta_t$$

and after substitution

$$\ddot{y} = v_x \gamma \dot{\theta}_t + \frac{v_y}{v_t} \gamma \dot{v}_t \quad (4.8)$$

The depth term is just

$$z = \gamma z \quad (4.9)$$

Thus

$$\underline{w}(k)^T = [(\gamma_{\dot{x}} \frac{v_x}{v_t} - \gamma_{\dot{y}} \frac{v_y}{v_t}) \quad (\gamma_{\dot{z}} v_x + \gamma_{\dot{v}_t} \frac{v_y}{v_t}) \quad \gamma_{\dot{z}}] \quad (4.10)$$

where from the assumption on the γ 's

$$E[\underline{w}(k)] = 0 \quad (4.11)$$

The excitation covariance matrix is thus found from

$$Q = E[\underline{w}(k)\underline{w}(k)^T] P^T \quad (4.12)$$

Let

$$\sigma_{\dot{x}}^2 = (\frac{v_x}{v_t}) \sigma_{\dot{v}_t}^2 + v_y^2 \sigma_{\dot{z}}^2 \quad (4.13a)$$

$$\sigma_{\dot{y}}^2 = (\frac{v_y}{v_t}) \sigma_{\dot{v}_t}^2 + v_x^2 \sigma_{\dot{z}}^2 \quad (4.13b)$$

$$\sigma_{\dot{x}\dot{y}} = v_x v_y [\frac{\sigma_{\dot{v}_t}^2}{v_t^2} - \sigma_{\dot{z}}^2] \quad (4.13c)$$

where the states are evaluated at the current state estimates $\underline{x}(k)$. Substituting these expressions in the Q matrix results in

$$Q = \begin{bmatrix} (\frac{T^2}{2})\sigma_{\ddot{x}}^2 & \frac{T^3}{2}\sigma_{\ddot{x}}^2 & (\frac{T^2}{2})\sigma_{\ddot{x}\ddot{y}}^2 & \frac{T^3}{2}\sigma_{\ddot{x}}\sigma_{\ddot{y}} & 0 \\ \frac{T^2}{2}\sigma_{\ddot{x}}^2 & T^3/2\sigma_{\ddot{x}\ddot{y}}^2 & T^2\sigma_{\ddot{x}\ddot{y}}^2 & 0 & \\ & & (\frac{T^2}{2})\sigma_{\ddot{y}}^2 & \frac{T^3}{2}\sigma_{\ddot{y}}^2 & 0 \\ & & & T^2\sigma_{\ddot{y}}^2 & 0 \\ & & & & T^2\sigma_{\dot{z}}^2 \end{bmatrix} \quad (4.14)$$

Symmetric

The excitation matrix serves not only to take into account the possibility of maneuvering, but of model inaccuracies as well [5]. Q is also used to prevent the gains of the filter from approaching zero as more and more data is processed, by insuring some uncertainty in the predicted state values.

The observation equations are nonlinear in the states and are given by

$$z(k) = \begin{bmatrix} T_C(k) \\ T_X(k) \\ T_Y(k) \\ T_Z(k) \end{bmatrix} = \begin{bmatrix} \frac{1}{VEL}[(x(k)+d/2)^2 + (y(k)+d/2)^2 + (z(k)+d/2)^2]^{\frac{1}{2}} + v(k) \\ \frac{1}{VEL}[(x(k)-d/2)^2 + (y(k)+d/2)^2 + (z(k)+d/2)^2]^{\frac{1}{2}} + v(k) \\ \frac{1}{VEL}[(x(k)+d/2)^2 + (y(k)-d/2)^2 + (z(k)+d/2)^2]^{\frac{1}{2}} + v(k) \\ \frac{1}{VEL}[(x(k)+d/2)^2 + (y(k)+d/2)^2 + (z(k)-d/2)^2]^{\frac{1}{2}} + v(k) \end{bmatrix} \quad (4.15)$$

The measurement noises, $v(k)$'s, are assumed to be zero-mean and independent with a covariance matrix

$$R(k) = \begin{bmatrix} \sigma_{T_C}^2 & 0 & 0 & 0 \\ 0 & \sigma_{T_X}^2 & 0 & 0 \\ 0 & 0 & \sigma_{T_Y}^2 & 0 \\ 0 & 0 & 0 & \sigma_{T_Z}^2 \end{bmatrix} \quad (4.16)$$

The magnitude of the transit times noise is a function of the signal-to-noise ratio at the hydrophone array, which is influenced by several environmental factors.

Discussions with NAVTORPSTA personnel indicate a typical accuracy of ± 10 microseconds and this value is used as the standard deviation for the simulation runs.

Equation (3.7a) can be used to give the linearized observation matrix. The result is

$$H(k) = \begin{bmatrix} \frac{\partial T_C}{\partial x} & \frac{\partial T_C(k)}{\partial v_x} & \frac{\partial T_C(k)}{\partial y} & \frac{\partial T_C(k)}{\partial v_y} & \frac{\partial T_C(k)}{\partial z} \\ \frac{\partial T_X(k)}{\partial x} & \frac{\partial T_X(k)}{\partial v_x} & \frac{\partial T_X(k)}{\partial y} & \frac{\partial T_X(k)}{\partial v_y} & \frac{\partial T_X(k)}{\partial z} \\ \frac{\partial T_Y(k)}{\partial x} & \frac{\partial T_Y(k)}{\partial v_x} & \frac{\partial T_Y(k)}{\partial y} & \frac{\partial T_Y(k)}{\partial v_y} & \frac{\partial T_Y(k)}{\partial z} \\ \frac{\partial T_Z(k)}{\partial x} & \frac{\partial T_Z(k)}{\partial v_x} & \frac{\partial T_Z(k)}{\partial y} & \frac{\partial T_Z(k)}{\partial v_y} & \frac{\partial T_Z(k)}{\partial z} \end{bmatrix} \quad (4.17)$$

When the derivatives are taken and evaluated at the predicted state values $x(k/k-1) = x'(k)$ the result is

$$H(k) = \begin{bmatrix} \frac{x'(k)+d/2}{DEN1} & 0 & \frac{y'(k)+d/2}{DEN1} & 0 & \frac{z'(k)+d/2}{DEN1} \\ \frac{x'(k)-d/2}{DEN2} & 0 & \frac{y'(k)+d/2}{DEN2} & 0 & \frac{z'(k)+d/2}{DEN2} \\ \frac{x'(k)+d/2}{DEN3} & 0 & \frac{y'(k)-d/2}{DEN3} & 0 & \frac{z'(k)+d/2}{DEN3} \\ \frac{x'(k)+d/2}{DEN4} & 0 & \frac{y'(k)+d/2}{DEN4} & 0 & \frac{z'(k)-d/2}{DEN4} \end{bmatrix} \quad (4.18)$$

where

$$DEN1 = [(x'(k)+d/2)^2 + (y'(k)+d/2)^2 + (z'(k)+d/2)^2]^{1/2}$$

$$DEN2 = [(x'(k)-d/2)^2 + (y'(k)+d/2)^2 + (z'(k)+d/2)^2]^{1/2}$$

$$DEN3 = [(x'(k)+d/2)^2 + (y'(k)-d/2)^2 + (z'(k)+d/2)^2]^{1/2}$$

$$DEN4 = [(x'(k)+d/2)^2 + (y'(k)+d/2)^2 + (z'(k)-d/2)^2]^{1/2}.$$

The Φ matrix, Q matrix, R matrix, and H matrix are then used in the Kalman filter equations (3.8).

B. THE SEQUENTIAL EXTENDED KALMAN FILTER

The Kalman filter equations described in the previous section represent a system that is characterized by a one-step estimation and prediction for each set of four transit time observables (T_C , T_X , T_Y , and T_Z). This one step process exhibits the following salient features:

1. The four transit times received during each 1.31 second measurement interval (time slot) are processed simultaneously by the filter equations. Updated covariance of error and state estimates are therefore obtained only once for each time slot.

2. A major part of the time period for the estimation calculation is spent in the gain equation where the inversion of a 4×4 matrix is required.

3. The Extended Kalman filter is based on a linearization about the predicted value of a period t_k to t_{k+1} . Unacceptably large or erroneous transit time measurements will cause the filter to ignore the update information for the entire time slot. The predicted estimate will become the new estimate for the time slot and the interval extended.

If one assumes that each of the four hydrophones in the array are statistically independent of one another, a sequential approach can be taken to process each of the four transit times separately. Thus, each observable will be processed in sequence, and the result of processing one measurement is used in the following computation to process the next measurement until all four observables have been used.

The advantages of the sequential approach over the traditional one-step estimation and prediction are:

1. Since the four transit times are independent and processed sequentially, the covariance of error matrix and

the state vector are updated four times during each time slot. Thus more accurate estimates of the filter states are achieved.

2. Modification of the filter equations for the sequential approach circumvented the matrix inversion in the gain equation. Therefore filter cycle time is reduced substantially.

3. An invalid transit time measurement will result in the filter ignoring the update information for that particular measurement only. For example, if only three of the four transit times are acceptable, the filter would be sequentially updated three times during that particular time slot. Thus, the filter is less sensitive to erroneous transit time measurements.

To utilize the sequential Extended Kalman filter, equations (3.8) must be modified. Calculations are performed on each of the four independent transit times in the following order: T_C , T_X , T_Y , and T_Z for each 1.31 second time slot. The estimate of the states $x(k/k)$, based on one transit time measurement are used as the prediction $x(k/k-1)$ for the calculations on the next measurement. Thus for the first time measurement T_C only the first row of the linearizing H matrix is calculated.

Next the first gain column corresponding to the first time measurement T_C is calculated by

$$G_{ic1} = \frac{P(k/k-1)H_{irow}^T}{H_{irow}P(k/k-1)H_{irow}^T + R_{ii}} \quad (4.19)$$

where $i = 1$ to 4 corresponding to the four measured transit times. Thus, the first row of the H matrix is used to calculate the first column of the gain matrix with both corresponding to the first measured time T_C .

Next, an estimate of the particular observation time is calculated using equation (3.8e) evaluated at the predicted state $\underline{x}(k/k-1)$.

The difference between observed transit time and the estimated transit times forms the residual which is used in the estimate equation

$$\underline{x}_i = \underline{x}(k/k-1) + G_{i\text{col}} [\text{Residual}] \quad (4.20)$$

This equation gives an estimate of the states based on one measurement.

Next, the covariance of error is calculated based on one measurement by

$$P_i = [I - G_{i\text{col}} H_{i\text{row}}] P_{i-1} \quad (4.21)$$

where

I = identity matrix

P_{i-1} = the covariance matrix calculated from the previous transit time measurement or if $i = 1$, the prediction $P(k/k-1)$.

After the first iteration, \bar{x}_1 becomes $\underline{x}(k/k-1)$ and P_1 becomes $P(k/k-1)$ for the second iteration which calculates the estimate of the states based on the second measurement T_X .

After four iterations ($k = 4$), \underline{x}_4 becomes the estimate for the time slot $x(k/k)$ and P_4 becomes the covariance of error $P(k/k)$.

The predictions for the next time slot are calculated using equations (3.8a) and (3.8d). This process is repeated for each time slot.

IV. TESTING AND SIMULATION

A. DESCRIPTION

The sequential Extended Kalman filter routine is tested using simulated torpedo tracks generated by the IBM-360 computer. A variety of track scenarios are produced to test the filter performance during single array tracking.

The first series of tests used constant course and speed tracks which transitioned multiple array quadrants including:

1. crossing north of the array
2. crossing above the array
3. crossing diagonally through the array

The next series of tests adds a number of typical torpedo maneuvers to the constant course and speed tracks. These maneuvers consisted of 10 and 20 °/sec turns with G forces ranging from 1/4-G to 1-G.

For the above tests filter initialization errors range from 0 to 40 feet/sec for X and Y velocity, and 0 to 60 feet for X and Y position. The Z depth is maintained constant at 300 feet which is approximately the average depth of water at Dabob bay. Zero mean Gaussian noise is added to corrupt the observed transit times for all runs.

The last series of tests demonstrates the ability of the filter to track through the areas of multiple arrays.

Before the above series of tests can be conducted, it is necessary to add operational features to the software which

provide the following capability:

1. detect erroneous transit time measurements
2. minimize position error during high dynamic maneuvers
3. track through multiple arrays

A more detailed explanation of these features is described below.

B. EDITING ERRONEOUS TIME MEASUREMENTS

The operation of the filter may be adversely affected by erroneous transit time measurements. Large errors in the transit time measurements will produce errors in the state vector estimate and the linearizing H matrix. This may cause the filter to become unstable and exhibit divergent characteristics. In some extreme cases catastrophic failure may result. Measurement errors can occur because of many factors including an error in the transit time of the acoustic pulse primarily due to the receipt of multi path signals from previous time slots that have reflected off the surface, bottom, or different density layers in the water.

To guard against catastrophic failures a three-sigma gate using the covariance of measurement noise (R) and the covariance of estimation error ($P(k/k)$) is implemented. For each calculation of a state estimate ($\underline{x}(k/k)$), the largest positional covariance of error is used, either \underline{x} , \underline{y} , or \underline{z} , and converted to time in seconds using the average velocity of sound in water for Dabob bay, 4860 ft/sec. The gate then is

written for each time measurement $i = 1$ to 4 :

$$\text{Gate} = \sqrt{\frac{(P_{jj})_{\text{maximum}} + R_{ii}}{4860}}$$

where $j = 1, 3, 5$. The gate expands or decreases depending on the confidence level of the position estimate and the transit time. If ZDIFF which is the difference between the actual transit time received and the predicted transit time to a particular hydrophone exceeds the gate, the measurement is considered unacceptable and the filter gain is set to zero causing the filter to ignore the data and take the prediction of the states as the estimate

$$\underline{x}(k/k) = \underline{x}(k/k-1)$$

An invalid time measurement zeros only the gain column for that particular hydrophone causing only that hydrophone's data to be ignored.

C. BOUNDING RESIDUAL BIAS ERROR

As previously mentioned, the torpedo dynamics are modeled in the filter's excitation covariance matrix Q.

During preliminary tests it becomes evident that torpedo turn rates between 5 and $20^\circ/\text{sec}$ yield position errors ranging from approximately 10 to 40 ft. Increasing the standard deviation parameters ($\sigma_\theta, \sigma_v, \sigma_z$) for the adaptive Q matrix helps to a certain extent, however as expected a point is reached where the noise starts to become the dominant error source. There are two major reasons why the filter develops errors during turns:

1. The filter's predicted state estimates are computed assuming a constant velocity over a 1.31 second sampling interval. During a turn the velocity vector of the torpedo is continuously rotating, therefore the filter's predicted estimate will be in error. A large magnitude error will require more than one time slot to remove. A faster sampling rate would reduce the error and may alleviate the problem; however, the Dabob tracking range system has been designed for a 1.31 second sampling rate and cannot be changed.

2. The adaptive Q matrix assumes that the torpedo accelerations are normally distributed and uncorrelated. Torpedo tracking maneuvers do not fit these assumptions.

To minimize position errors during maneuvers a procedure has been developed in order that repeated estimates of the state vector are obtained during a single sampling period (1.31 second time slot) until the transit time residual error falls below a preset threshold.

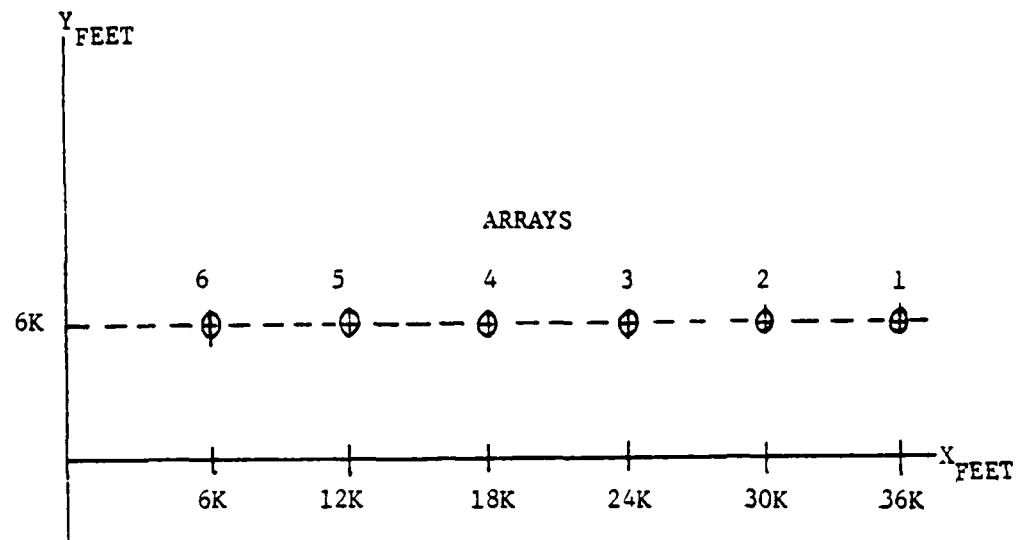
In Section IV it was stated that during each time slot the gain, covariance, and state estimate equations (4.19-4.21) were iteratively solved for each of the four sequential transit times T_C , T_X , T_Y , and T_Z . Subsequently additional software was incorporated to calculate the estimated transit time to each of the four hydrophones based on the last updated state vector. Four time residuals are then computed by subtracting the estimated time to each hydrophone from the observed transit time. The average of the absolute value of

the time residuals is then formed. If the average residual error exceeds the preset threshold in the software, which is indicative of large error in the state vector, Q is calculated and added to the last updated covariance of error matrix P . The filter then reiterates the gain, covariance, and state estimate equations for the same time slot. If the new state vector generates an average residual error still exceeding the threshold value, then the process is repeated. This procedure continues until the average residual error falls below the preset threshold at which time an acceptable state vector estimate has been obtained for the time slot. Once this occurs the prediction equations (3.8a) and (3.8d) are solved and the filter proceeds to the next time slot and commences processing new transit time measurements. As will be shown later the filter did successfully bound the position error during turning maneuvers. For these tests the threshold constant is set at 10 microseconds, which is the value of RMS measurement noise.

C. MULTIPLE ARRAY TRACKING

Initial tests were performed on tracks in the area of one array. In order to more closely simulate a typical run on the range, a scheme was designed to track the torpedo through multiple arrays [2].

First, a coordinate system is defined as shown in Figure 3. The center of the coordinate system is geographically



Coordinate System for Multiple Array Tracking

A R R A Y S	C HYDRO			X HYDRO			V HYDRO			Z HYDRO		
	X	Y	Z	X	Y	Z	X	Y	Z	X	Y	Z
	36000	6000	0	36030	6000	0	36000	6030	0	36000	6000	30
A	30000	6000	0	30030	6000	0	30000	6030	0	30000	6000	30
R	24000	6000	0	24030	6000	0	24000	6030	0	24000	6000	30
R	18000	6000	0	18030	6000	0	18000	6030	0	18000	6000	30
A	12000	6000	0	12030	6000	0	12000	6030	0	12000	6000	30
Y	6000	6000	0	6030	6000	0	6000	6030	0	6000	6000	30

HYDRO--Hydrophone Location Matrix

Figure 3

near the entrance to Dabob bay in the simulation. Array number 6 is the closest array to the coordinate center. In the simulation array 1 is at 36,000 feet from coordinate center and array 6 is 6,000 feet. The C hydrophone is assumed to be the axis location of each array. Then each X position for the X hydrophone in each array is $X_C + 30$, each Y position for the Y hydrophone is $Y_C + 30$ and each Z position for the Z hydrophone is $Z_C + 30$. These 72 positions, an XYZ position for each of 4 hydrophones in 6 arrays, are placed into a 6×12 matrix HYDRO and referenced throughout the routine. The torpedo position is referenced to a central level rectangular coordinate system. The nonlinear observation equations become

$$z(k) = \begin{bmatrix} T_C(k) \\ T_X(k) \\ T_Y(k) \\ T_Z(k) \end{bmatrix} = \begin{bmatrix} \frac{1}{VEL} [(x'(k) - X_{iC})^2 + (y'(k) - Y_{iC})^2 + (z'(k) - Z_{iC})^2]^{1/2} \\ \frac{1}{VEL} [(x'(k) - X_{iX})^2 + (y'(k) - Y_{iX})^2 + (z'(k) - Z_{iX})^2]^{1/2} \\ \frac{1}{VEL} [(x'(k) - X_{iY})^2 + (y'(k) - Y_{iY})^2 + (z'(k) - Z_{iY})^2]^{1/2} \\ \frac{1}{VEL} [(x'(k) - X_{iZ})^2 + (y'(k) - Y_{iZ})^2 + (z'(k) - Z_{iZ})^2]^{1/2} \end{bmatrix}$$

where $T_C(k)$, $T_X(k)$, $T_Y(k)$, and $T_Z(k)$ are the transit times to each of the four hydrophones and $x'(k)$, $y'(k)$, and $z'(k)$ are the filter estimates $x'(k/k)$ evaluated at the predicted positions $\underline{x}(k/k-1)$. The subscripted variables X, Y, and Z are the coordinates of a particular array being used.

The decision parameter used to determine the switching from array to array is a straight handoff. If the predicted x position is greater than 3,000 feet from the array in use, then an index (I8) is incremented and the next row of HYDRO is implemented. This placed into the routine the X, Y, and Z positions of the hydrophones in the next array. The handoff can easily be utilized in real range operations, as the transit times from adjacent arrays are present at the computer for a particular time slot. For simulation, it is assumed that in all the arrays each axis pointed in the same direction. In actual range operations each array is tilted about both the X and Y axis. Since the true transit times are derived in a tilted coordinate frame, the filter's estimate of transit time must also be calculated in a tilted coordinate frame. The tilt angle measurements along with the level rectangular coordinates of the array with respect to the central rectangular coordinate system can be input into the matrix HYDRO to rotate the coordinates of each hydrophone in the array.

VI. TEST RESULTS AND DISCUSSION

A. SERIES ONE--STRAIGHT RUNS

This series of tests includes constant speed and heading tracks. Initial position and velocity errors are set to zero. Measurement noise is added to all runs. Torpedo velocity ranged from 20 to 55 knots. Figure 4 shows the true trajectory of the torpedo in the horizontal X-Y plane. The center of the hydrophone array is located at positional coordinates (0,0). Figure 5 describes the filter's RMS estimate of position error as a function of sampling time. The RMS estimates are obtained by taking the square-root of the appropriate diagonal terms of the covariance matrix. It should be noted that the propagation of RMS estimates are a function of the position of the torpedo with respect to the hydrophone array. As shown in Figure 4, if Y = 0, the torpedo path is inbound toward the array along the "X" axis. Upon examining Figure 5, it is evident that the RMS estimate of X position error or the uncertainty in the filter's X position estimate is small and relatively constant throughout the entire trajectory. The uncertainty in the filter's Y position estimate decreases as the torpedo approaches the array, becomes a minimum at the closest point of approach (CPA), and increases as the torpedo moves outbound away from the array. This behavior in the filter's RMS estimates can be explained by recognizing

that the cluster of four hydrophones in the array actually describe a position fixing system. The torpedo position is located by the intersection of circular lines of position (range arcs) originating from each hydrophone on the array. In general, the greater distance the torpedo is located from the array, the shallower the range arc intersections become and the more uncertainty exists in the actual torpedo position. For the case where the torpedo is moving along the X axis, the uncertainty in position exists only in the Y direction. If the torpedo's X distance from the array becomes infinite, the range arcs from each hydrophone appear to originate from a single point source. The position fixing system then reduces to a single dimension ranging system along the X axis with the uncertainty in the Y position estimate becoming infinite. If the torpedo approaches the array along the Y axis ($X = 0$), the filter's RMS estimate of Y position error will be relatively small, and as the torpedo's Y distance from the array becomes infinite, the filter's uncertainty in the X position estimate becomes infinite.

In order to keep RMS position error estimates within allowable tolerance the Dabob range tracking system requires the torpedo remain within a 3,000 foot radius of the center of the hydrophone array.

Figures 6 and 7 depict the error in both position and depth for the straight run trajectory along the X axis. The position errors are computed by subtracting the filter

position estimate, $x(k/k)$, from the computer generated true position for each time slot. From Figure 6, it is observed that the Y position error magnitude, which is caused by system noise, decreases on the inbound leg and increases on the outbound leg. Since the torpedo path originated on the outer tracking perimeter ($X = 3,000$ feet), the noise in the Y channel will be amplified due to the large uncertainty in the Y position estimate. The magnitude of noise error in the Y direction also decreases as the torpedo approaches the array and increases as the torpedo moves outbound. The steady state X and Y position errors ranged between -11 and +4 feet throughout the trajectory.

Figure 8 describes a straight inbound torpedo path that passes north of the array at a constant Y distance of 2121 feet. Torpedo velocity is maintained at 20 knots. A comparison of the RMS x estimates of this track with the preceding one, Figures 5 and 9, reveal that both estimates are relatively constant, however the X estimate in Figure 9 is significantly larger. Since the torpedo path is parallel to the X axis, a larger uncertainty in the X position estimate will result. A comparison of the RMS Y position error estimates reveals identical propagation characteristics. This is due to the symmetry in the east-west direction of the two trajectories.

Figures 10 and 11 show that the steady state position and depth magnitude errors are less than 10 feet. The noise

induced error in the X position is due to the uncertainty in the filter X position estimate.

A torpedo path which is inbound along a 45° diagonal to the array is depicted in Figure 12. For this run torpedo velocity is constant at 28 knots. Figure 13 shows that the filter's X and Y RMS estimates of position error are approximately equal. Likewise Figure 14 shows that X and Y position error propagation is also similar. These results are consistent since the X and Y position magnitudes of the torpedo trajectory are identical. At the point of closest approach ($X = 0$, $Y = 0$) the uncertainty in both the X and Y positions becomes a minimum and increases as the torpedo moves past the array. Steady state position and depth errors range between -4 and +6 feet.

B. SERIES TWO--MANEUVERING RUNS

The results of the straight run analyses discussed in the previous subsection show that the propagation of the filter's estimate of RMS position error is dependent on the path of the torpedo with respect to the hydrophone array. Thus the errors in X and Y position, and Z depth are also a function of the torpedo trajectory. In this series of tests maneuvers are added to the three straight path trajectories. These maneuvers consist of 360° turns at turn rates of 10 and 20°/sec. G forces range between 1/4-G and 1-G. G forces are changed using the same turn rate by varying velocity. A typical test

run on the tracking range at Dabob would include these type maneuvers.

Figure 16 describes an inbound torpedo path which maintains a Y distance from the array between -200 and +600 feet. Initial position and velocity are 30 and 20 feet in X and Y position and 30 and -20 feet/second in X and Y velocity. Torpedo velocity is maintained constant at 20 knots throughout the trajectory. Four 360° $1/4$ -G turns are executed during the run. Figures 17 and 18 describe the position and depth errors. Within approximately three time slots the filter achieved steady state performance. Upon observing the error propagation it is apparent that the filter is insensitive to turn rate maneuvers. Negligible degradation in position and depth is observed. Thus the error bound routine discussed in the previous section successfully bounds position and depth errors during turns. As expected the position errors decrease as the torpedo approaches the array and increase as the torpedo proceeds outbound from the array. Since position and depth errors exhibit approximately equal oscillations about zero indicates that the system noise is the dominant error source driving the filter. Bias errors on the time residuals due to maneuvers are negligible. Steady state errors in position and depth ranged between -1 and +5 feet throughout the run.

The next test describes an inbound torpedo trajectory, Figure 19, which passes north of the hydrophone array. The torpedo maintained a Y distance from the array between 1600

and 2400 feet. Four $10^\circ/\text{sec}$ $1/4\text{-G}$ turns are executed during this test. Filter initialization errors are 20 and 11 feet in X and Y position and 20 feet/sec in both X and Y velocity. The error in position and depth is described in Figures 20 and 21. The X position error demonstrates larger deviations than the Y position error. As noted during the straight runs, this is due to the difference in the filter's X and Y RMS position error estimates for this type trajectory. The oscillatory characteristics of the position error indicate again that noise is the dominant error source and the filter is tracking the torpedo through the maneuvers. Position errors range between -8 and +8 feet with one X channel error reaching a maximum of -15 feet, which occurred at time slot 140. The exact cause of the -15 foot error is unknown but may have been caused by an anomaly in the IBM-360 subroutine SNORM which generates the zero mean Gaussian noise for the filter. Errors in torpedo depth, Figure 21, are consistent and range between -2 and +5 feet.

For the next test the torpedo exhibits an inbound trajectory along a 45° diagonal with respect to the array. Figure 22 shows that four $10^\circ/\text{sec}$ $1/4\text{-G}$ turns are executed on this run: 2 on the inbound leg and 2 on the outbound leg. Filter initialization errors are 60 feet in both X and Y position and 30 feet in X and Y velocity. Steady state conditions are achieved in approximately four time slots. As expected for this type trajectory, the X and Y position

errors portray similar propagation characteristics, Figure 23. This similarity can be explained by the equivalent X and Y RMS error estimates generated by the filter for a 45° diagonally inbound trajectory. Position and depth errors, Figure 24, ranged between -7 and +10 feet.

The preceding tests discussed filter performance for straight runs with 10°/sec 1/4-G turns. Using the same basic torpedo trajectories as above, similar tests are performed with 10°/sec turn rates at 1/2-G. Figures 25 through 33 describe the torpedo paths and the corresponding position and depth error propagation plots for each run. Filter initialization errors ranged between 10 and 40 feet in position and 10 and 40 feet in velocity. Torpedo velocity is maintained constant at 55 knots. An analysis of the position and depth plots reveals that filter performance is similar to that described in the previous tests. In Figures 26 and 32 the larger errors incurred after time slot 135 are due to the torpedo trajectory exceeding the radial tracking range limit of 3,000 feet. This is more clearly described in the torpedo trajectory curves, Figures 25 and 31. The additional 1/4-G acceleration during the turns did not produce visible degradation in the filter's position and depth estimates.

The next set of maneuvering tests increased the turn rate to 20°/sec with G forces at 1/2-G. The same basic inbound and outbound straight runs trajectories are used. Initialization errors ranged between 20 and 40 feet in position and -10 and

and 35 feet/second for velocity. Figure 34 describes a torpedo inbound trajectory which maintains a Y distance from the array between -275 and 500 feet. Four turns are executed on this run. The X and Y position errors reveal essentially the same characteristics described before. In general the position and depth errors decreased as the torpedo approaches the array, become a minimum at the closest point of approach, and increase as the torpedo moves outbound past the array. The higher turn rates experienced on this test do not degrade the X and Y position errors. Figures 35 and 36 show that position and depth errors ranged between -1 and +5 feet.

Figure 37 depicts a torpedo path which maintains a Y distance from the array between 1760 and 2760 feet. Three $20^\circ/\text{sec}$ $1/2\text{-G}$ turns are performed during this run. Figures 38 and 39 describe the position and depth errors which range between -7 and +9 feet during steady state.

The diagonally inbound trajectory with four $20^\circ/\text{sec}$ $1/2\text{-G}$ turns is displayed in Figure 40. Position and depth errors for this run, Figures 41 and 42, ranged between +10 and -10 feet. Again note the similarity in the position error behavior for each channel for this type trajectory. The larger errors in position after time slot 125 are due to the filter's RMS position error estimates increasing as the torpedo approaches the radial tracking limit of the hydrophone array.

The last set of maneuvering tests increased the G force during the $20^\circ/\text{sec}$ turns from $1/2\text{-G}$ to 1-G . The three basic

inbound-outbound trajectories are again repeated. Figures 43 through 51 describe the torpedo trajectories and corresponding position and depth errors. Overall performance indicates that during steady state conditions the magnitude of position and depth errors are below 10 feet.

Due to the presence of system noise position errors reached a maximum of 14 feet, when the torpedo trajectory exceeded the radial tracking limit of the hydrophone array. As was also observed in the preceding tests, errors induced by the turn rate appeared to have a negligible effect on filter performance.

C. SERIES THREE--MULTIPLE ARRAY TRACKING

The purpose of the last series of tests is to functionally demonstrate that the filter is able to track the torpedo through multiple arrays using the simulated tracking range set up and handoff scheme described in the previous section. Figure 52 depicts a straight run trajectory which traverses the six hydrophone arrays. The position and depth errors are described in Figures 53 and 54.

Note that the handoff from array to array was accomplished with negligible effect on position and depth errors. The magnitude of the errors compare well with those observed on the single array straight run tracking.

VII. CONCLUSIONS

The sequential Extended Kalman filter satisfactorily provided real time estimates of torpedo position and depth. The magnitude of steady state position and depth errors ranged between 0 and 10 feet for torpedo tracks within the specified radial tracking range.

The iterative error bound routine furnished the capability to estimate torpedo position and depth during turning maneuvers up to 1-G. Errors generated during maneuvers are comparable to those observed during straight runs.

The filter's RMS estimates of position and depth errors are dependent on system noise and the distance the torpedo is from the center of the hydrophone array. In general larger errors are encountered at more remote distances from the hydrophone array.

The simulated trajectories were performed using constant measurement noise sequences. Since the filtering problem is non-linear the error, in the filter's state estimate vector is a function of the statistical properties of the noise. Future tests should include a Monte Carlo simulation where filter performance is investigated for an ensemble of measurement noise sequences.

Additional tests should also include evaluating filter performance using trajectories generated from actual torpedo

runs on the Dabob test range. These tests would verify the adequacy of the noise model in the filter and the ability of the software to edit erroneous transit time measurements.

FIGURES

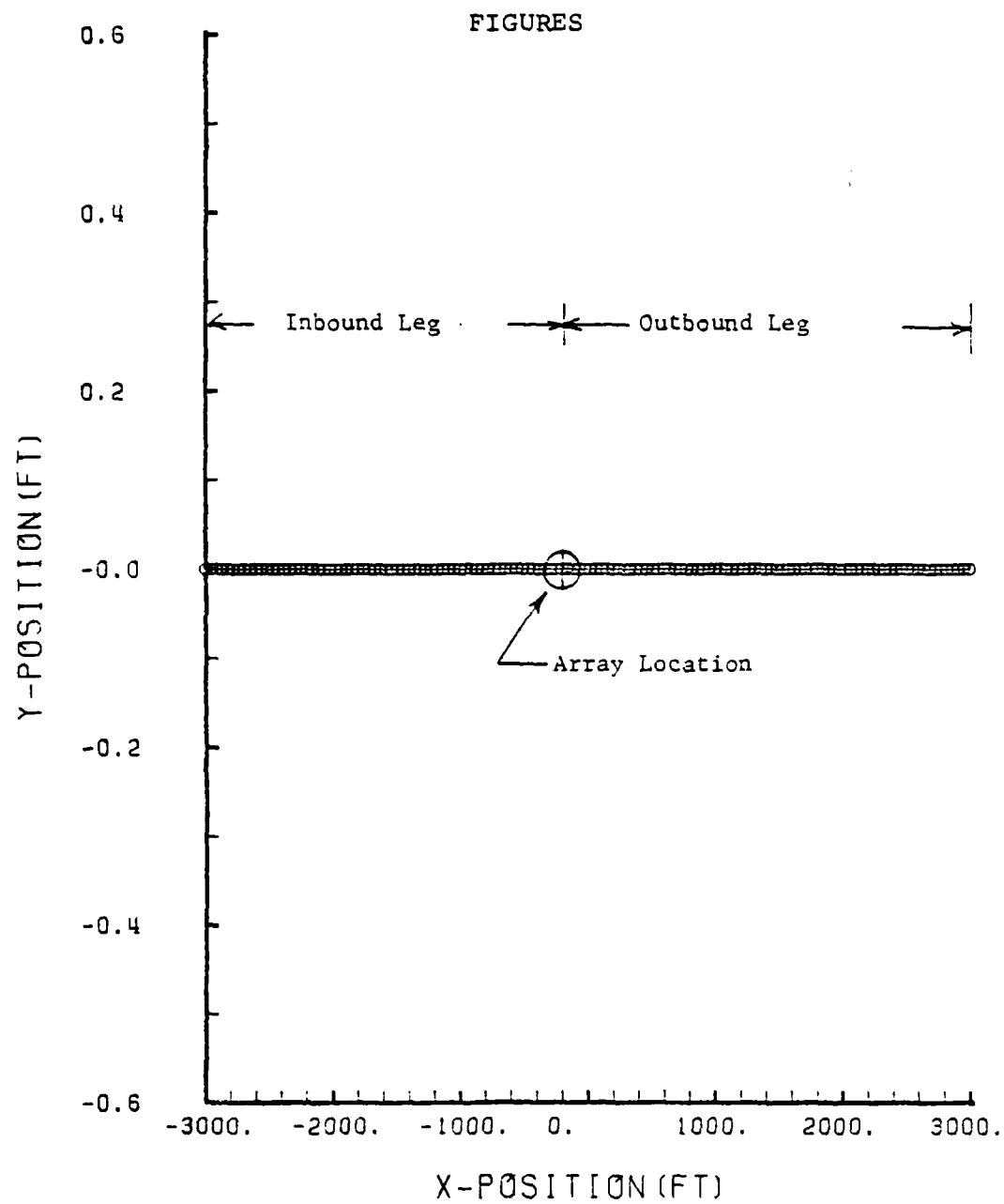


Figure 4. True Trajectory of the Torpedo in the Area of a Single Array

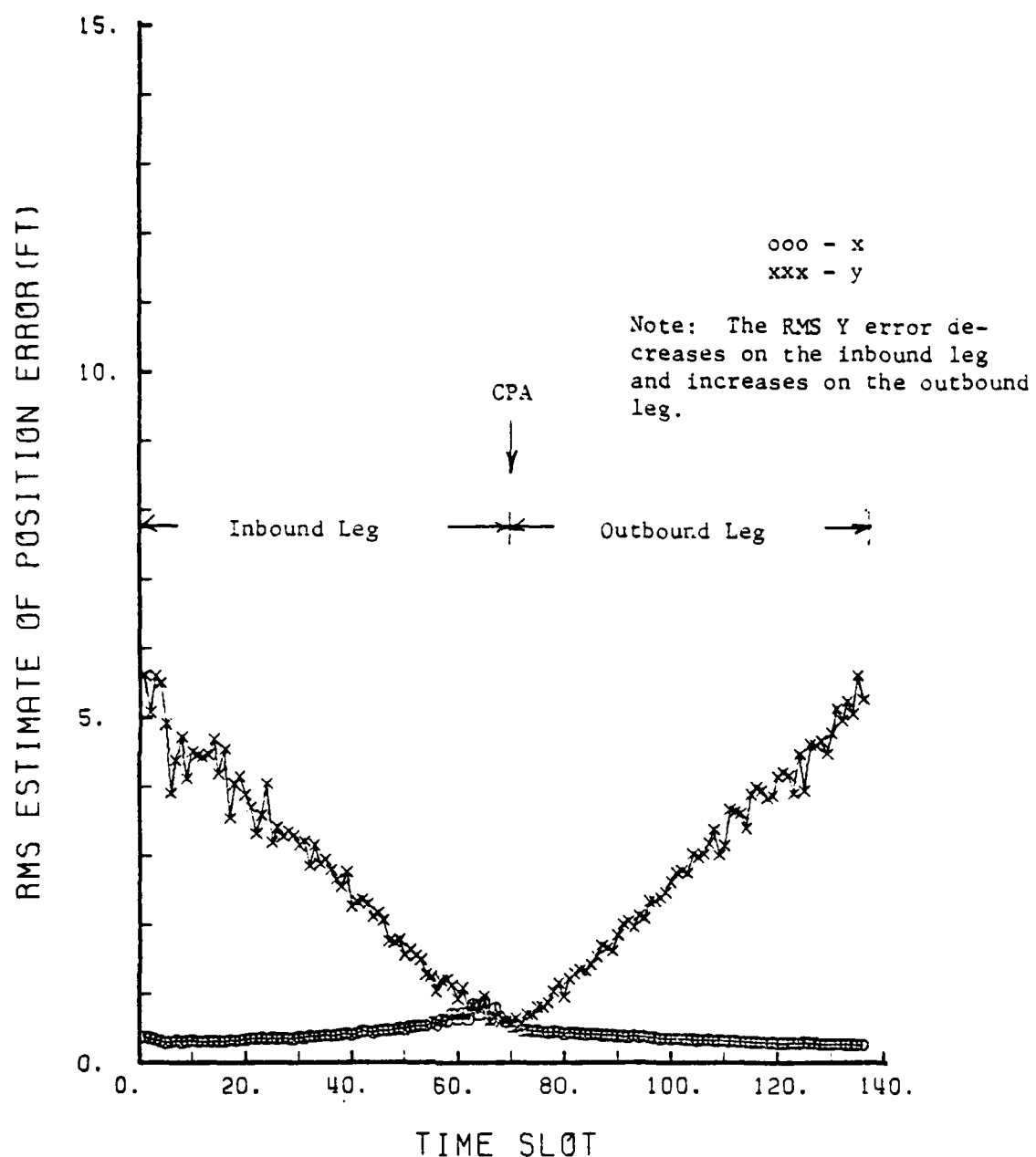


Figure 5. Filter Estimate of RMS Position Error During a Straight Run in the Area of a Single Array

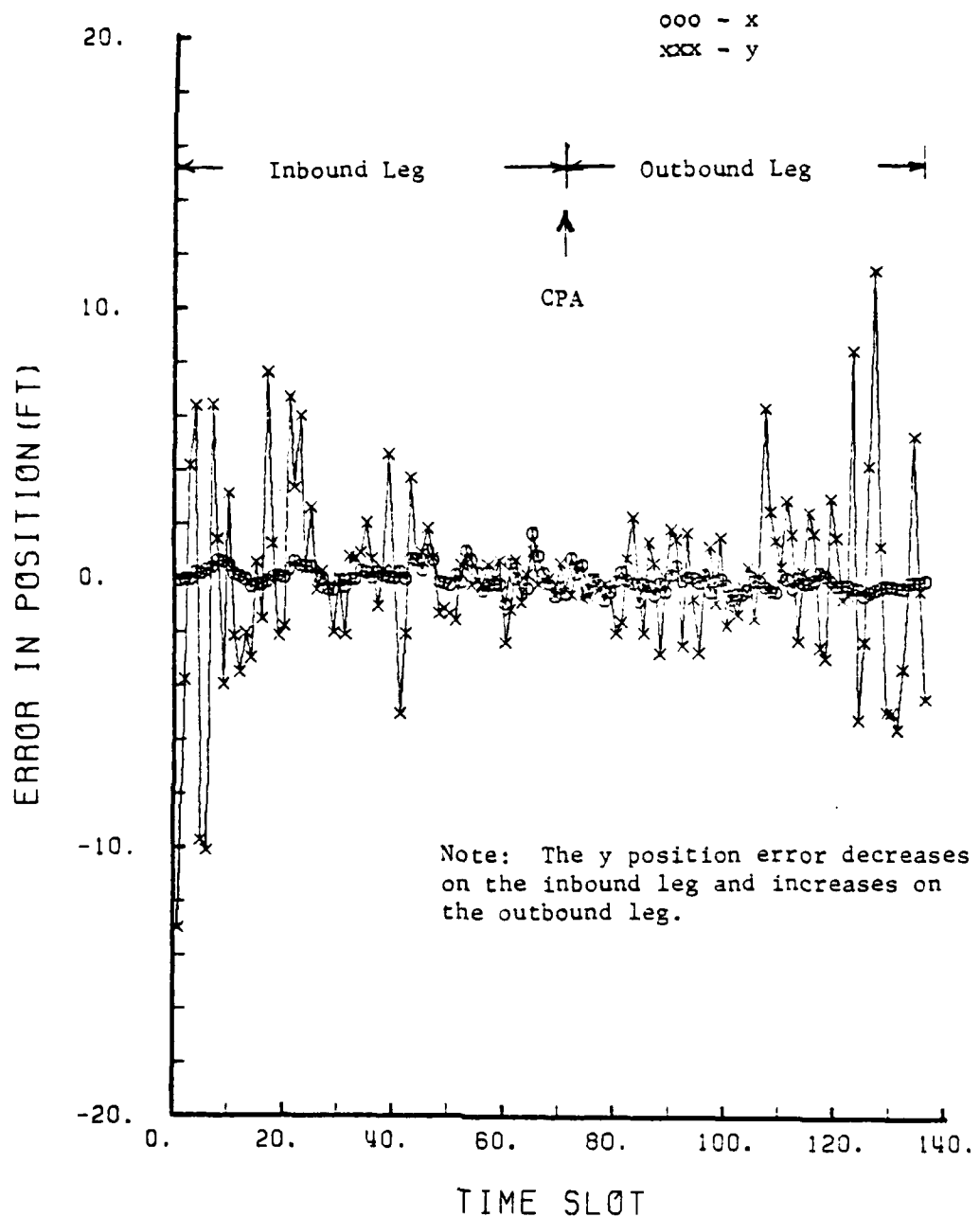


Figure 6. Error in Torpedo Position During A Straight Run in the Area of a Single Array

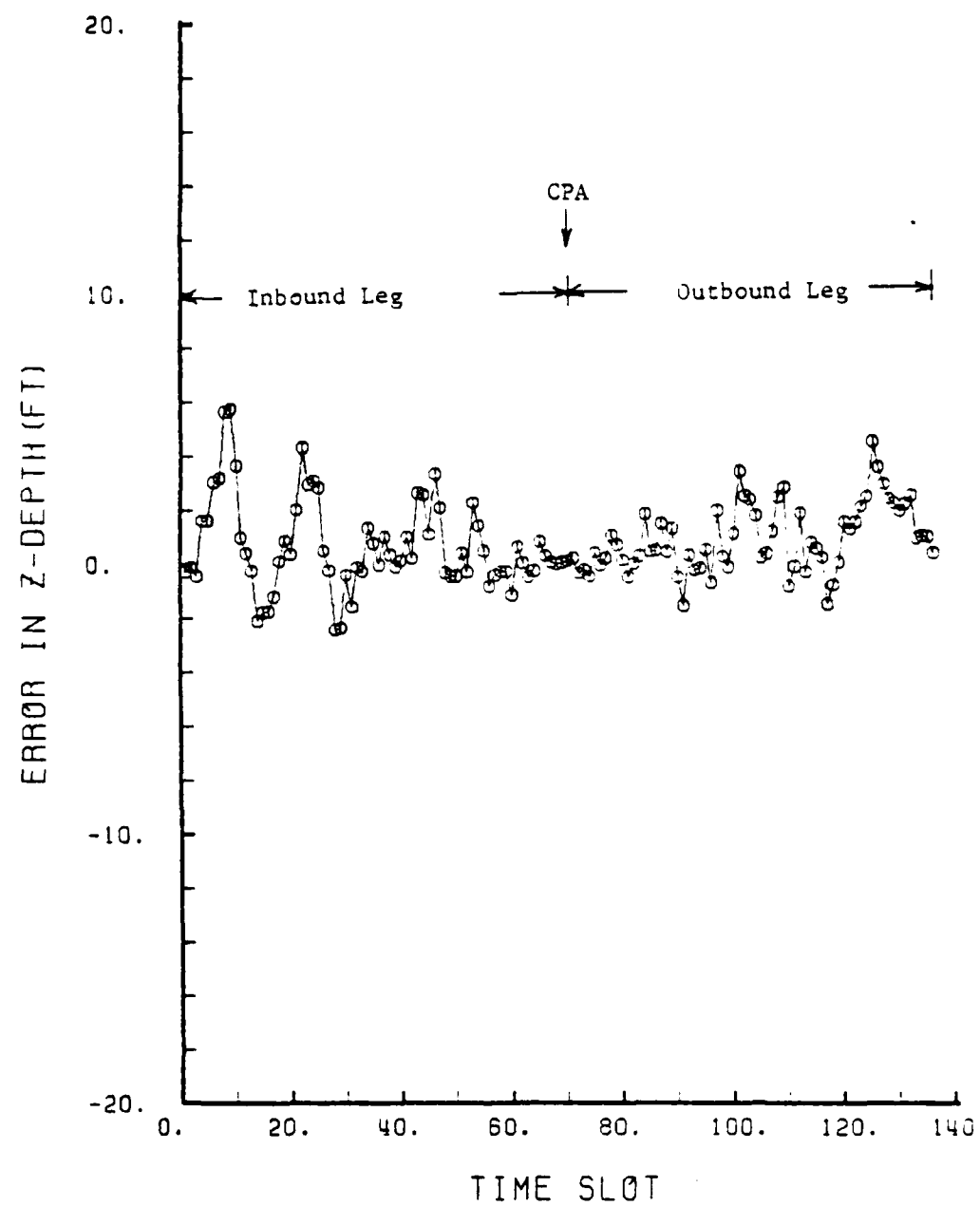


Figure 7. Error in Torpedo Depth During a Straight Run
in the Area of a Single Array

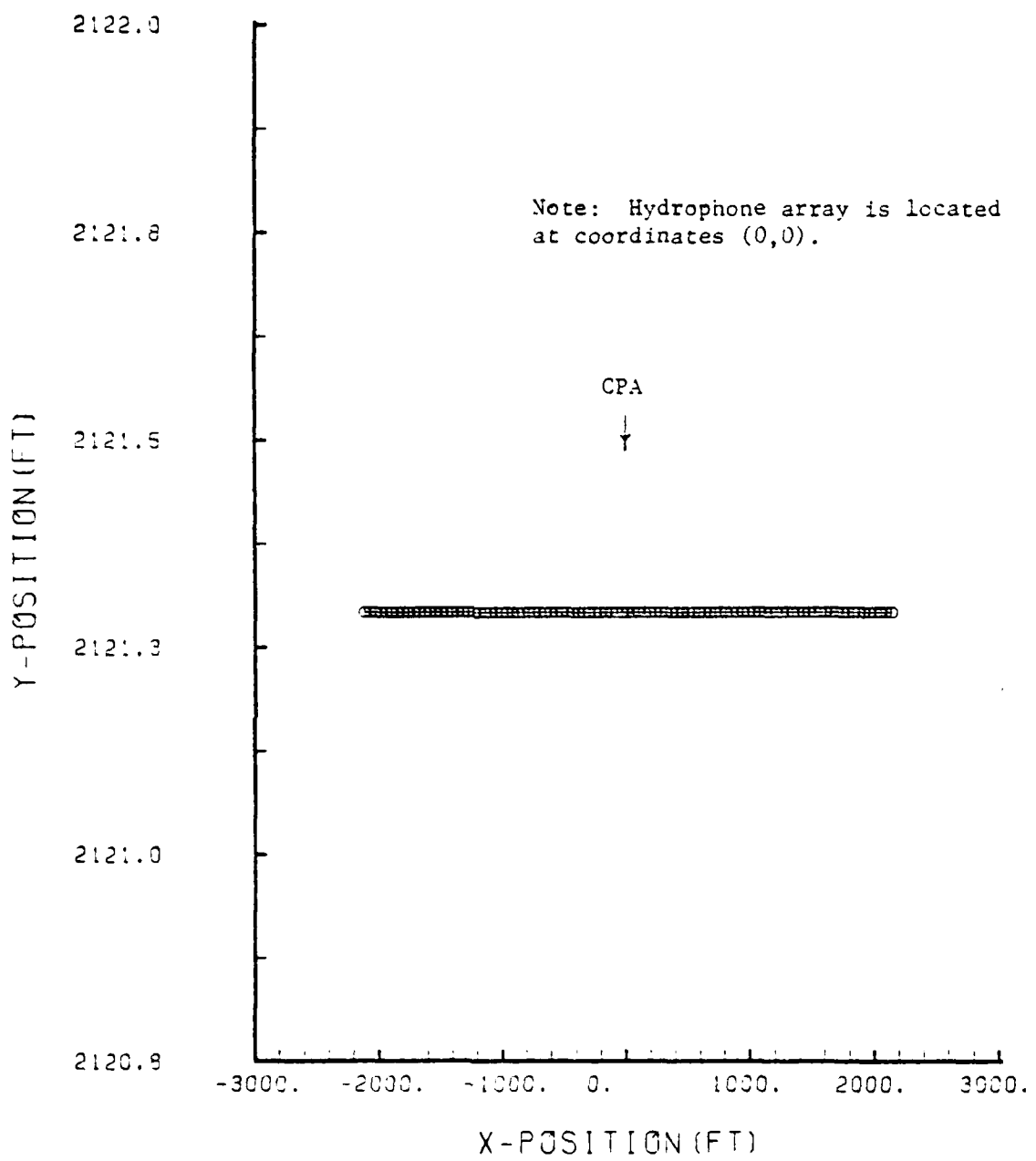


Figure 8. True Trajectory of the Torpedo During a Straight Run in the Area of a Single Array.

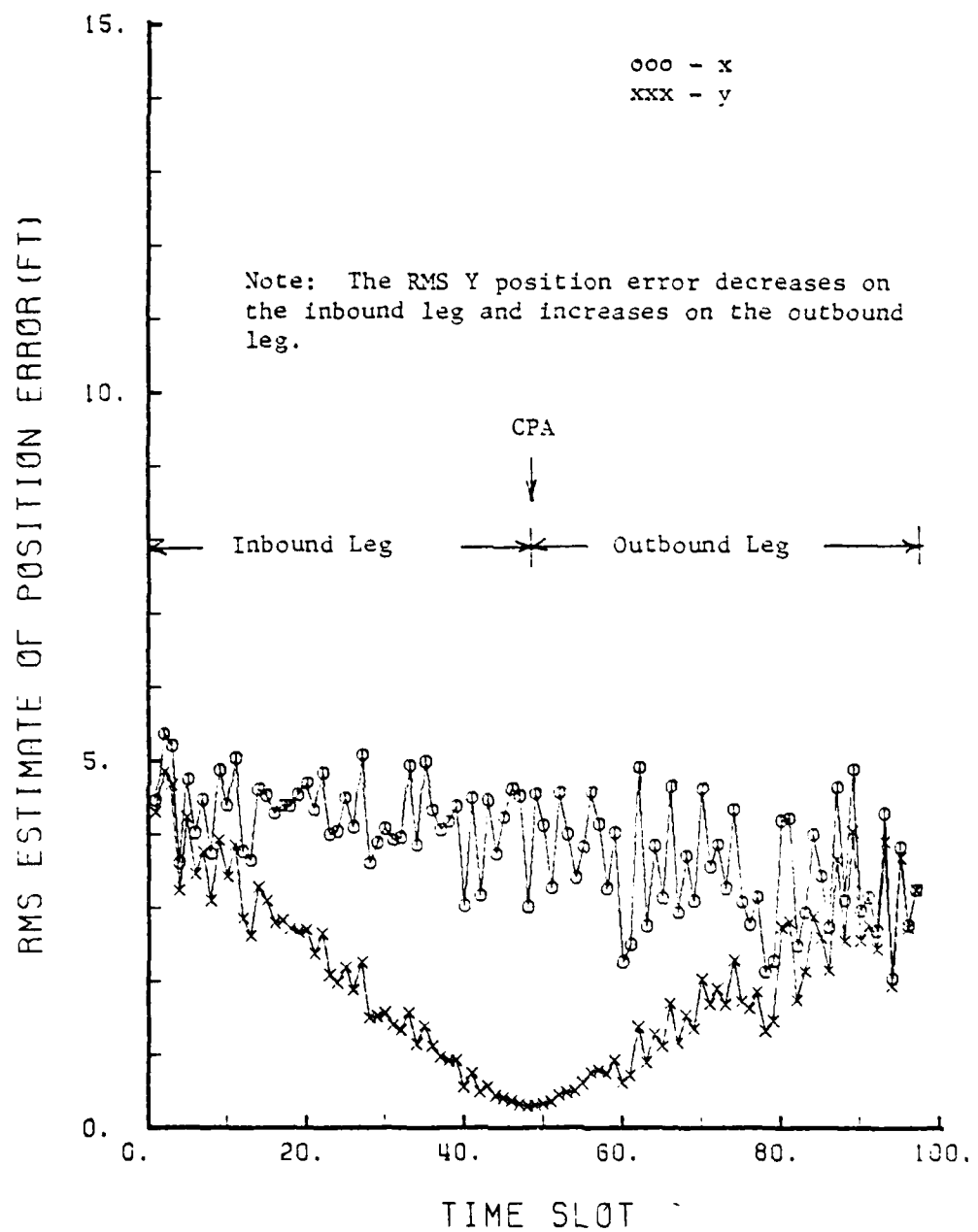


Figure 9.. Filter Estimate of the RMS Position Error During a Straight Run in the Area of a Single Array

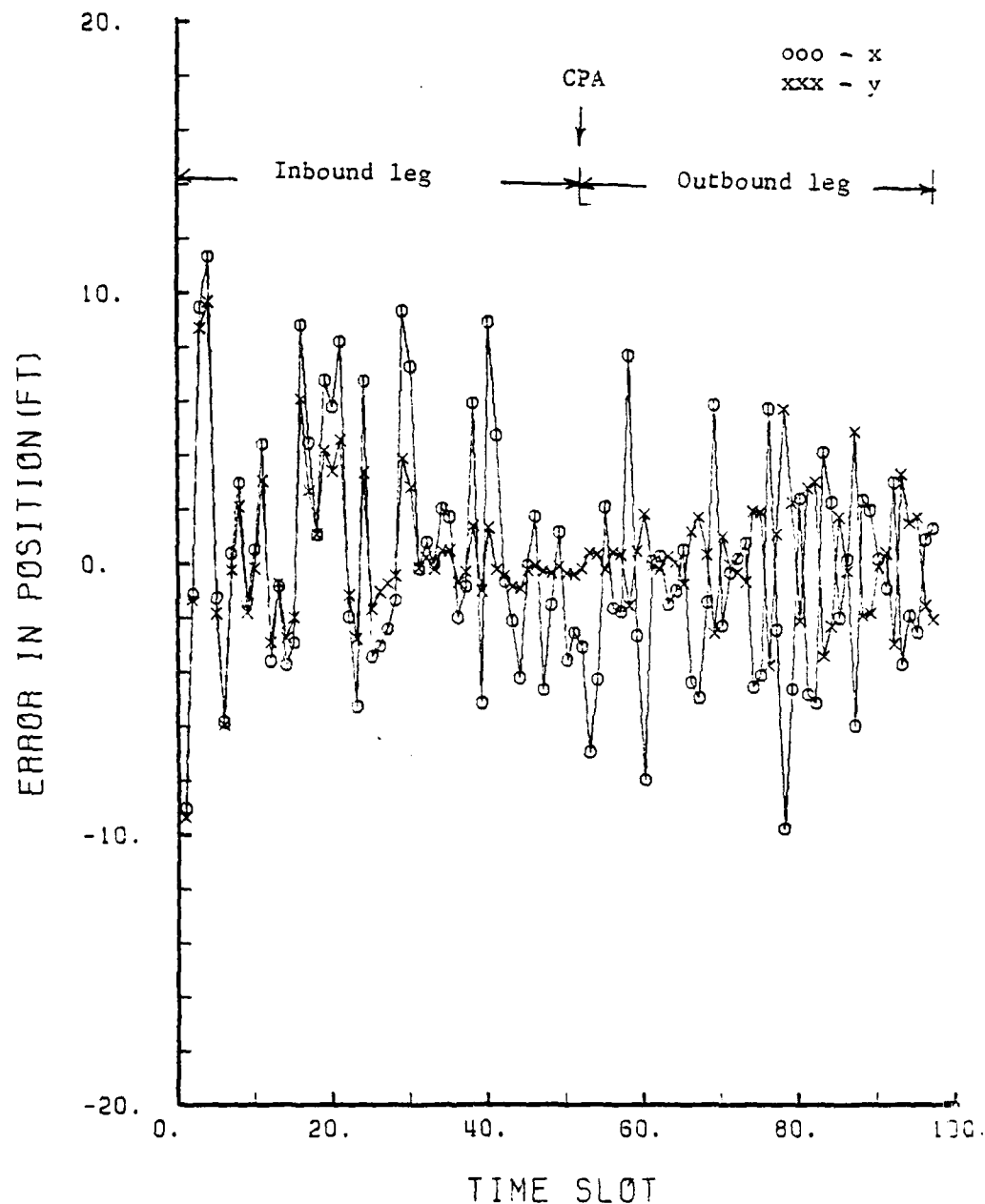


Figure 10. Error in Torpedo Position During a Straight Run in the Area of a Single Array

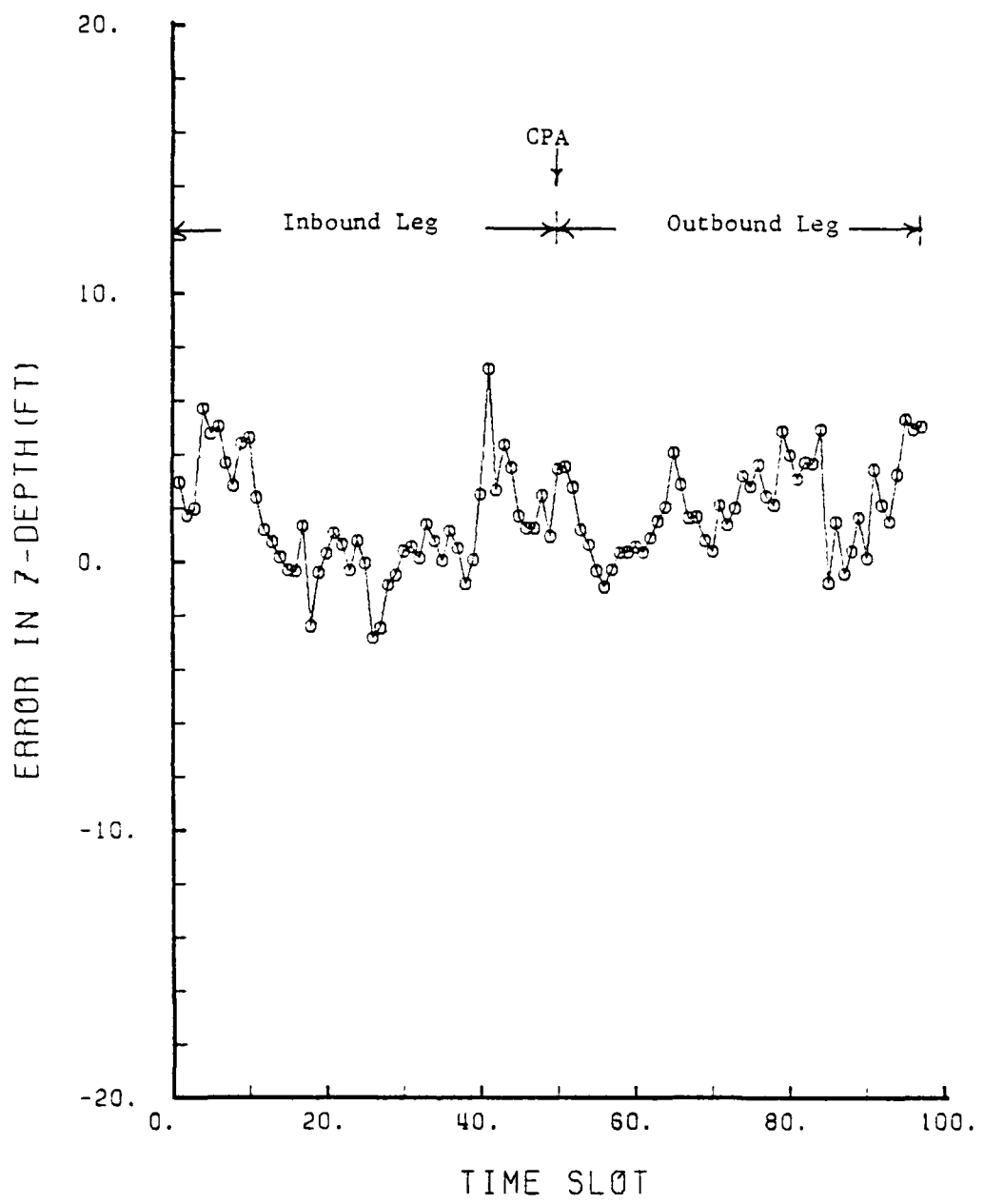


Figure 11. Error in Torpedo Depth During a Straight Run
in the Area of a Single Array

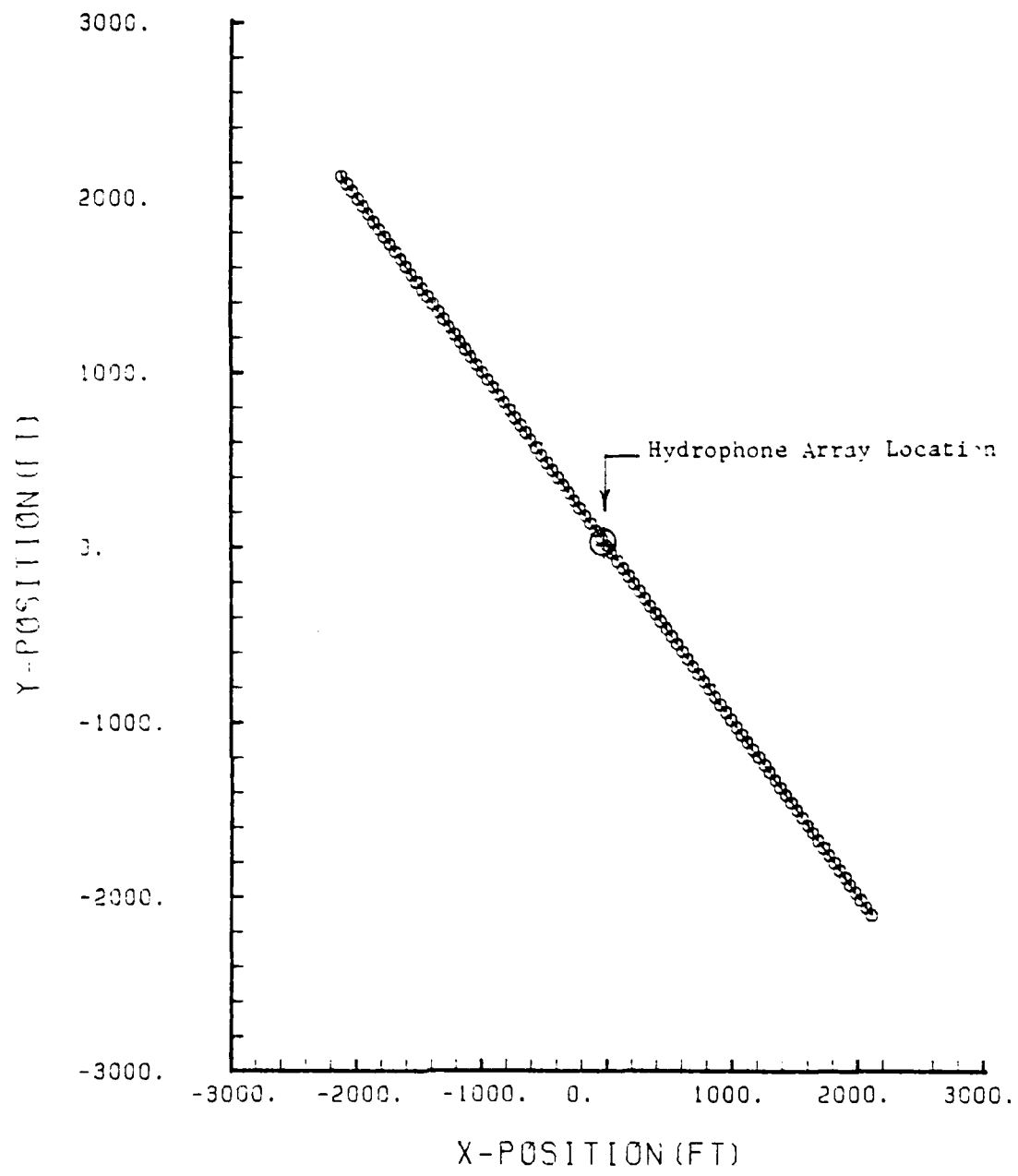


Figure 12. True Trajectory of the Torpedo During a Straight Run in the Area of a Single Array

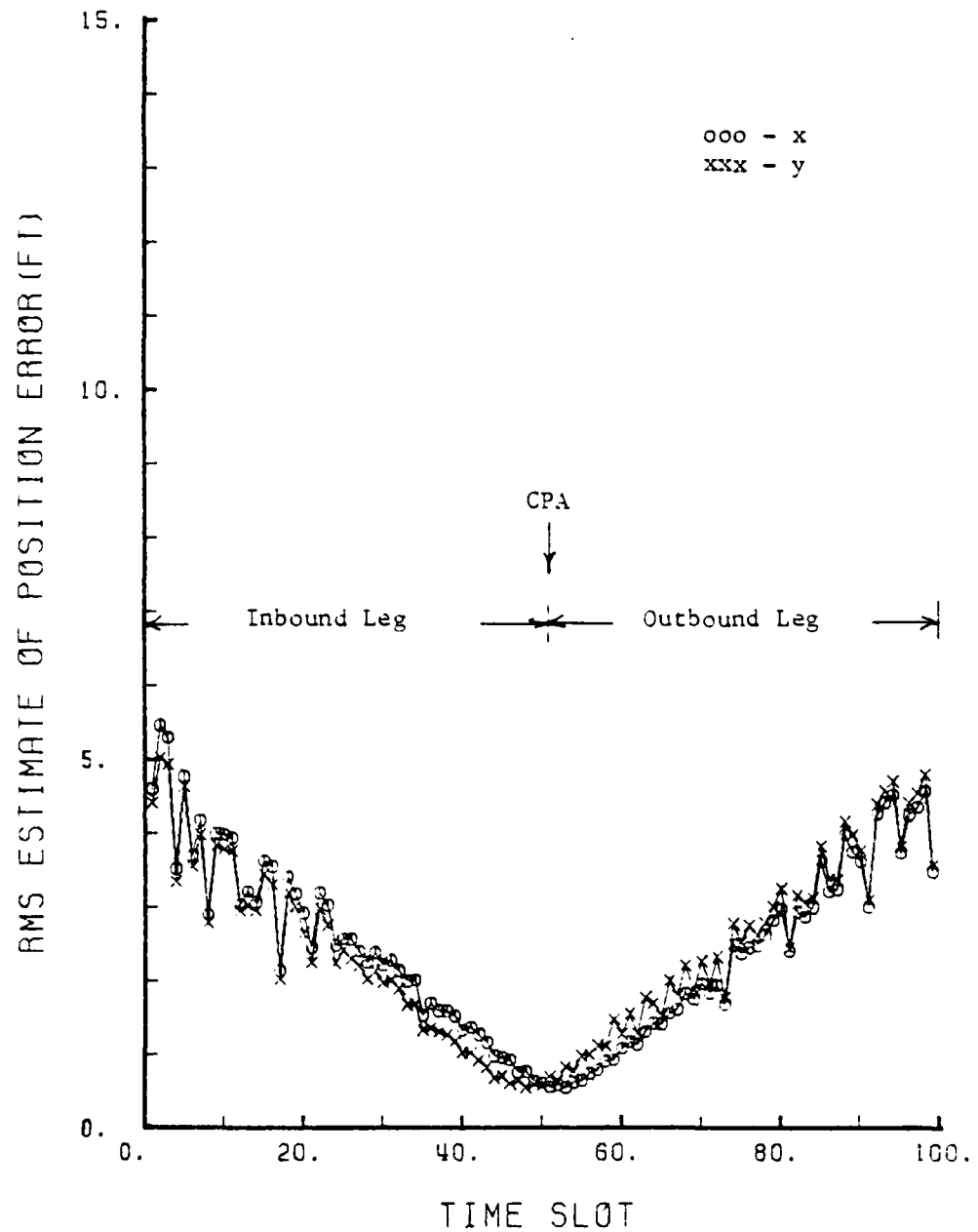


Figure 13. Filter Estimate of RMS Position Position Error During a Single Run in the Area of Single Array

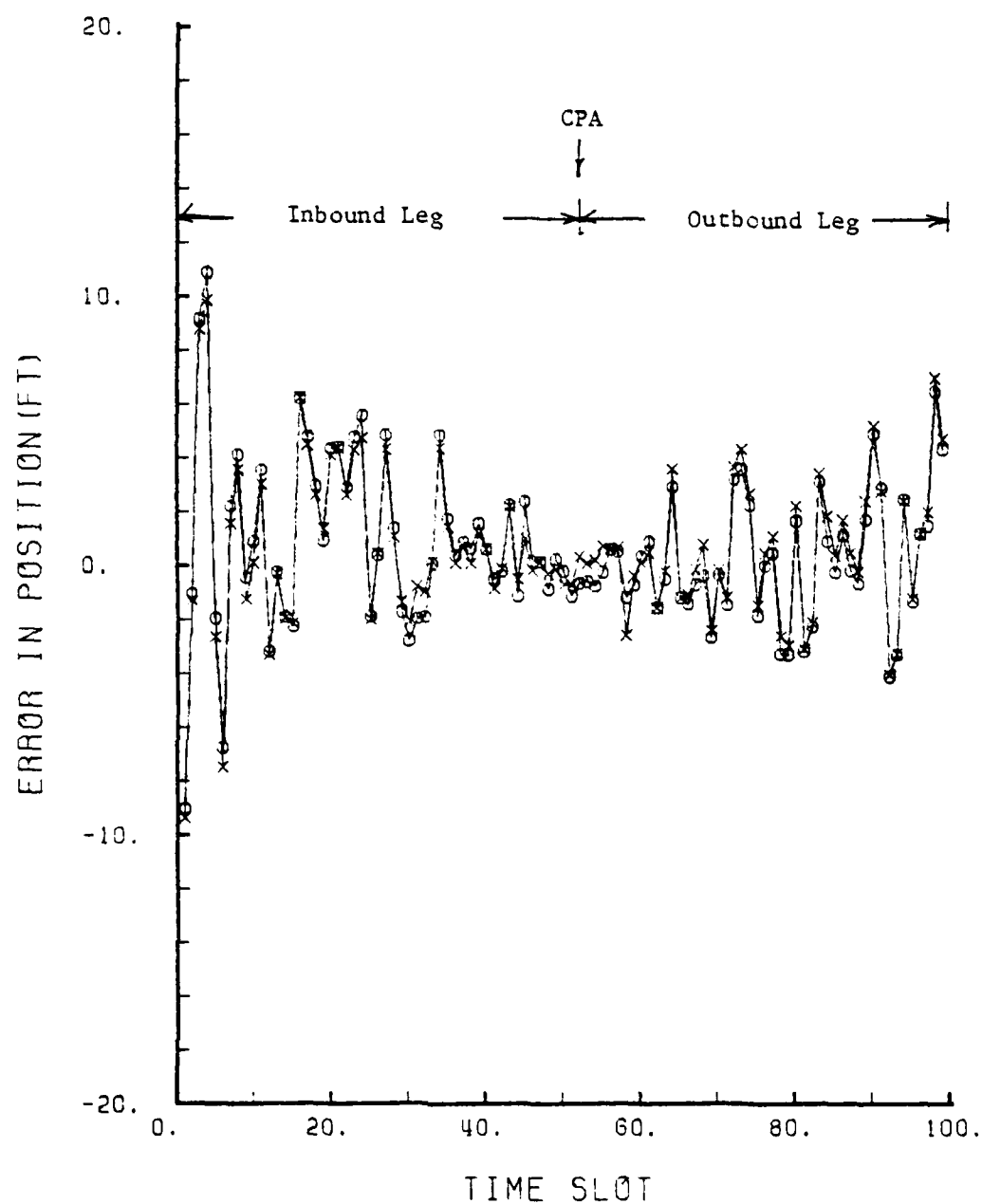


Figure 14. Error in Torpedo Position During a Straight Run in the Area of a Single Array

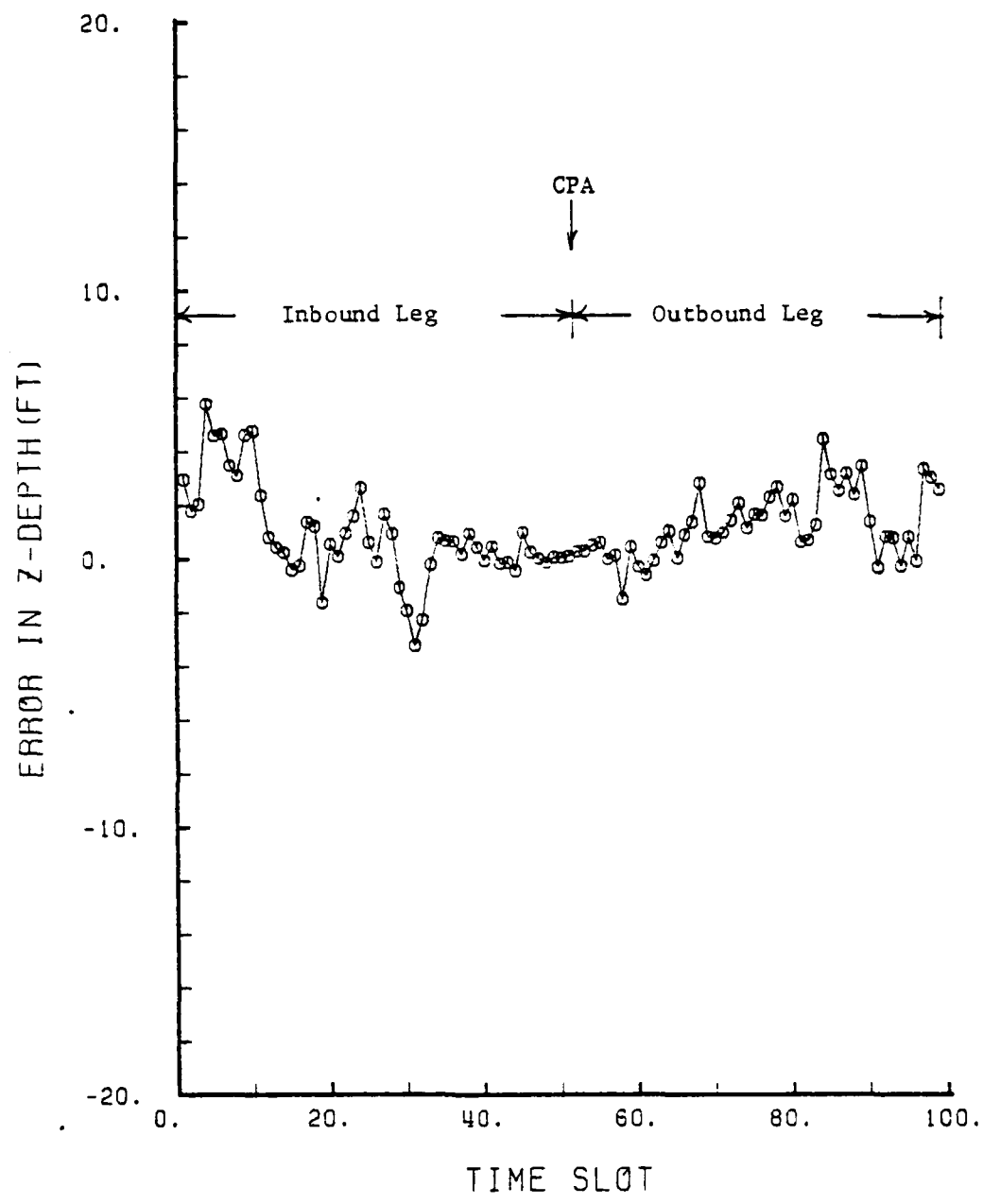


Figure 15. Error in Torpedo Depth During a Straight Run in the Area of a Single Array

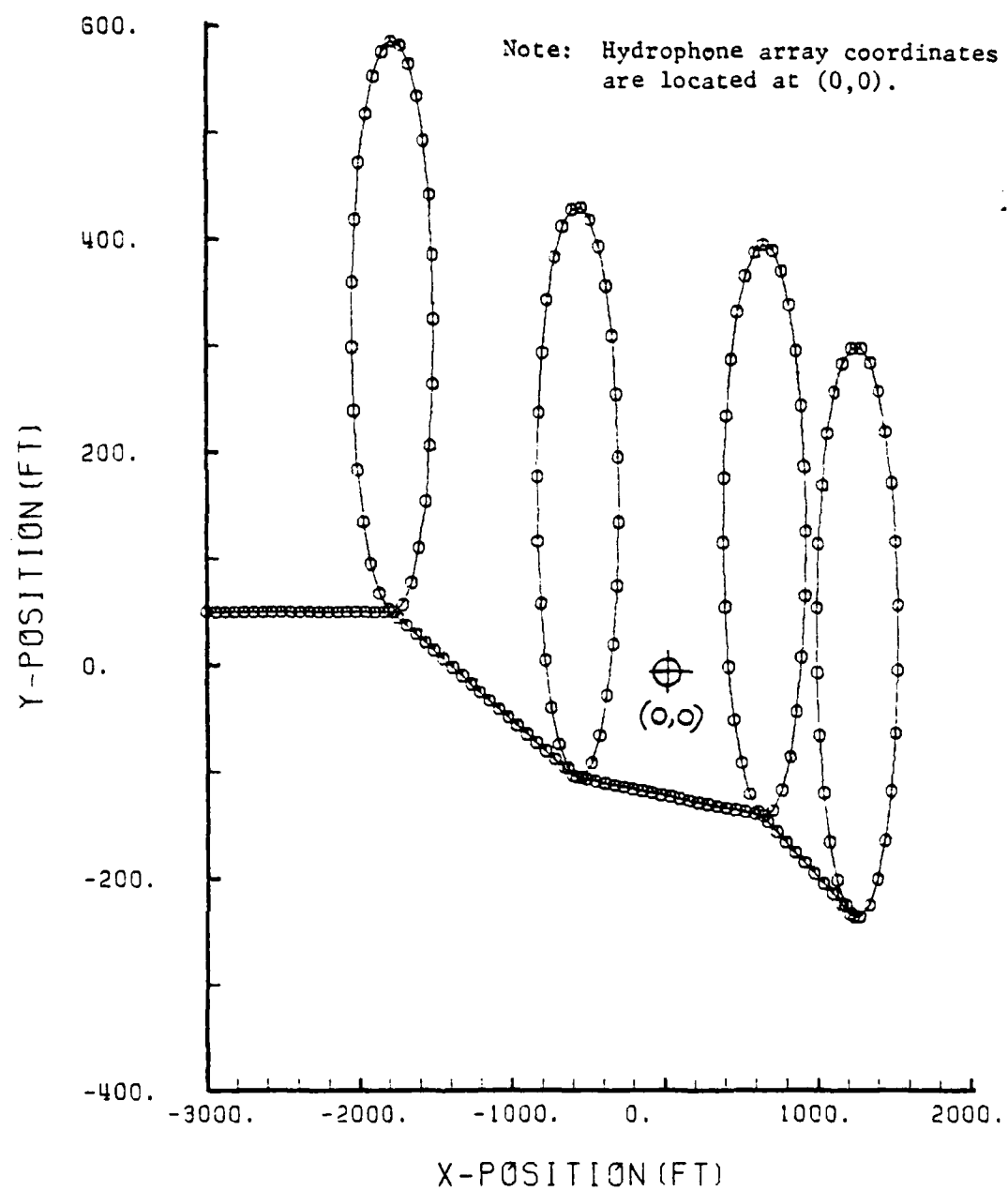


Figure 16. True Trajectory of the Torpedo in the Area of a Single Array

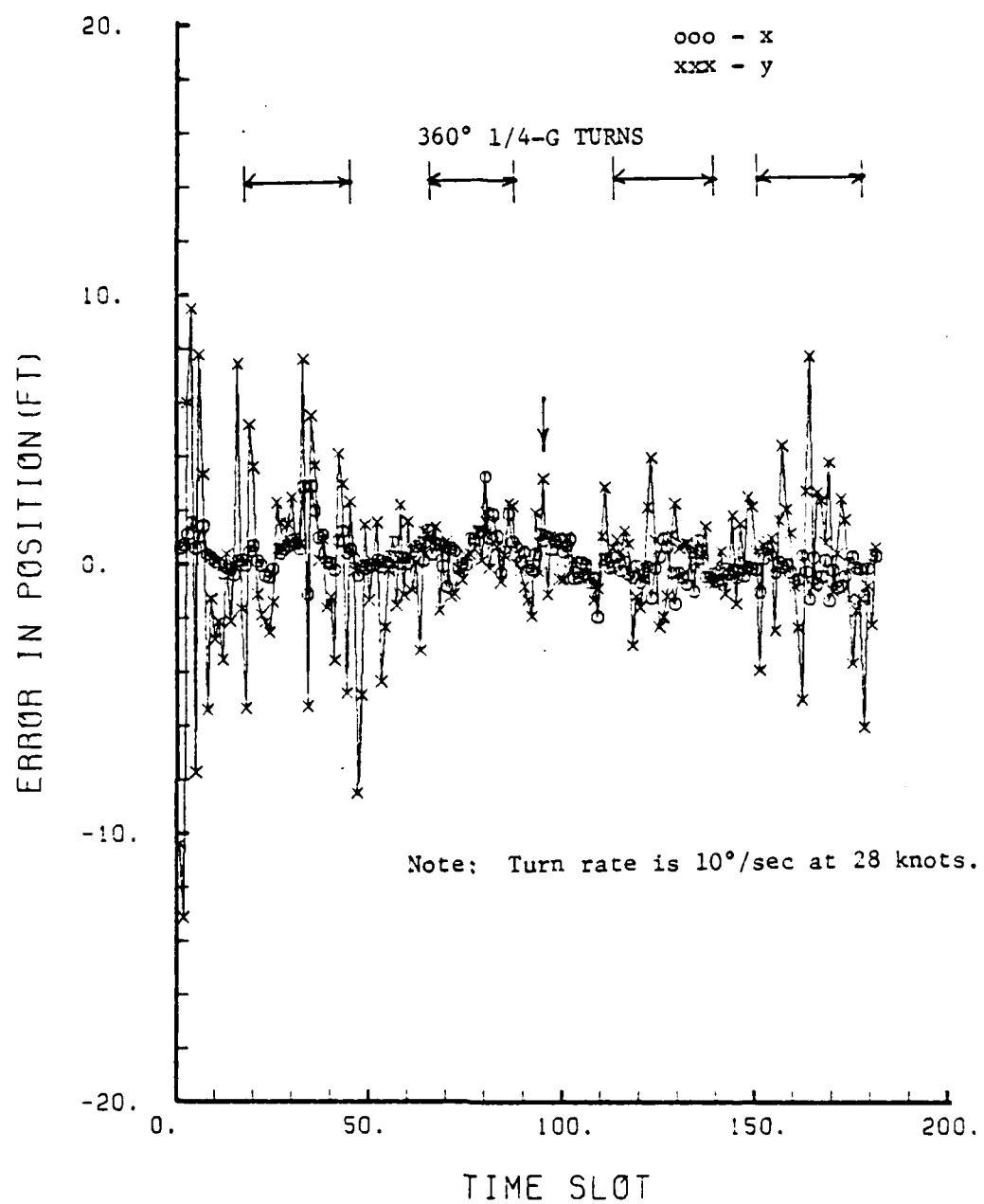


Figure 17. Error in Torpedo Position During a Maneuvering Run in the Area of a Single Array

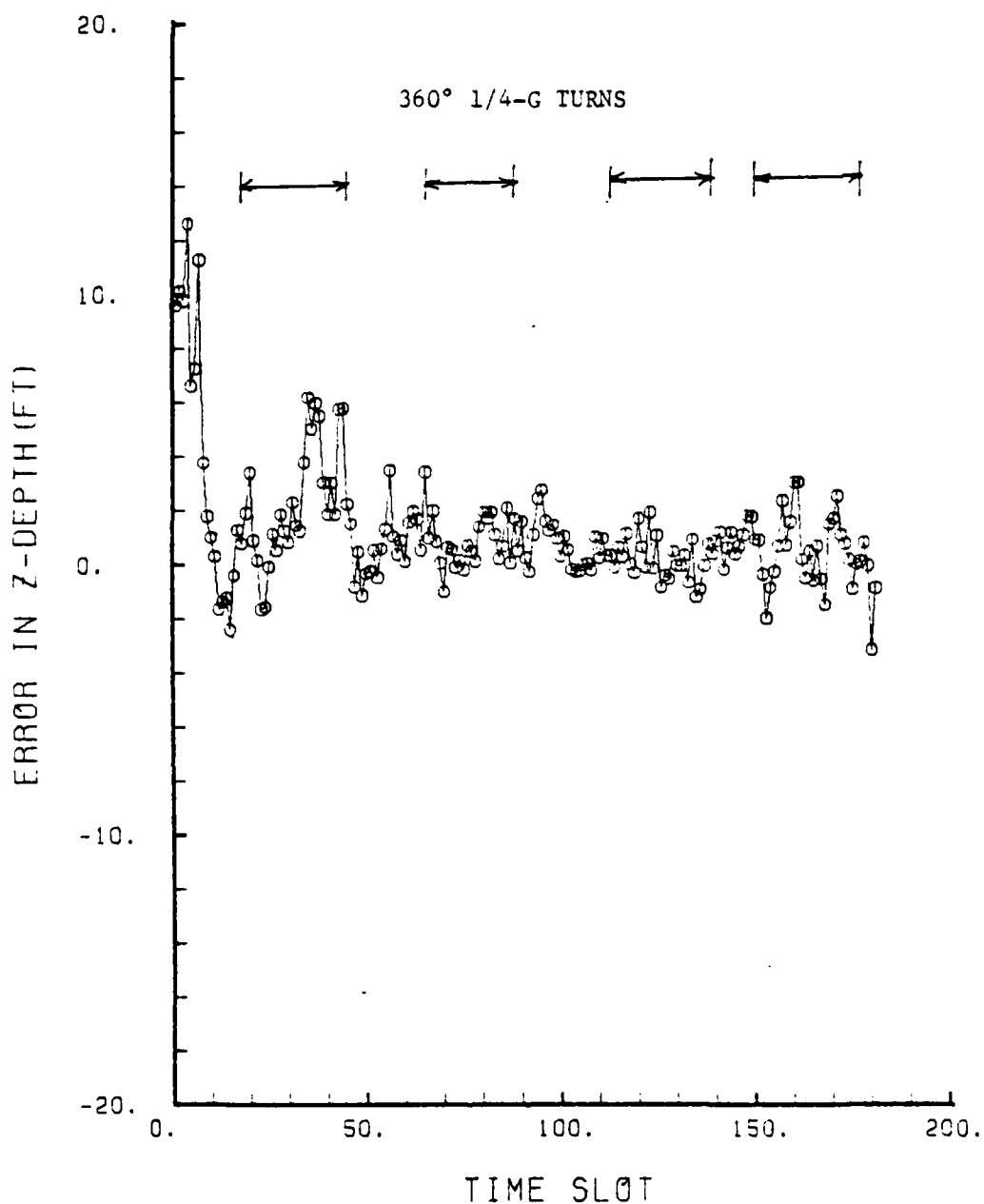


Figure 18. Error in Torpedo Depth During a Maneuvering Run in the Area of a Single Array

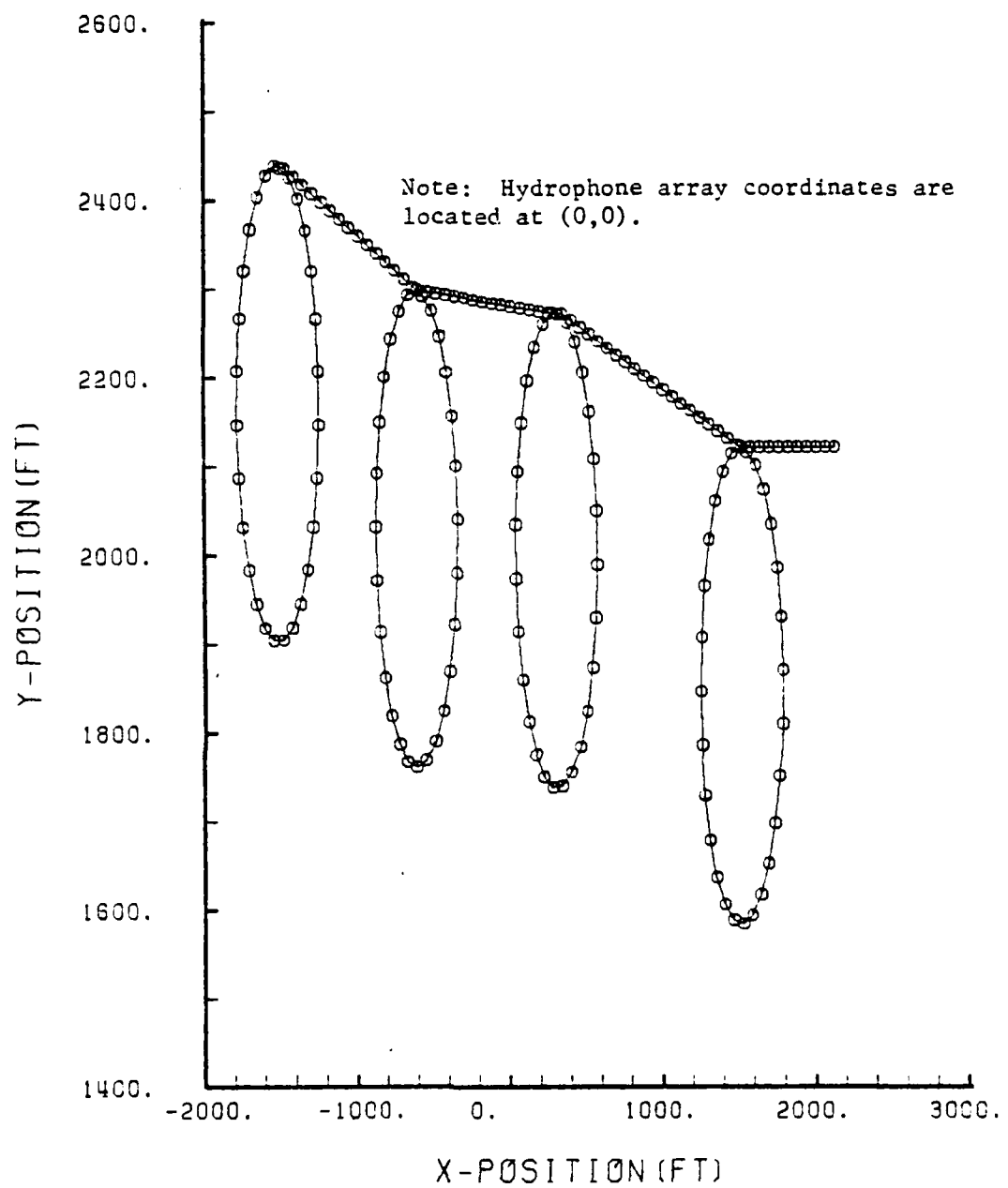


Figure 19. True Trajectory of the Torpedo During a Maneuvering Run in the Area of a Single Array

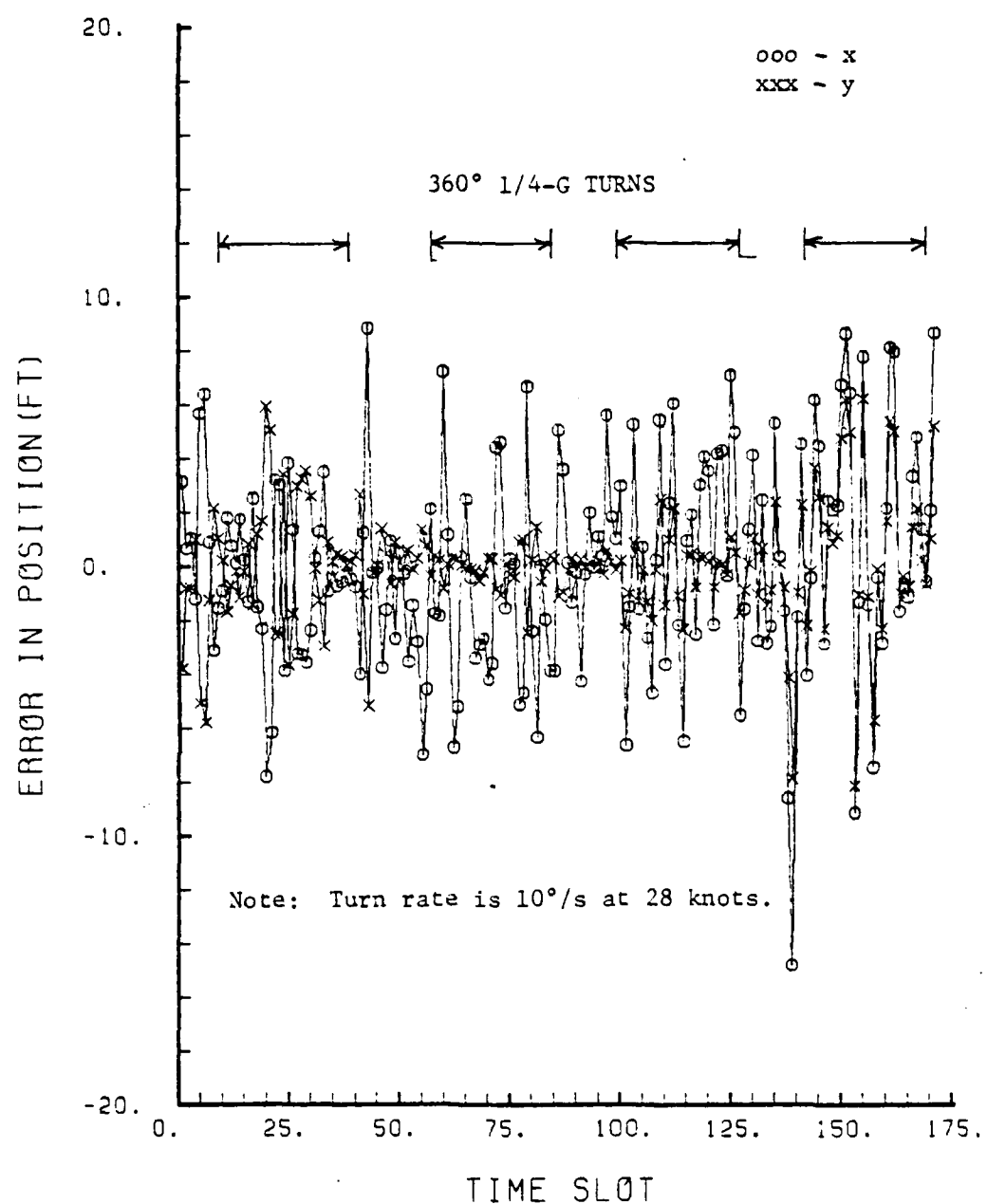


Figure 20. Error in Torpedo Position During a Maneuvering Run in the Area of a Single Array

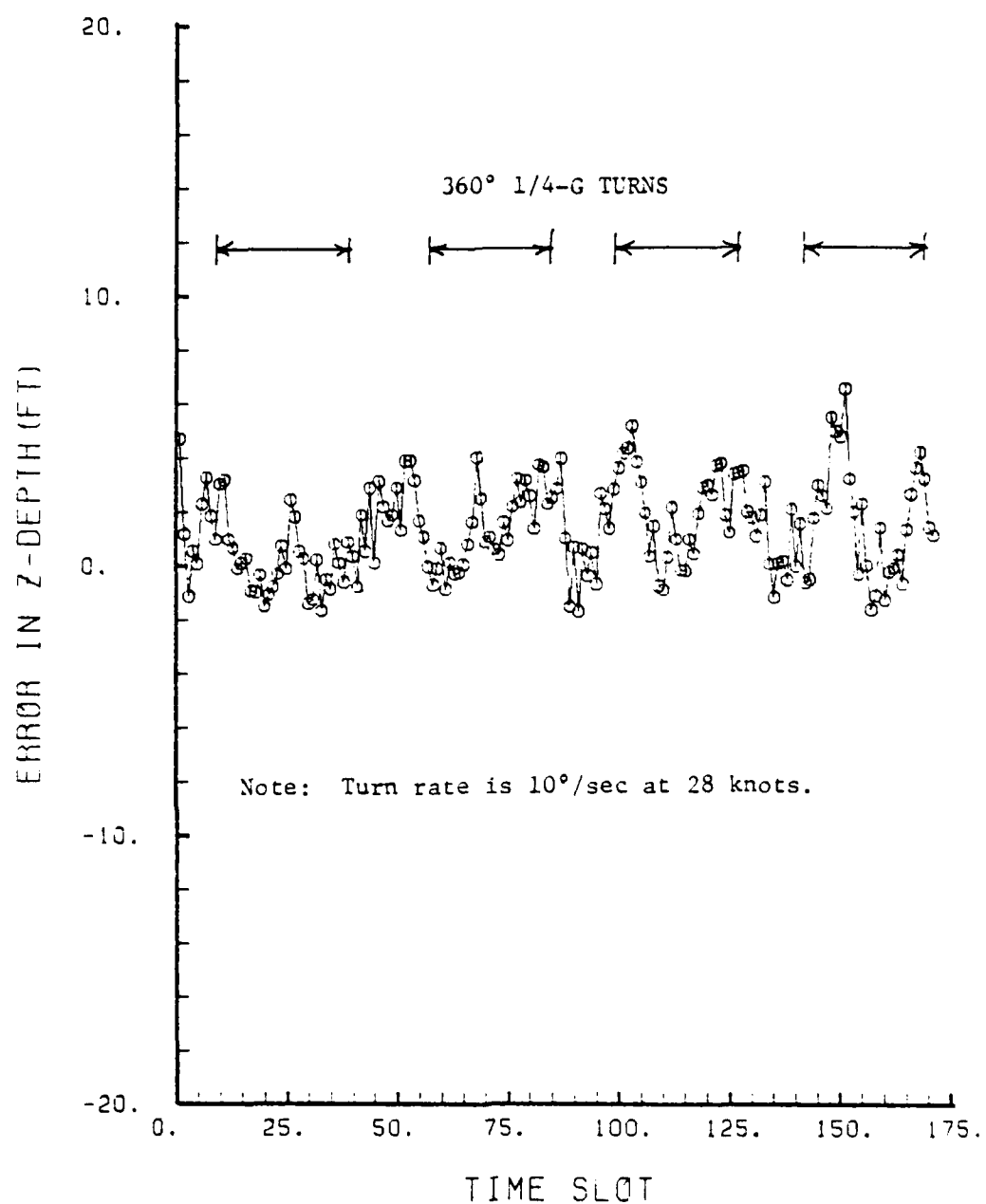


Figure 21. Error in Torpedo Depth During a Maneuvering Run in the Area of a Single Array

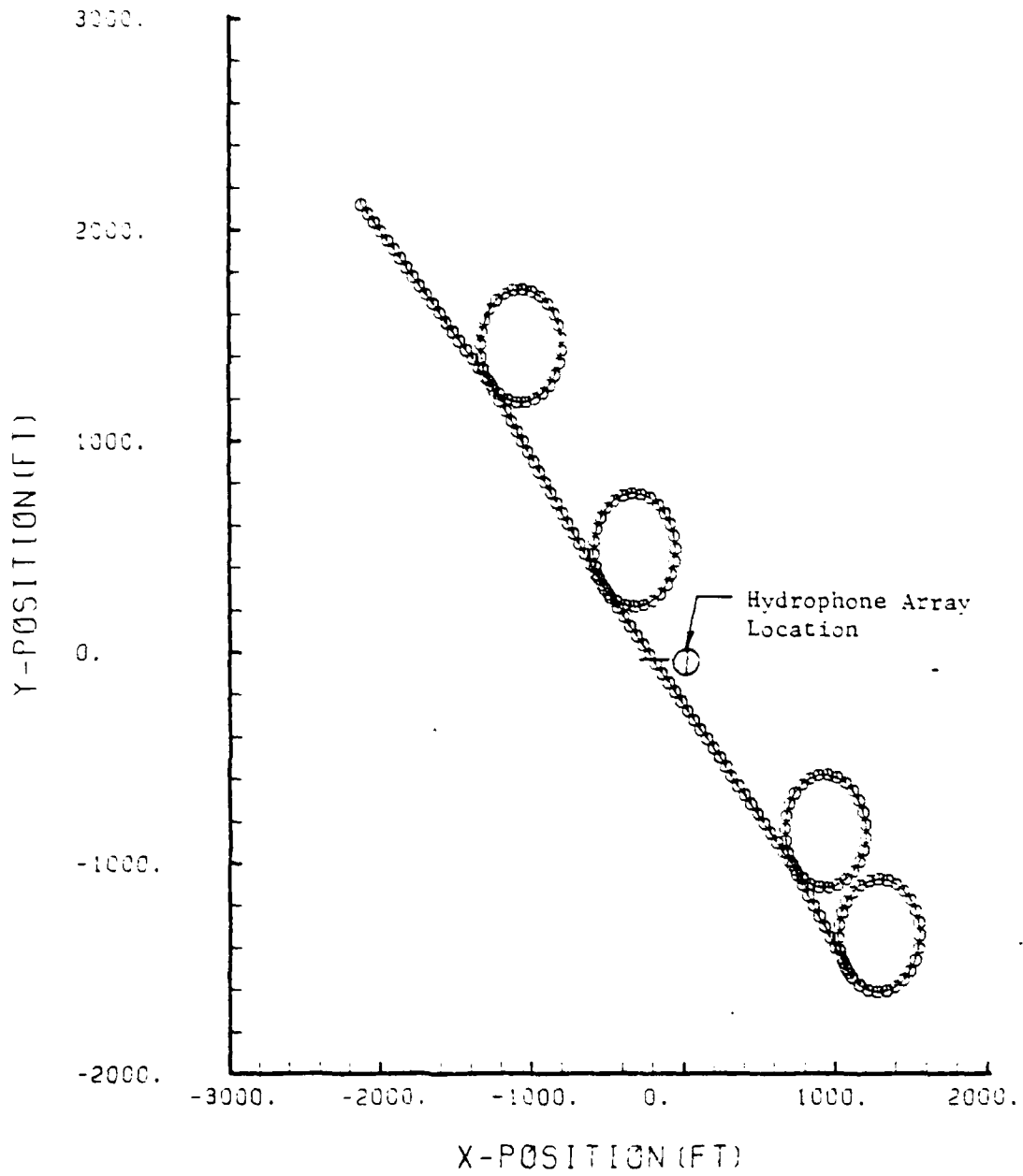


Figure 22. True Trajectory of the Torpedo During a Maneuvering Run in the Area of A Single Array

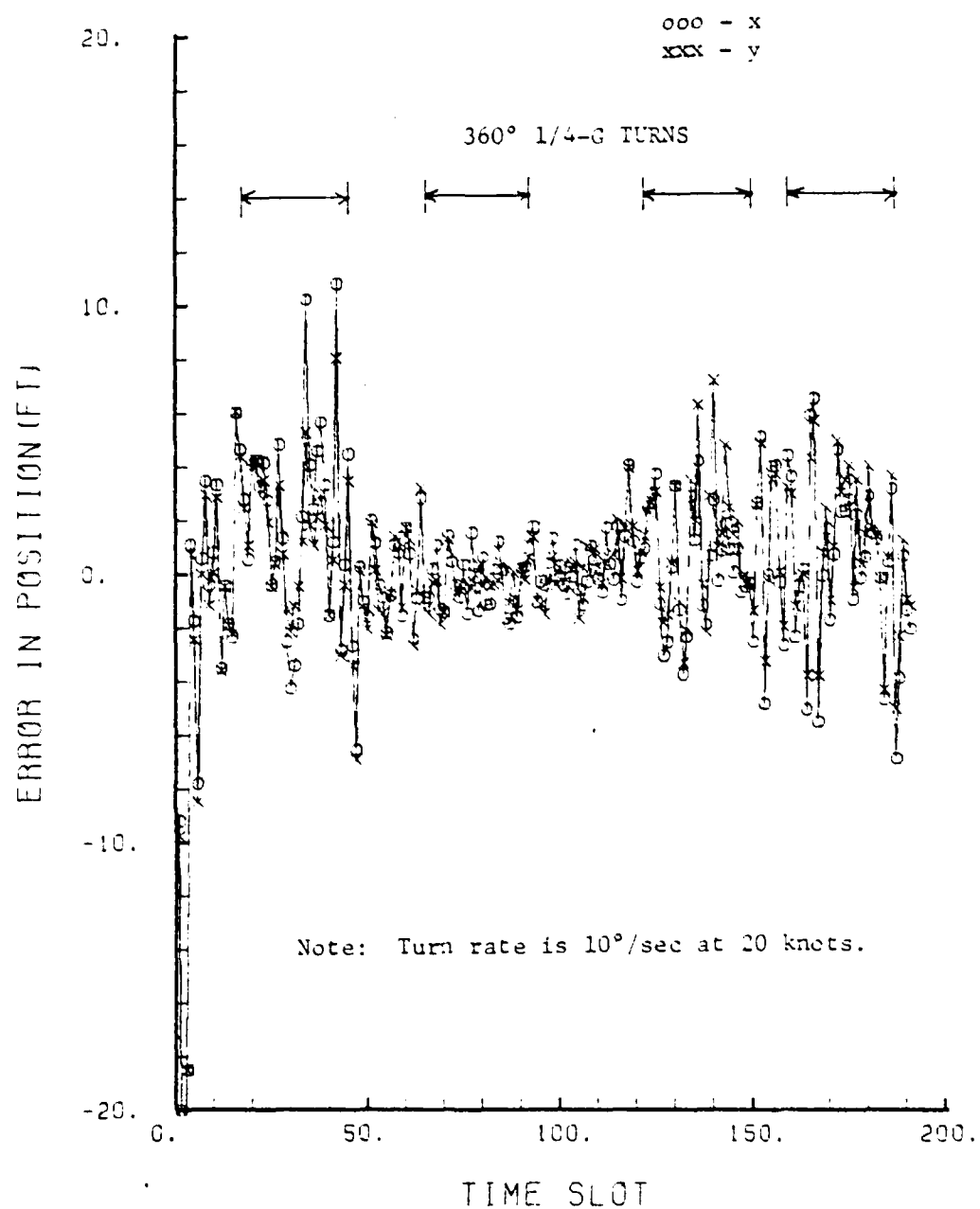


Figure 23. Error in Torpedo Position During a Maneuvering Run in the Area of a Single Array

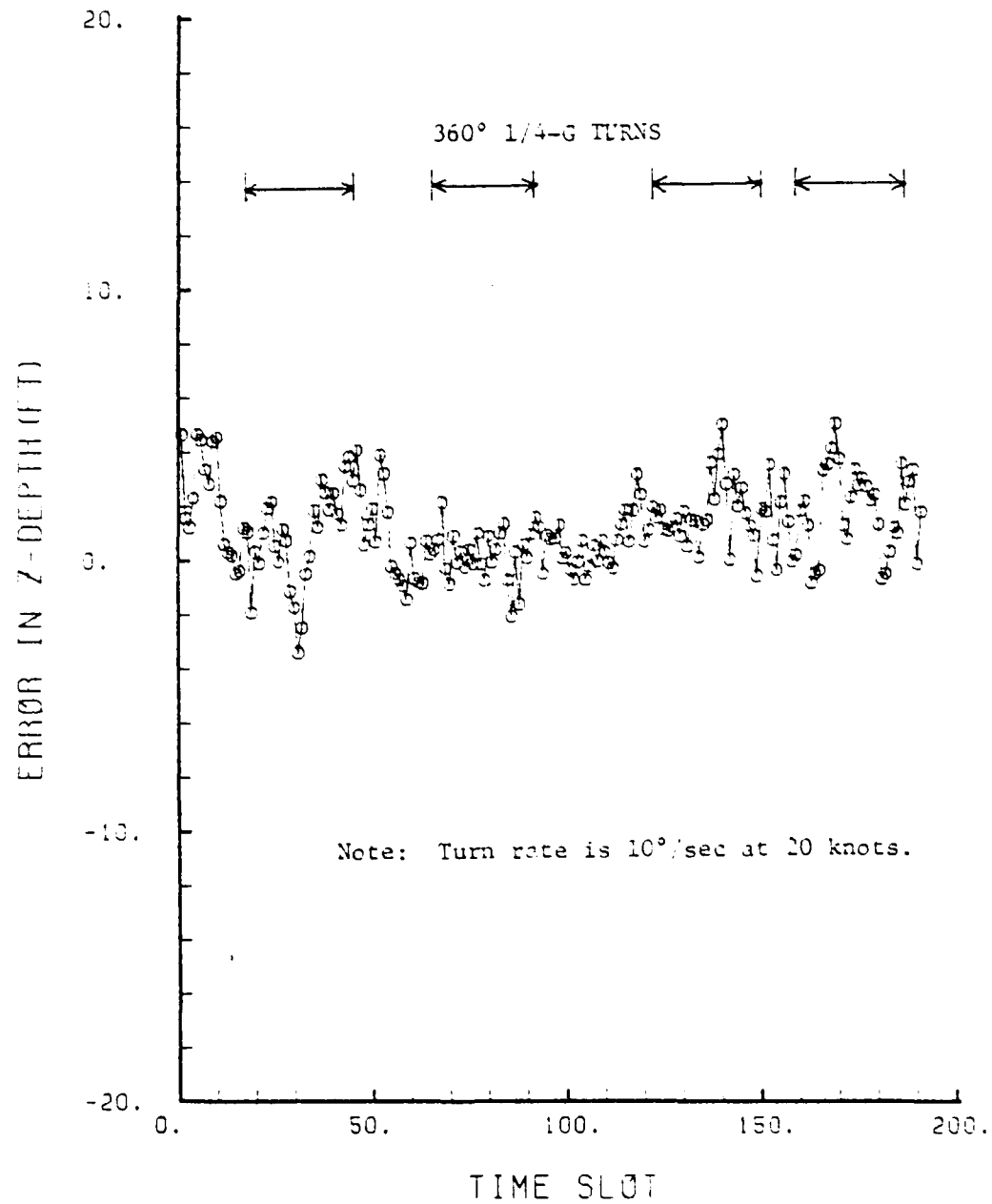


Figure 24. Error in Torpedo Depth During a Maneuvering Run in the Area of a Single Array

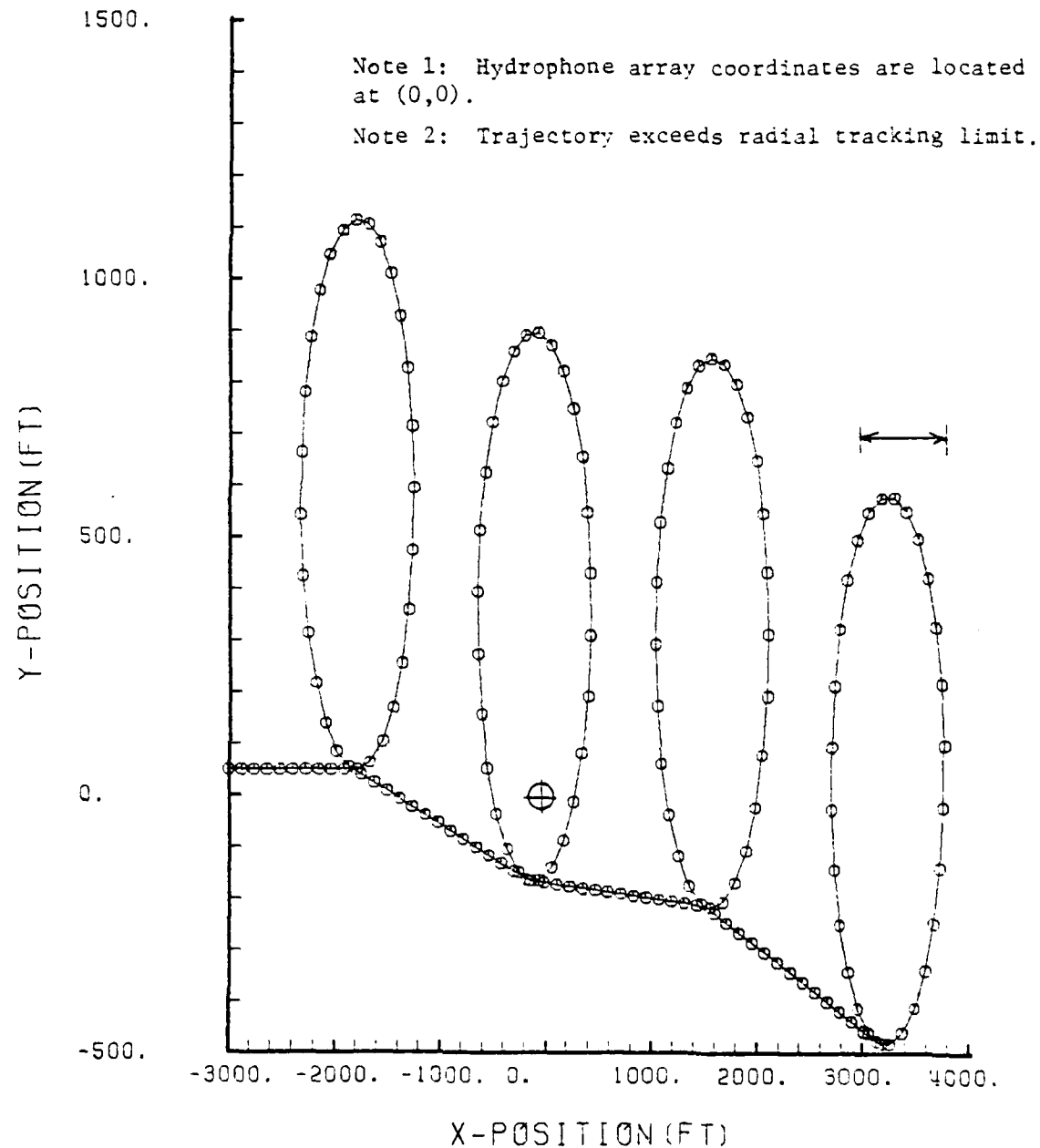


Figure 25. True Trajectory of the Torpedo During a Maneuvering Run in the Area of a Single Array

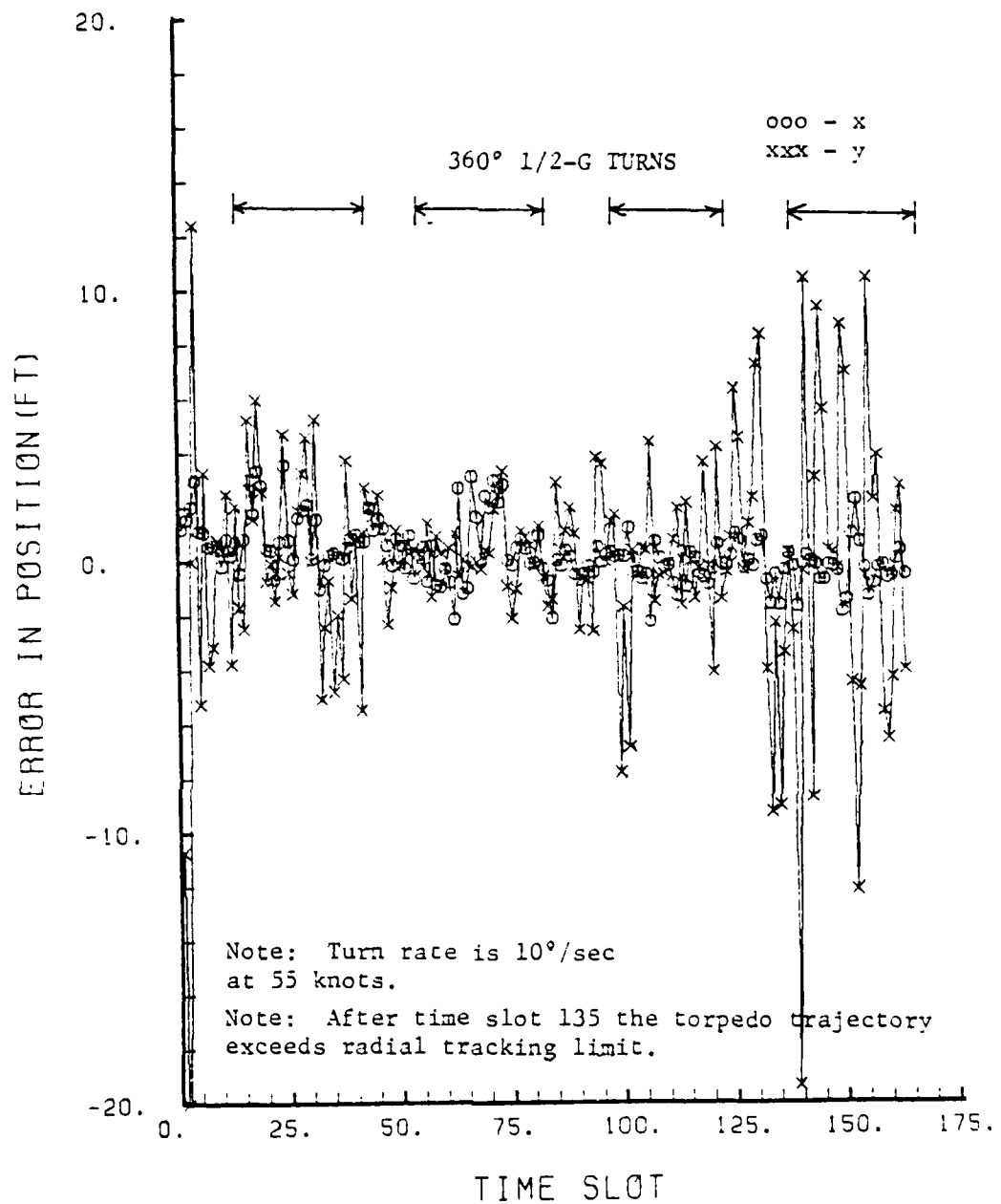


Figure 26. Error in Torpedo Position During a Maneuvering Run in the Area of a Single Array

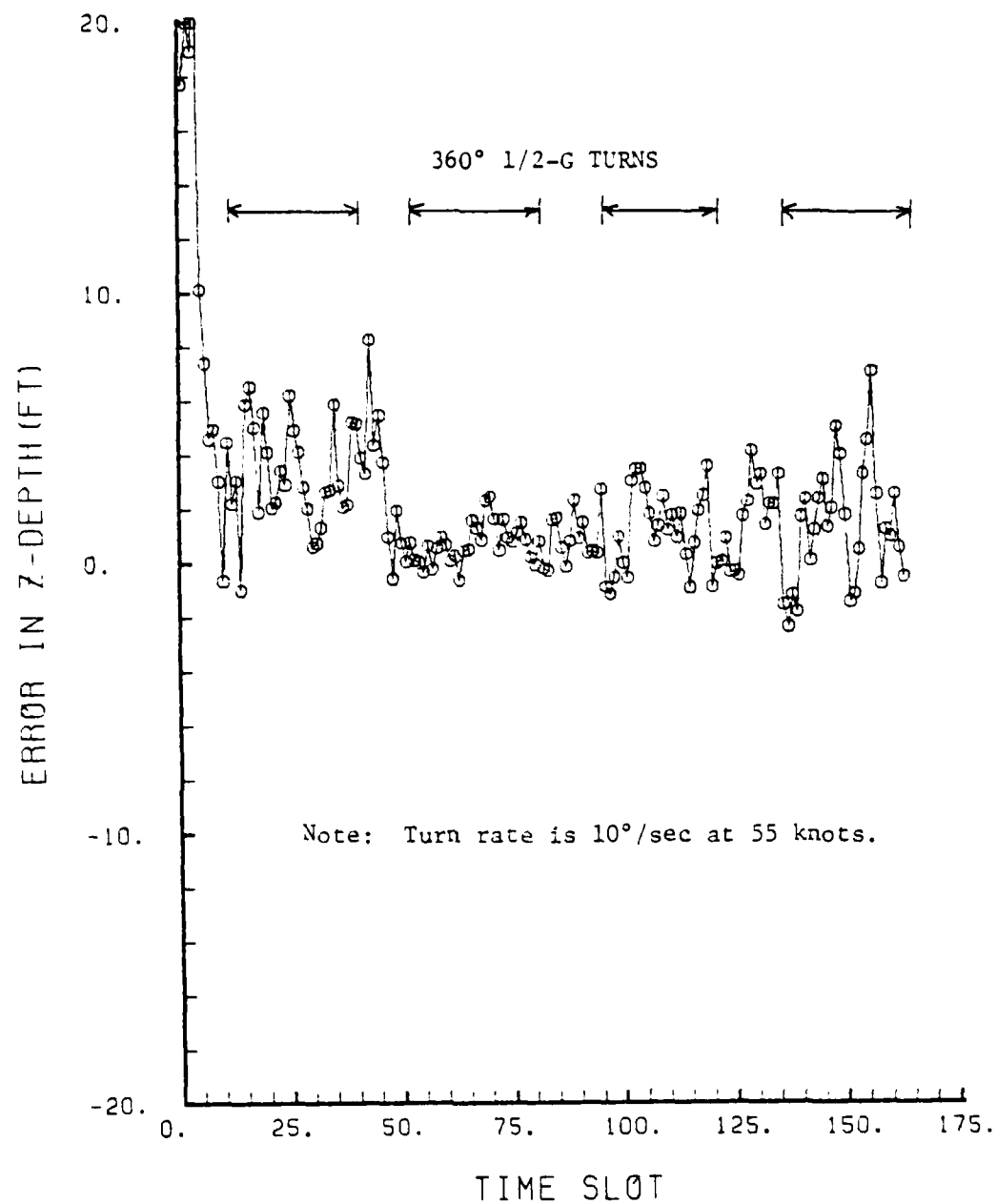


Figure 27. Error in Torpedo Depth During a Maneuvering Run in the Area of a Single Array

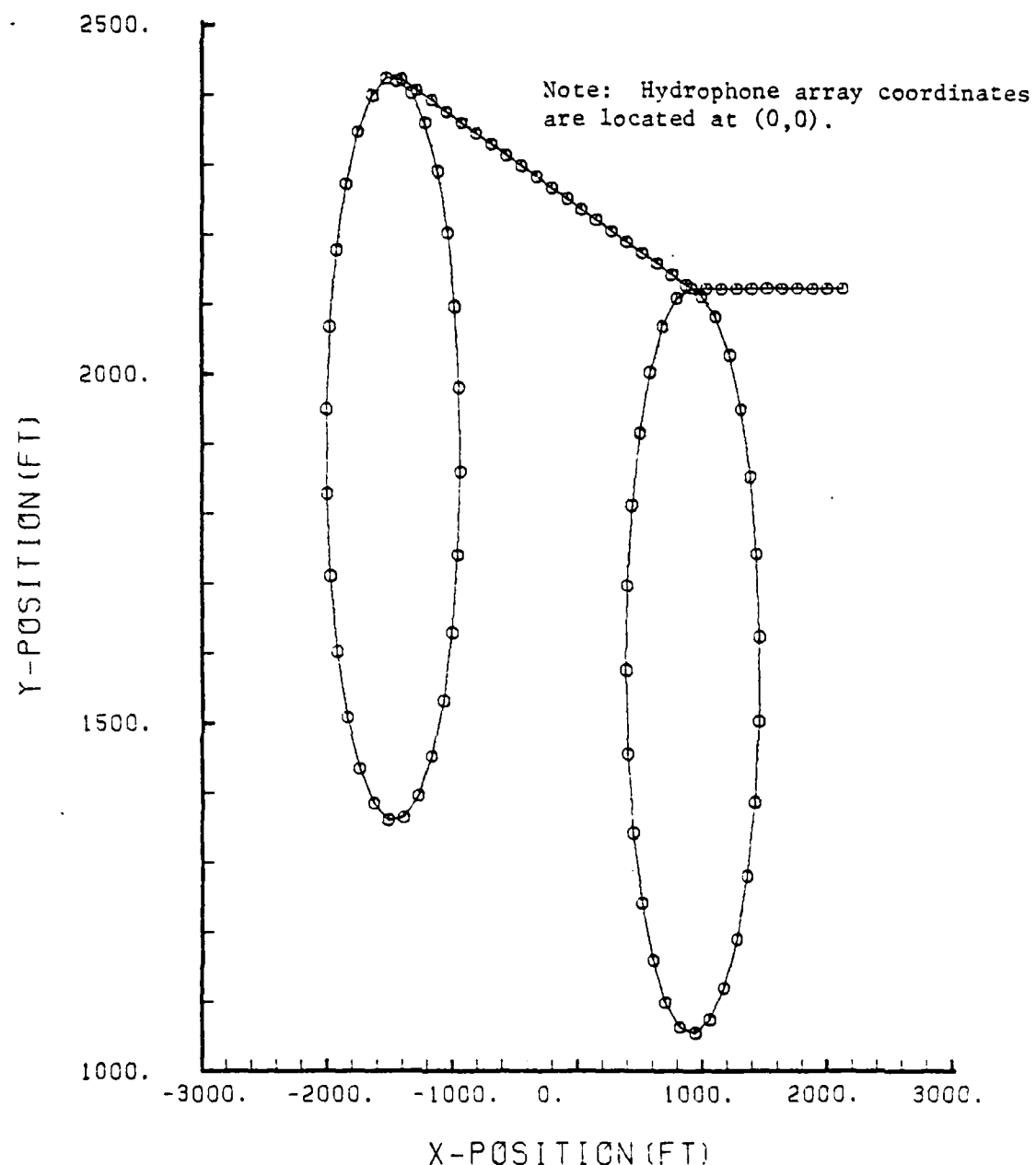


Figure 28. True Trajectory of the Torpedo During a Maneuvering Run in the Area of a Single Array

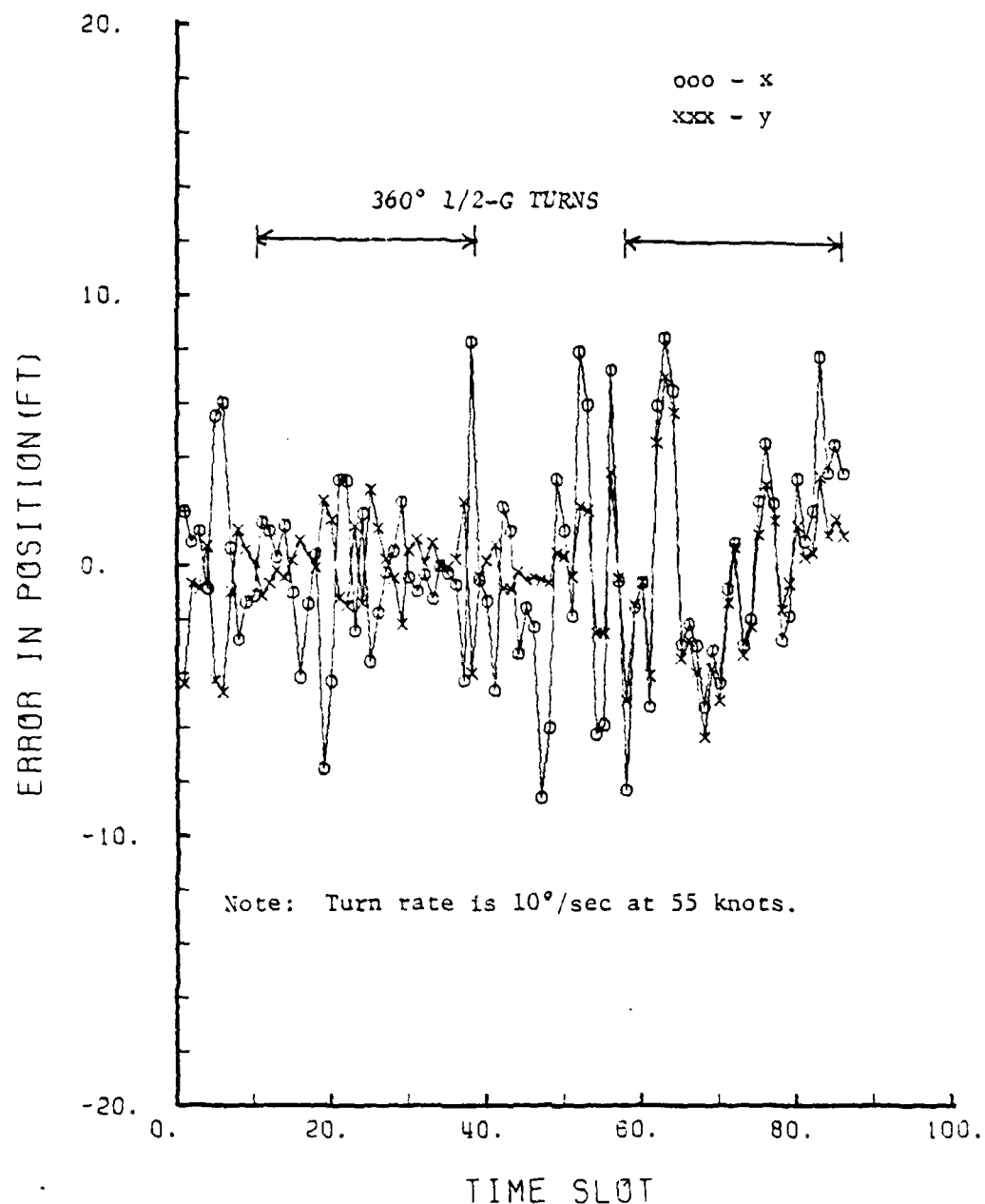


Figure 29. Error in Torpedo Position During a Maneuvering Run in the Area of a Single Array

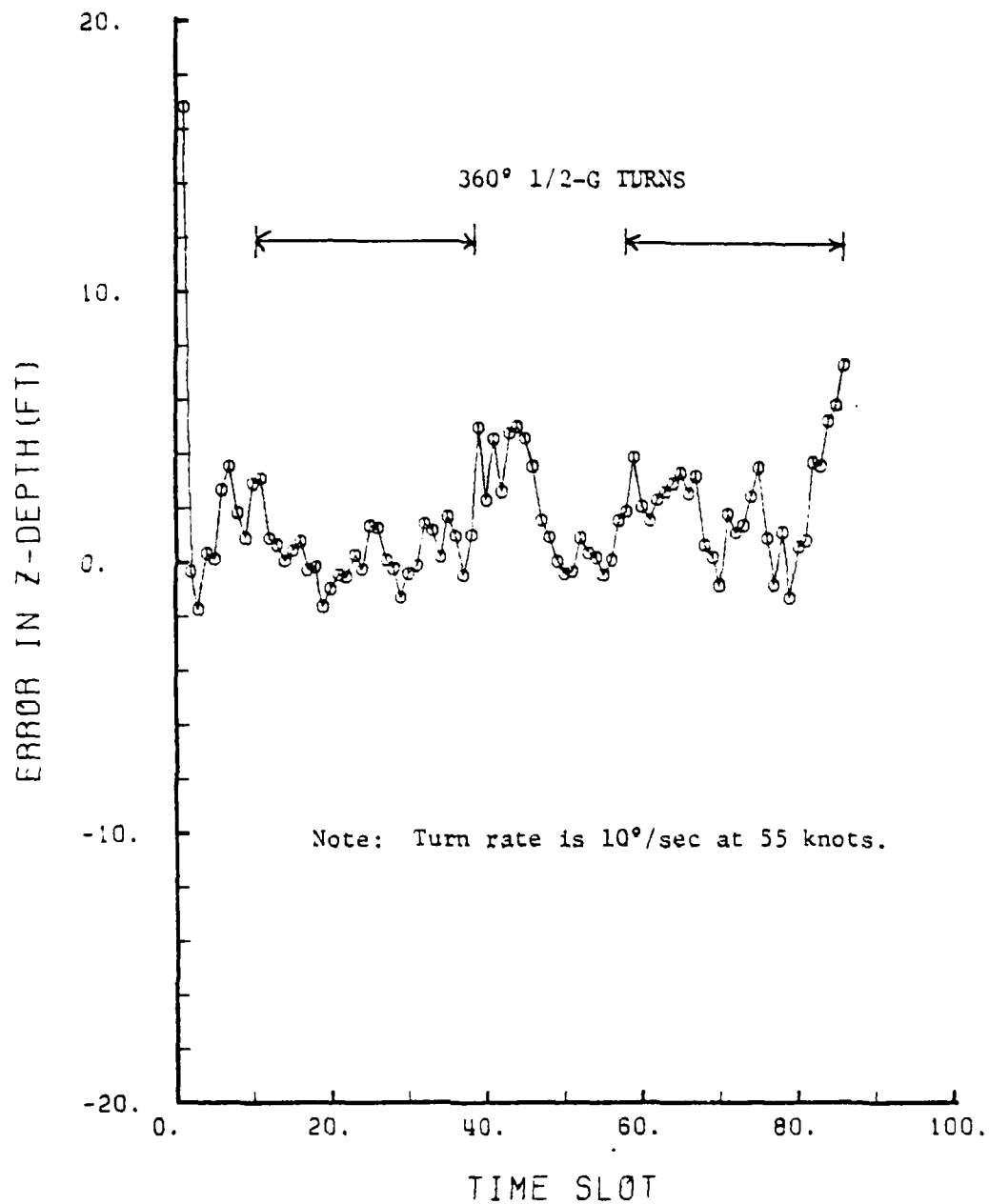


Figure 30. Error in Torpedo Depth During a Maneuvering Run in the Area of a Single Array

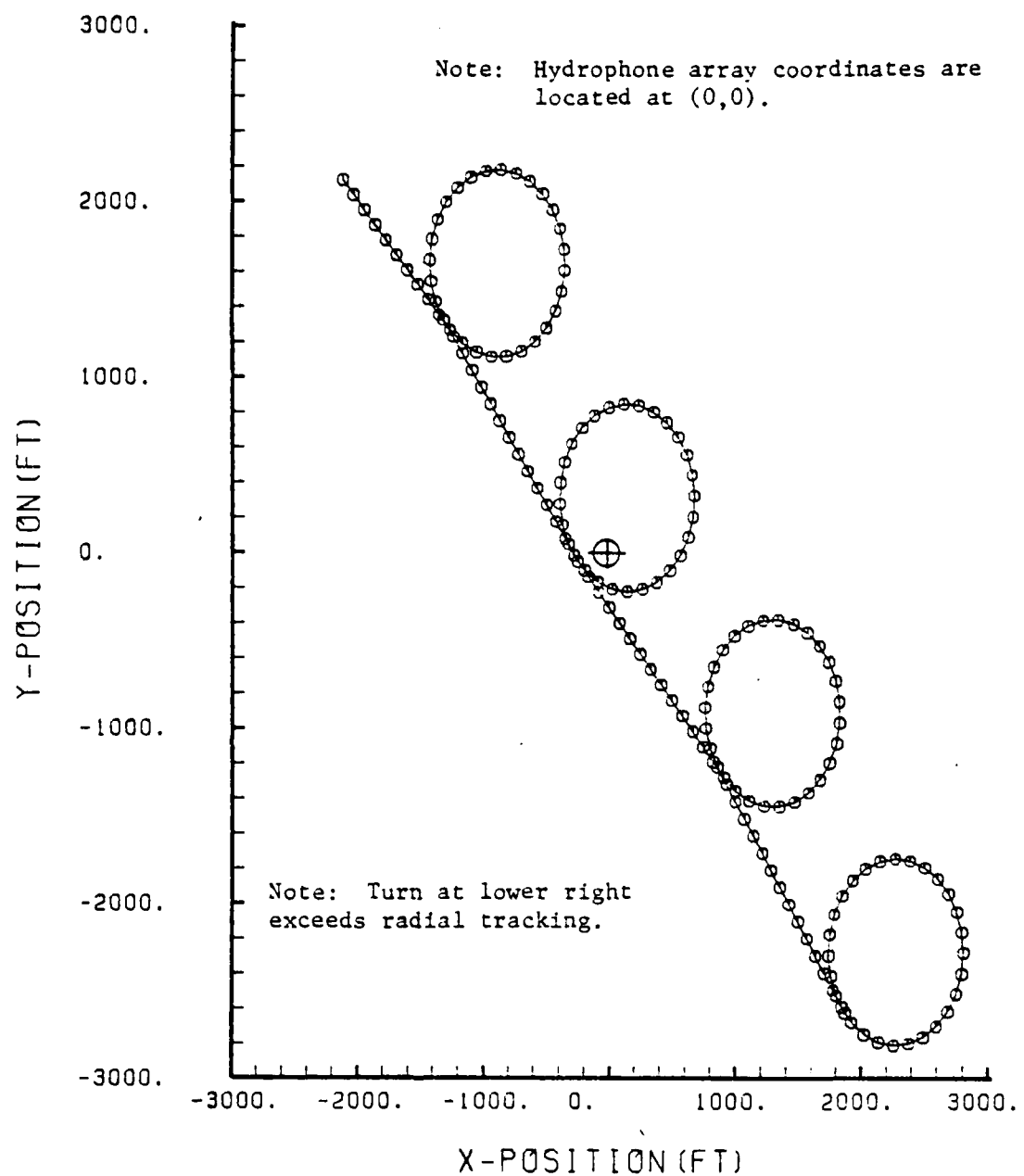


Figure 31. True Trajectory of the Torpedo During a Maneuvering Run in the Area of a Single Array

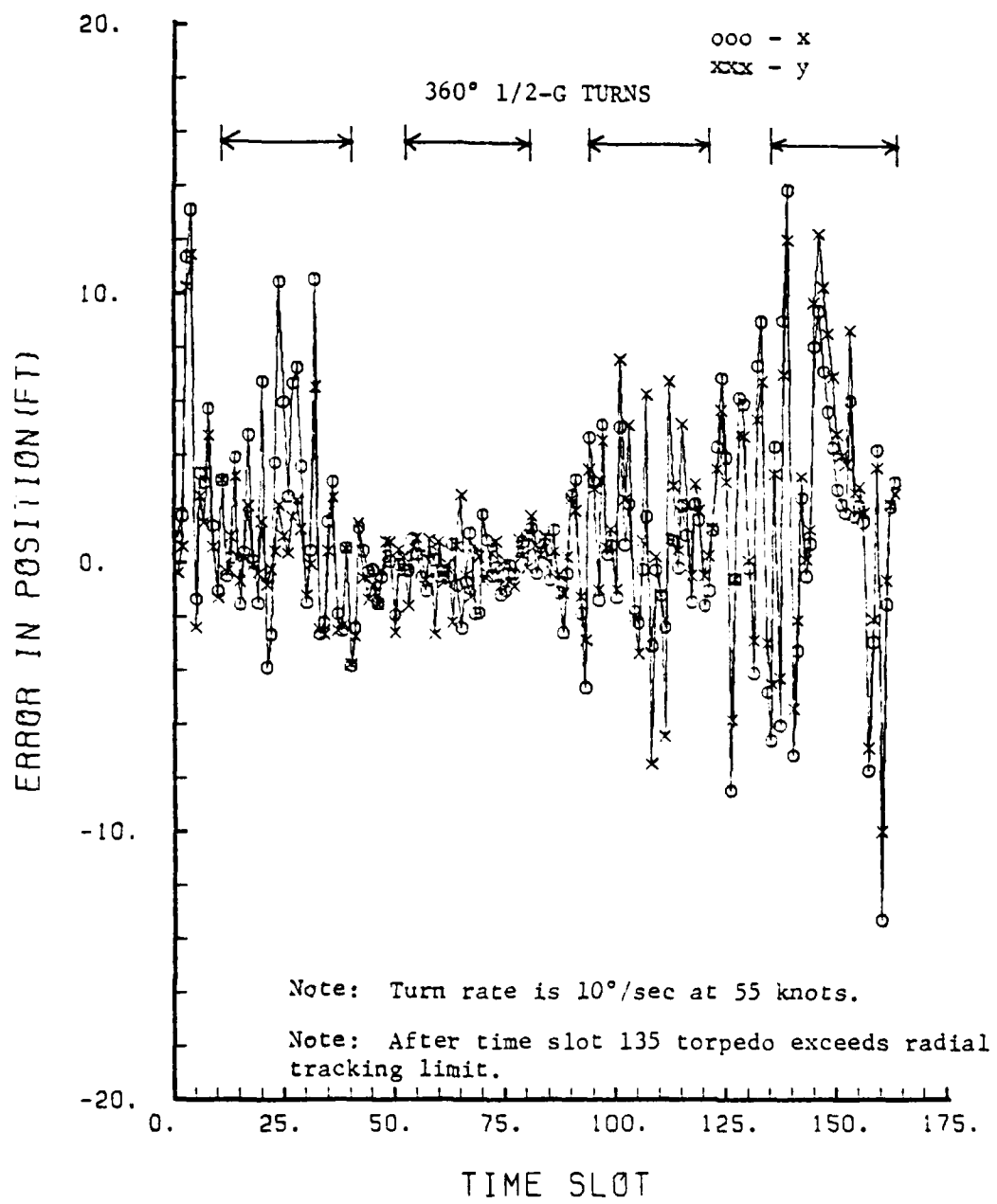


Figure 32. Error in Torpedo Position During a Maneuvering Run in the Area of a Single Array

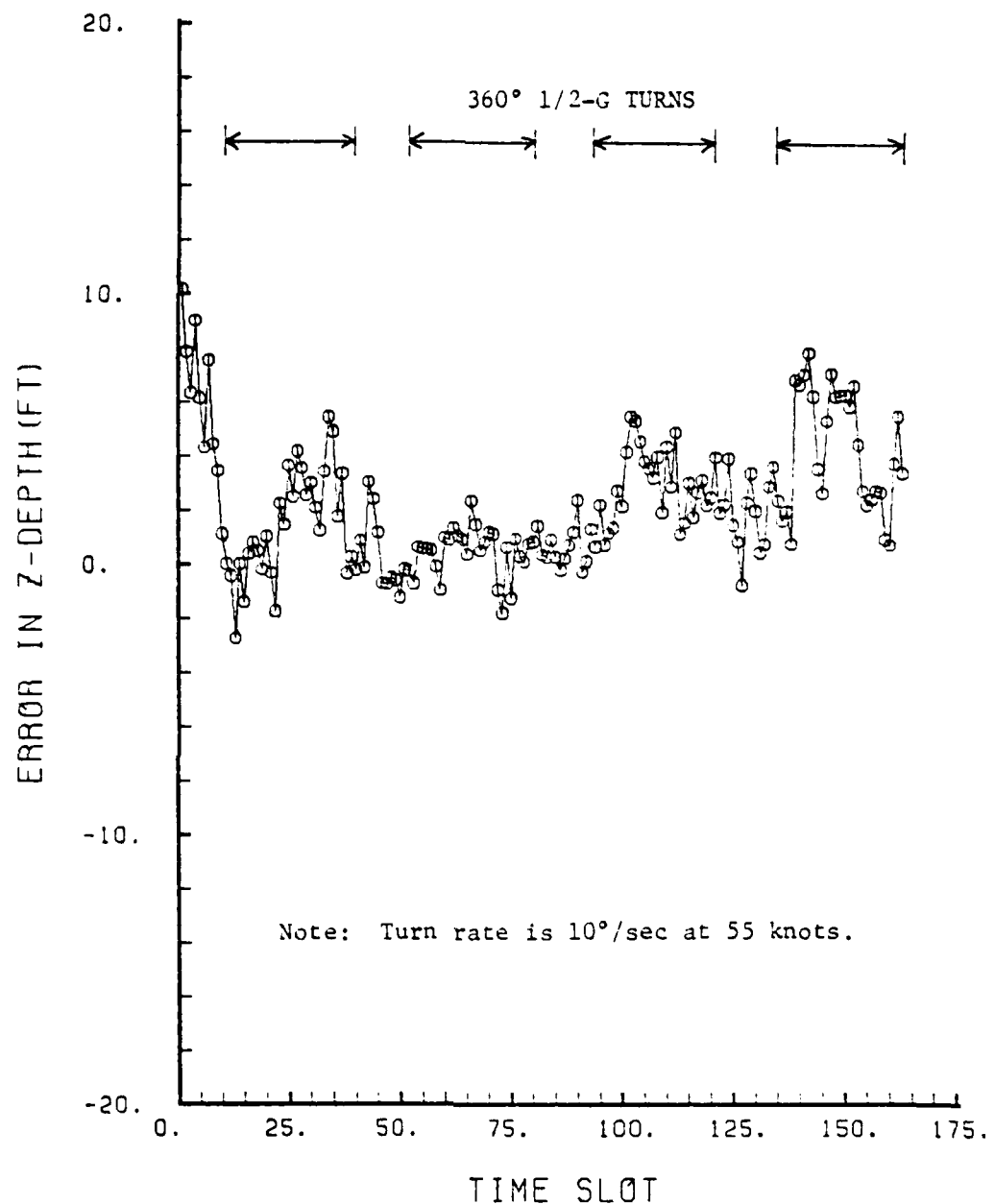


Figure 33. Error in Torpedo Position During a Maneuvering Run in the Area of a Single Array

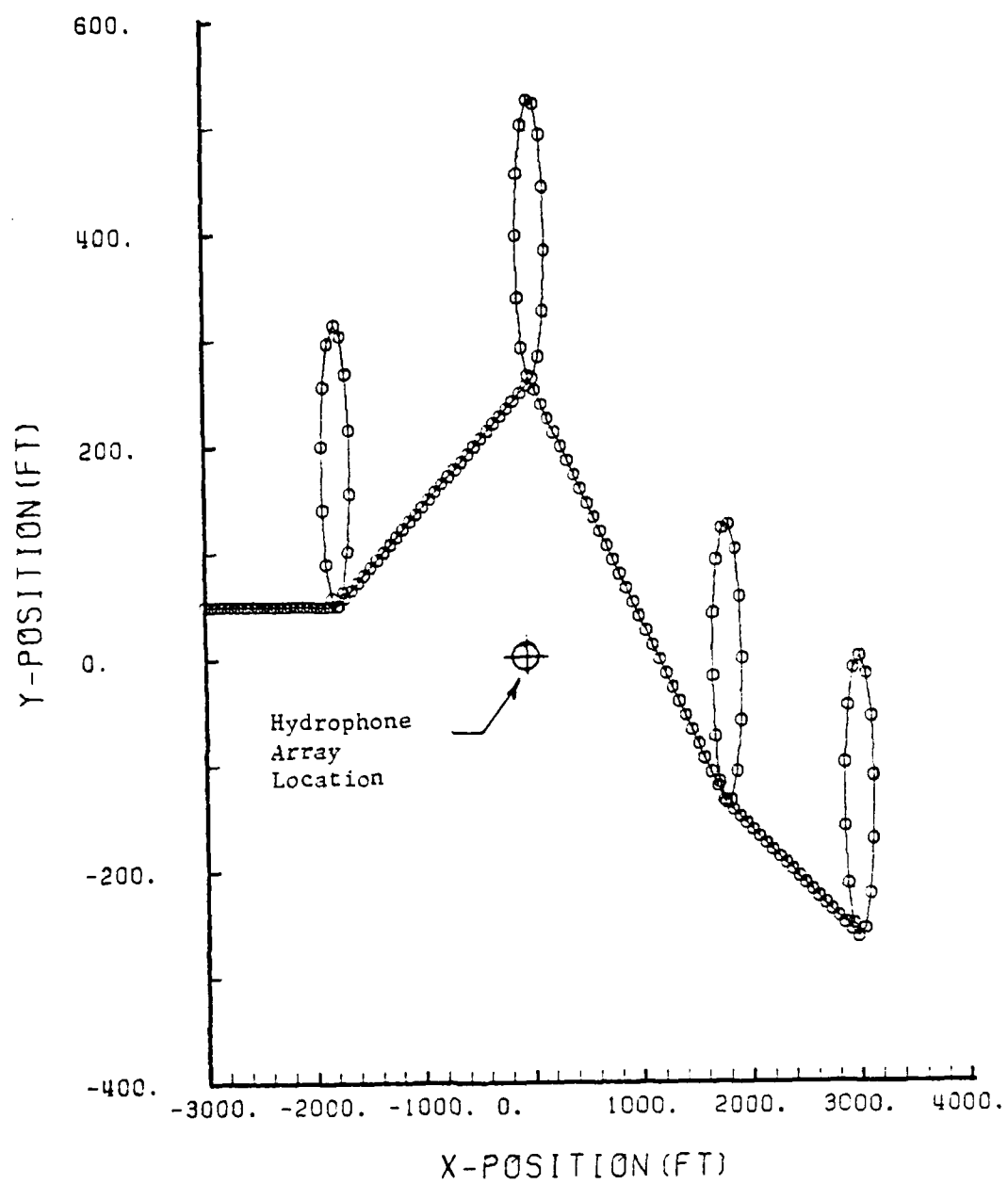


Figure 34. True Trajectory of the Torpedo During a Maneuvering Run in the Area of a Single Array

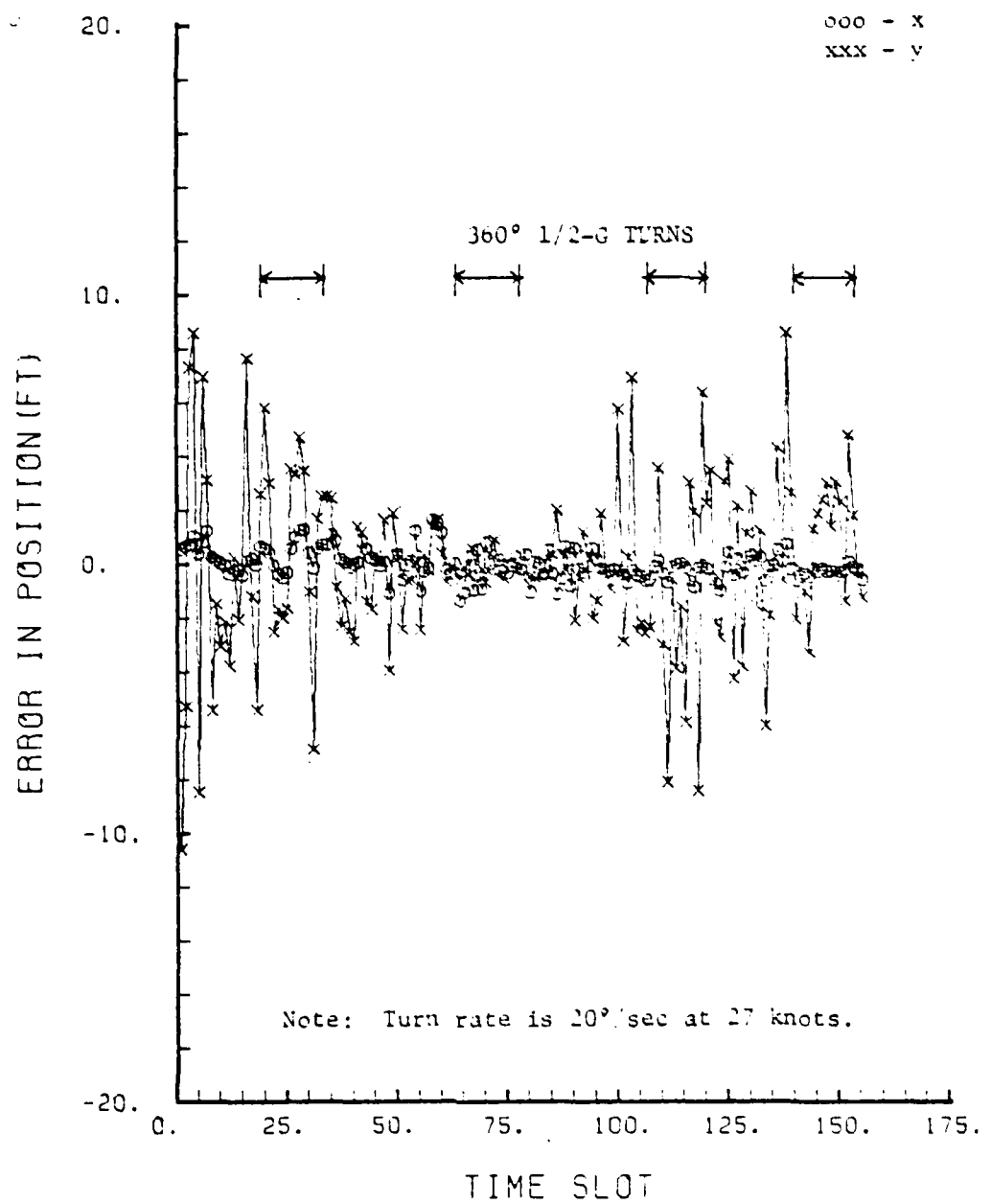


Figure 35. Error in Torpedo Position During a Maneuvering Run in the Area of a Single Array

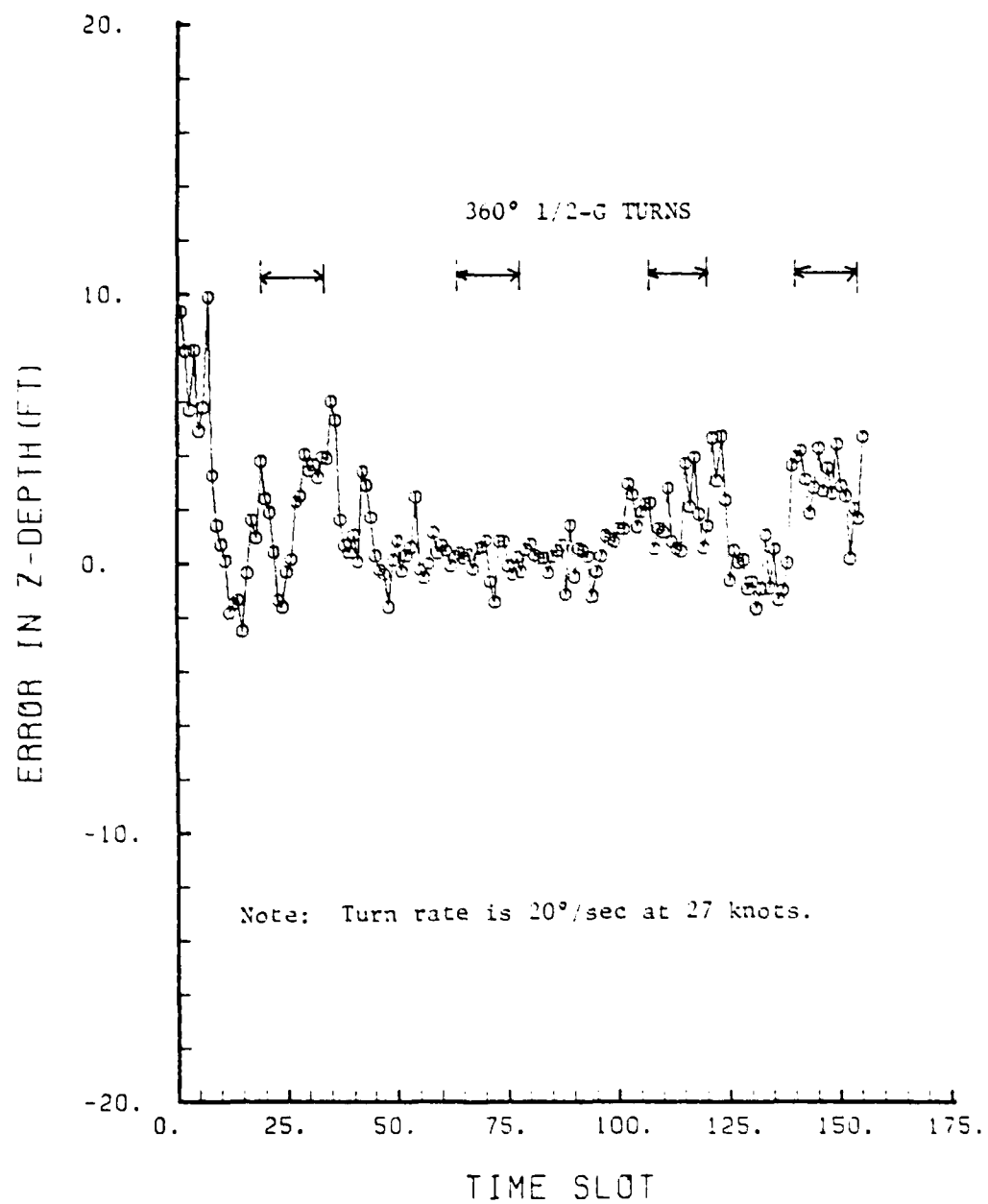


Figure 36. Error in Torpedo Depth During a Maneuvering Run in the Area of a Single Array

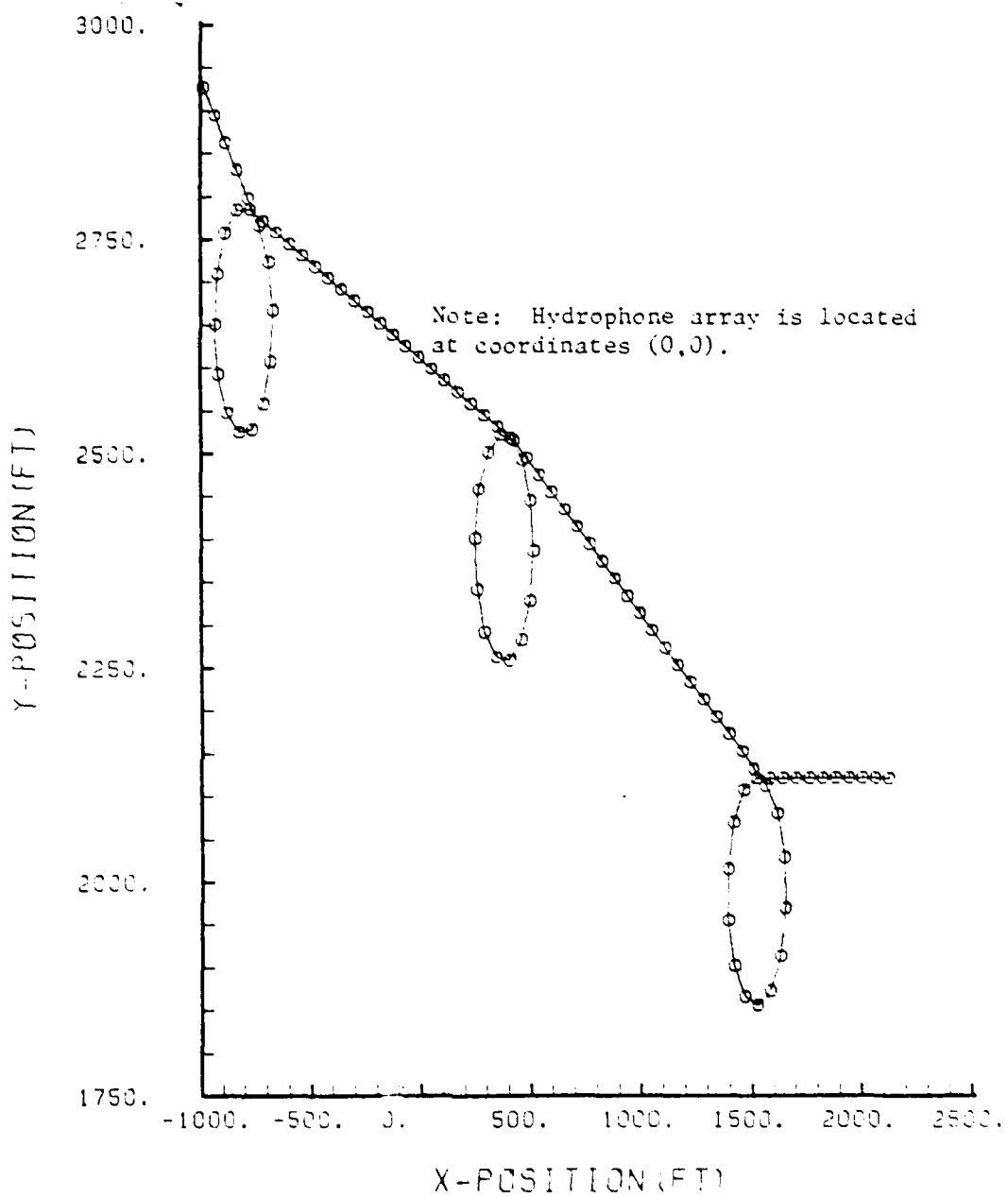


Figure 37. True Trajectory of the Torpedo During a Maneuvering Run in the Area of a Single Array

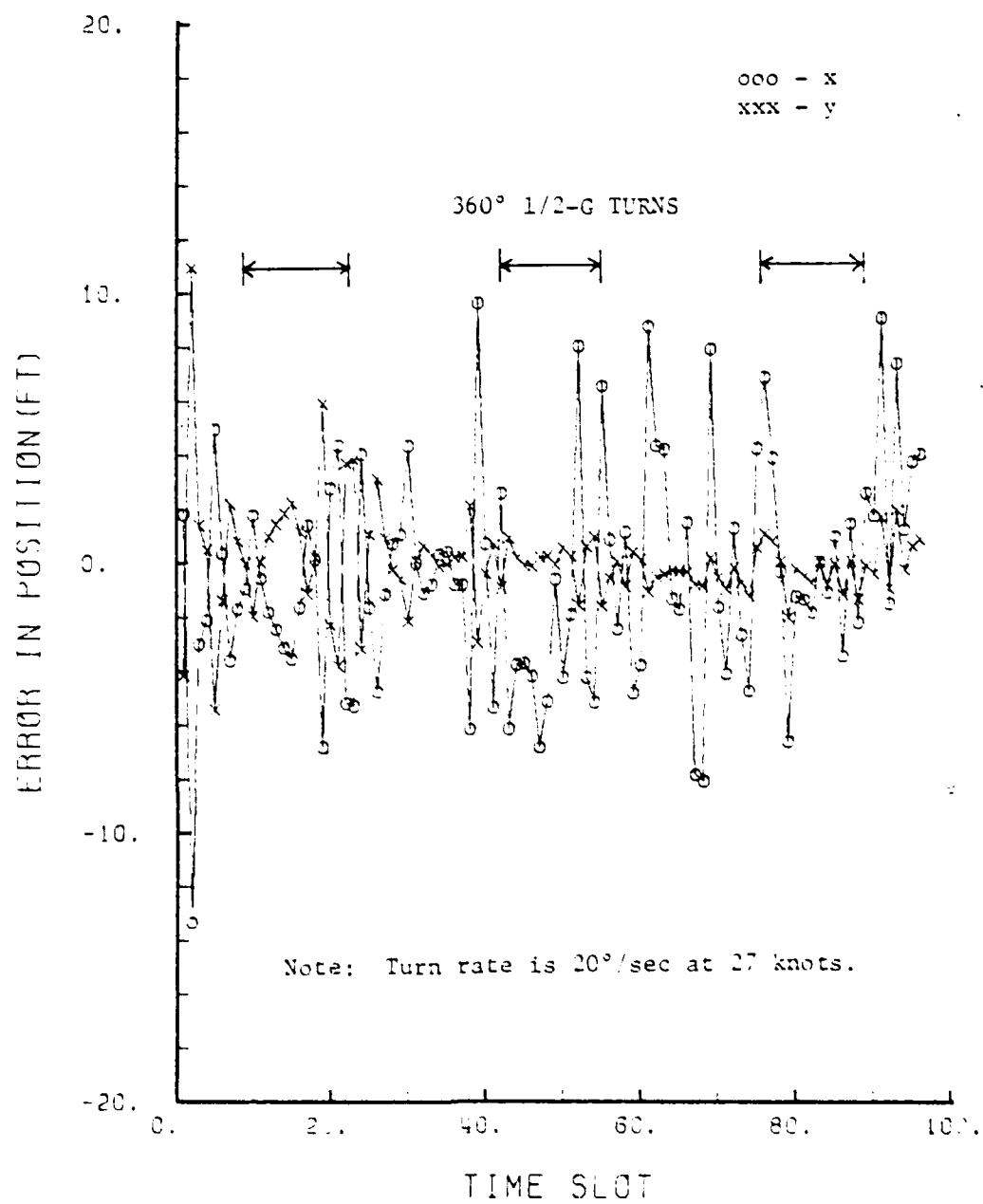


Figure 38. Error in Torpedo Position During a Maneuvering Run in the Area of a Single Array

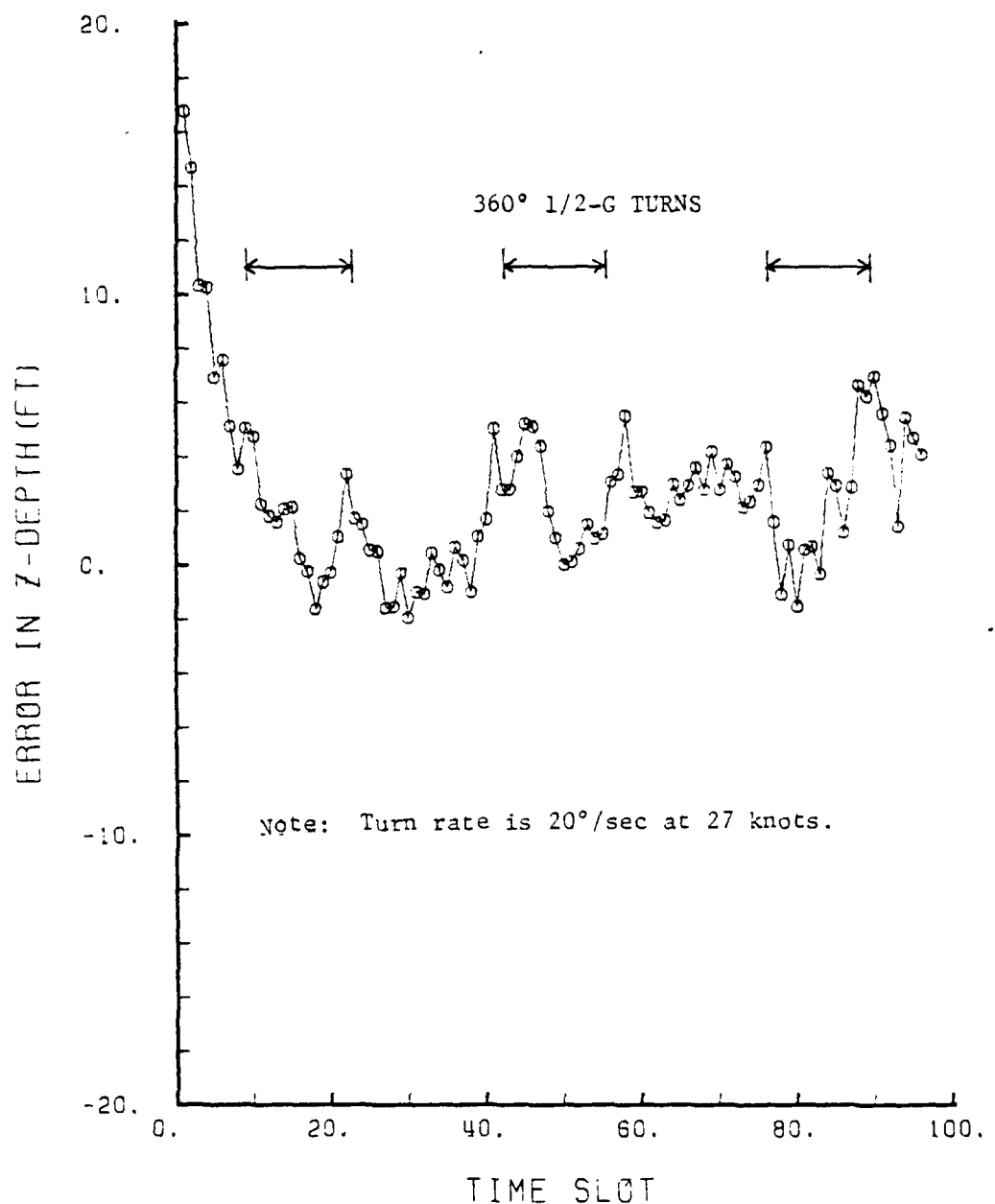


Figure 39. Error in Torpedo Depth During a Maneuvering Run in the Area of a Single Array

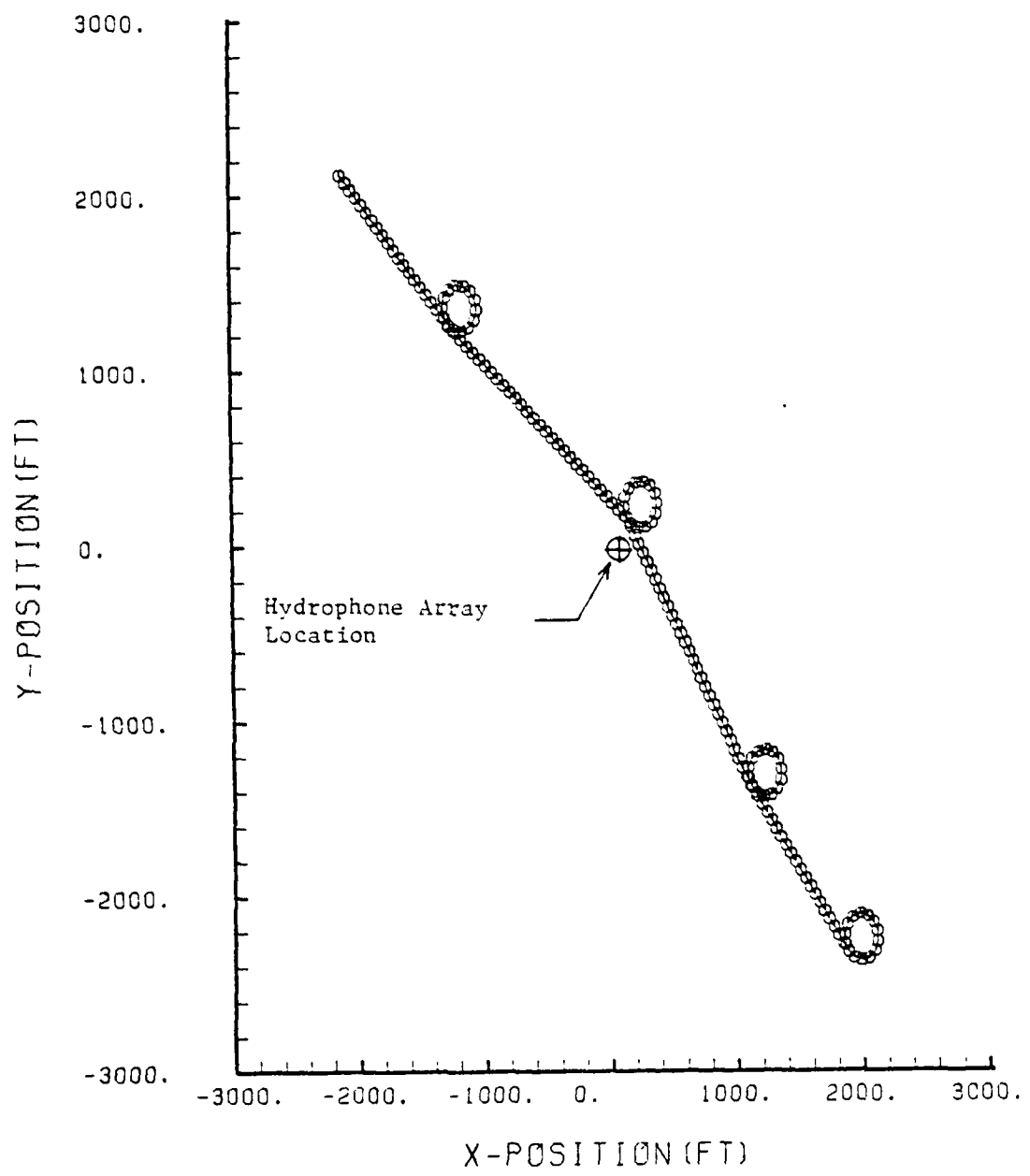


Figure 40. True Trajectory of the Torpedo During a Maneuvering Run in the Area of a Single Array

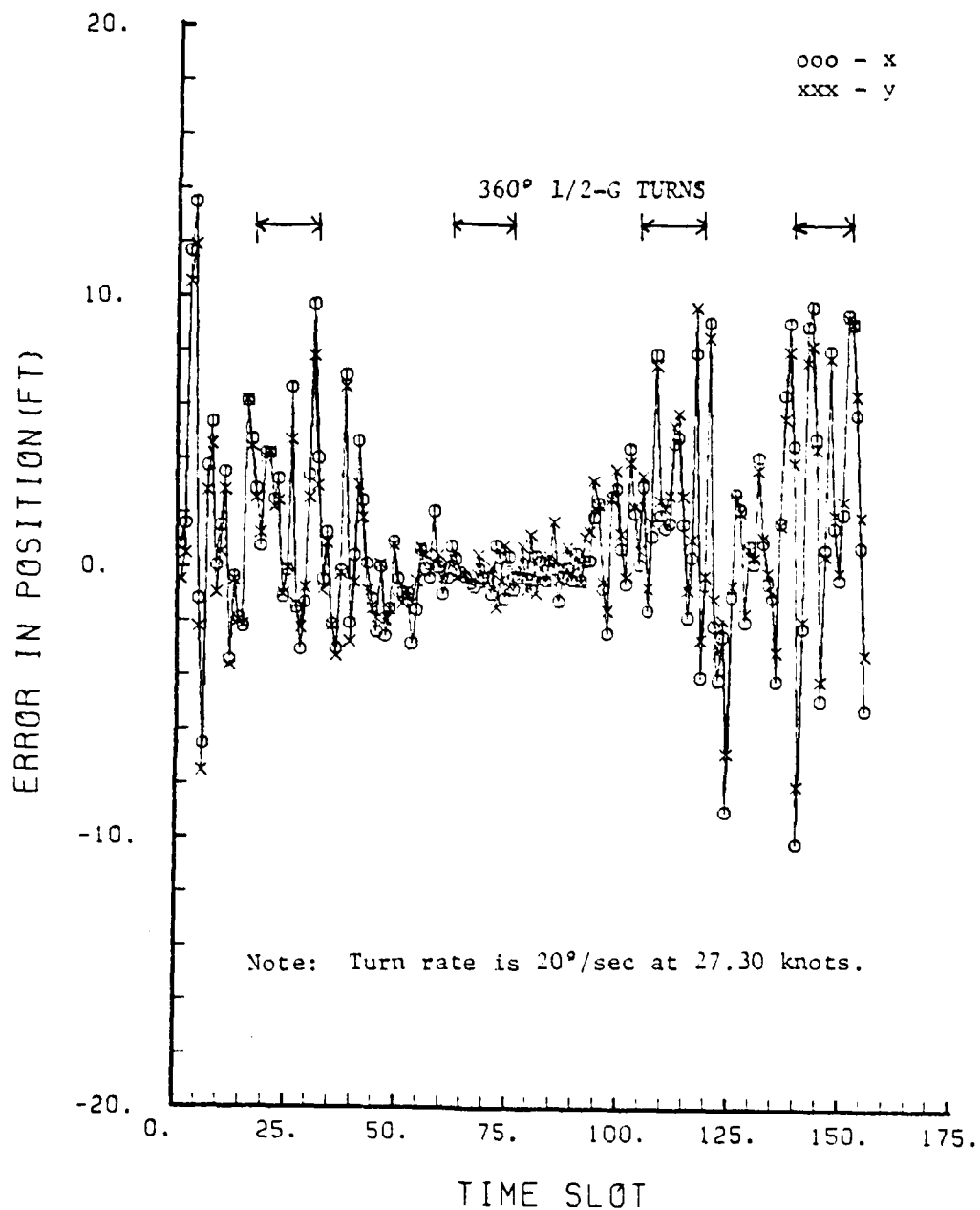


Figure 41. Error in Torpedo Position During a Maneuvering Run in the Area of a Single Array

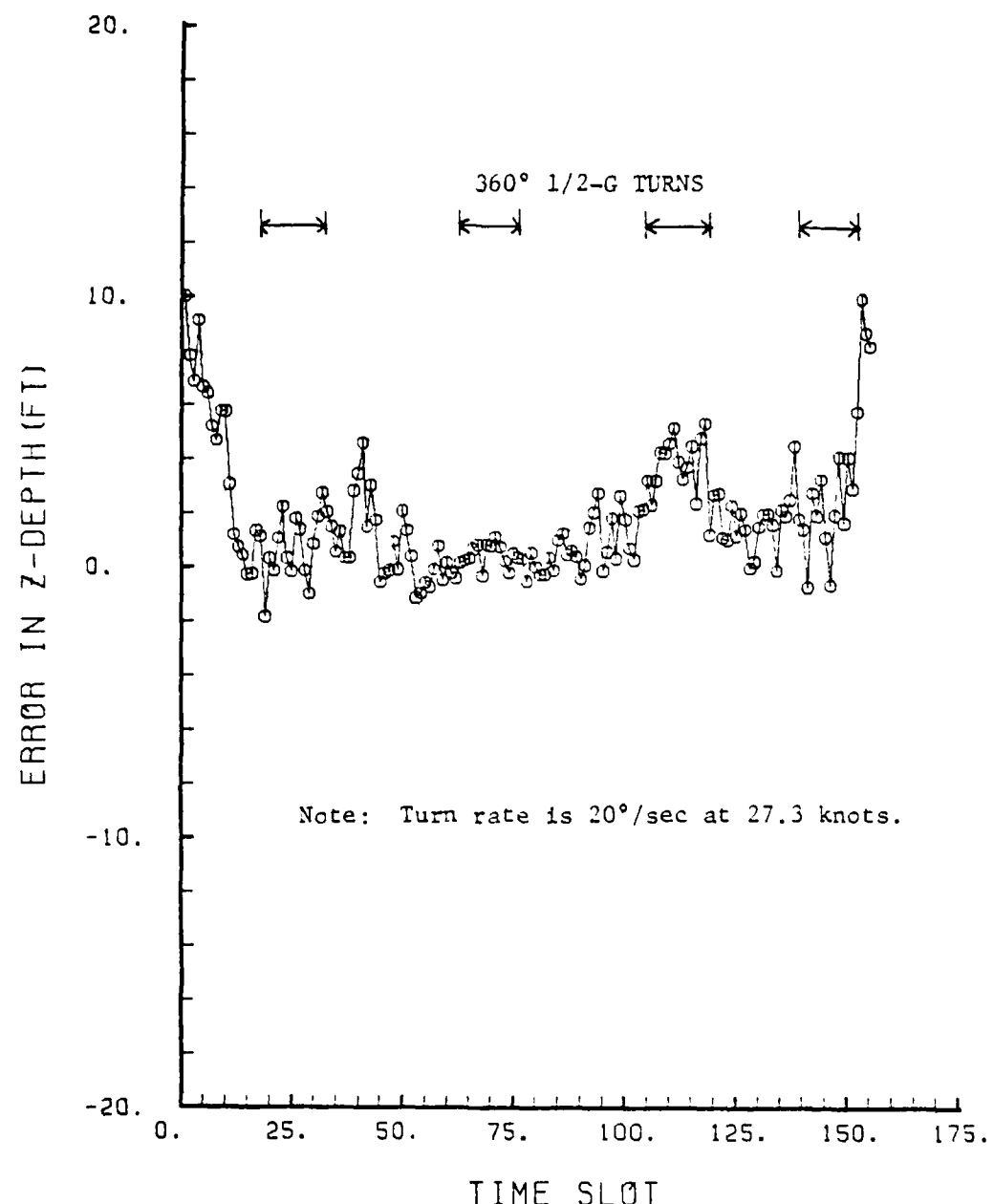


Figure 42. Error in Torpedo Depth During a Maneuvering Run in the Area of a Single Array

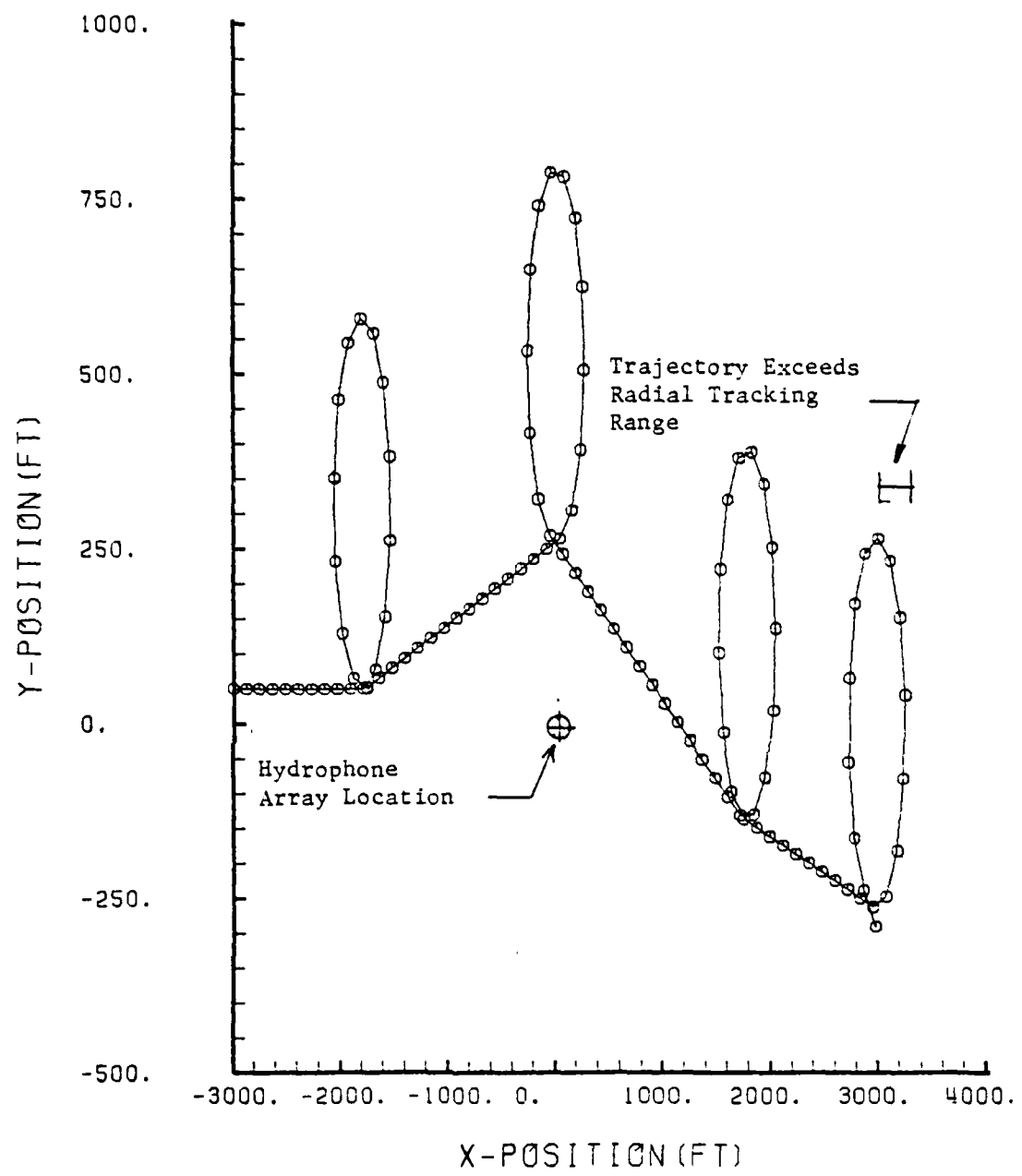


Figure 43. True Trajectory of the Torpedo During a Maneuvering Run in the Area of a Single Array

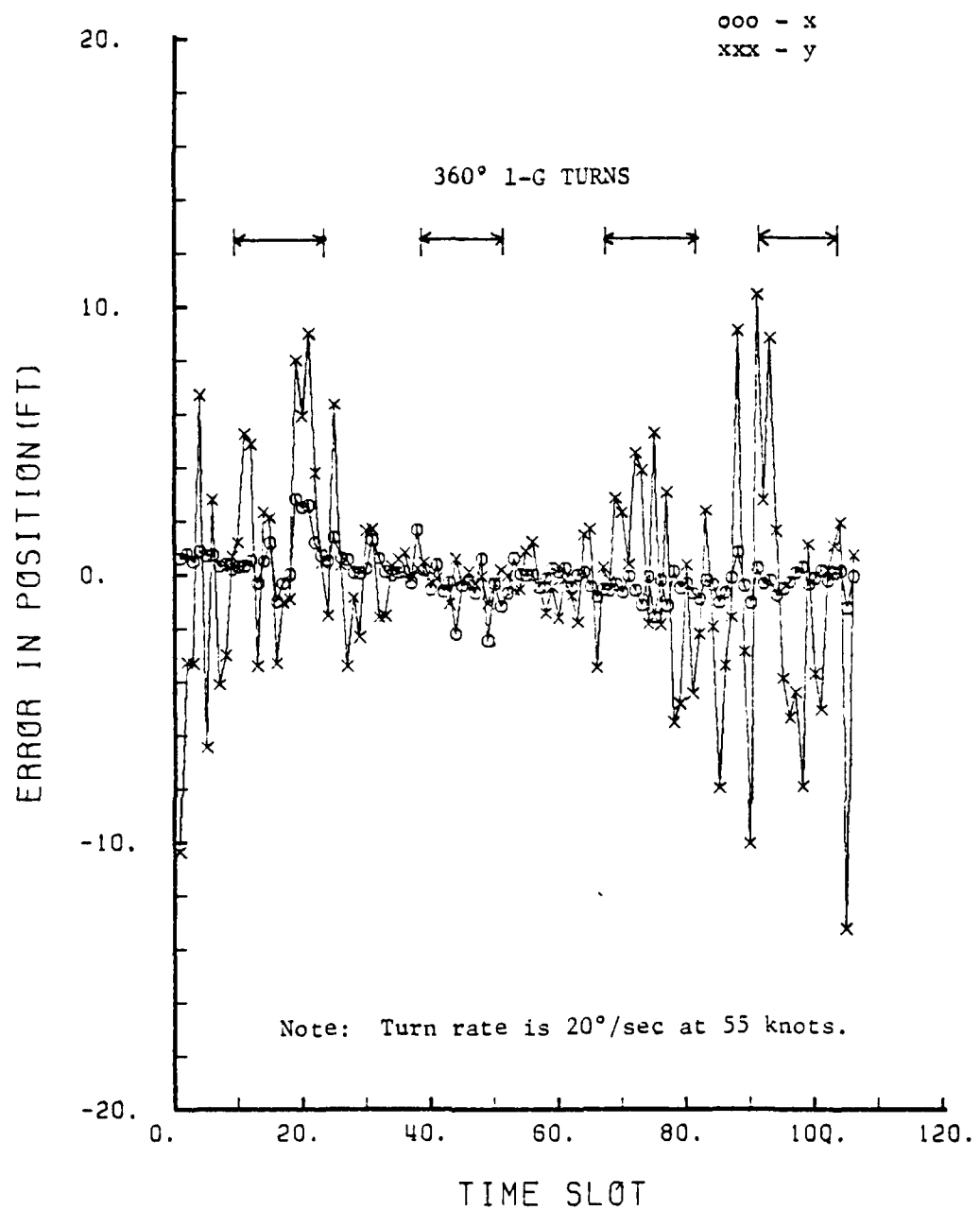


Figure 44. Error in Torpedo Position During a Maneuvering Run in the Area of a Single Array

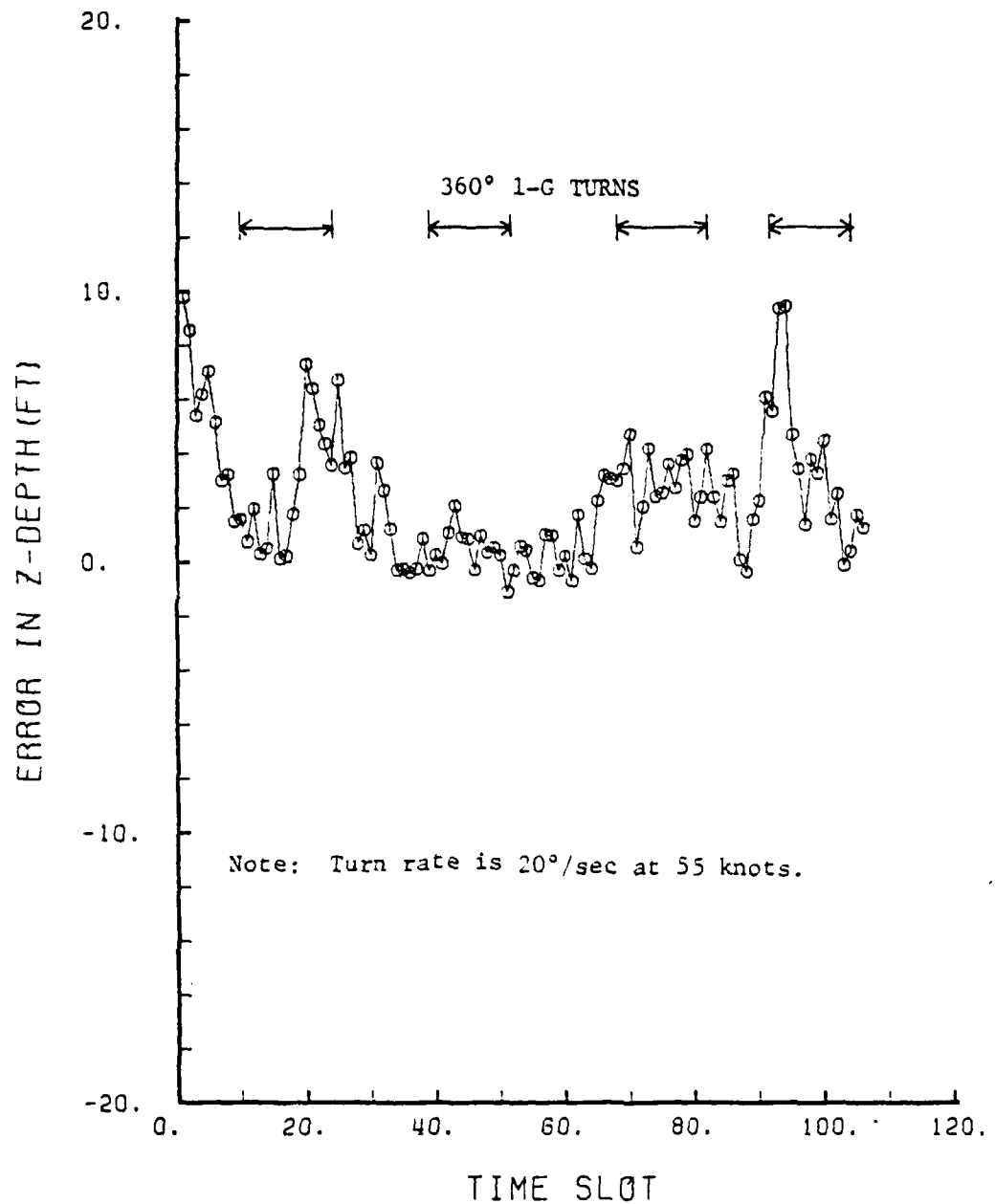


Figure 45. Error in Torpedo Depth During a Maneuvering Run in the Area of a Single Array

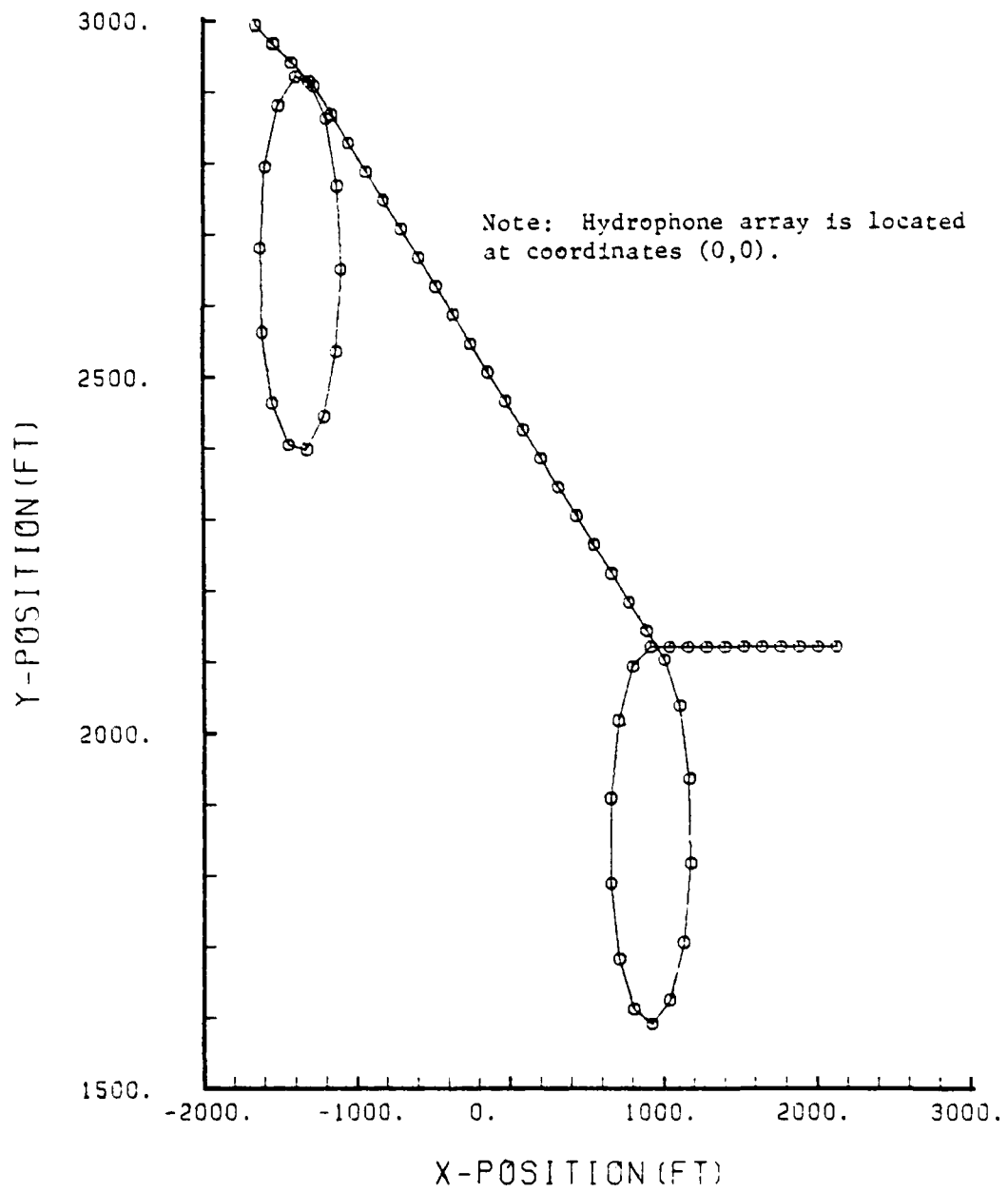


Figure 46. True Trajectory of the Torpedo During a Maneuvering Run in the Area of A Single Array

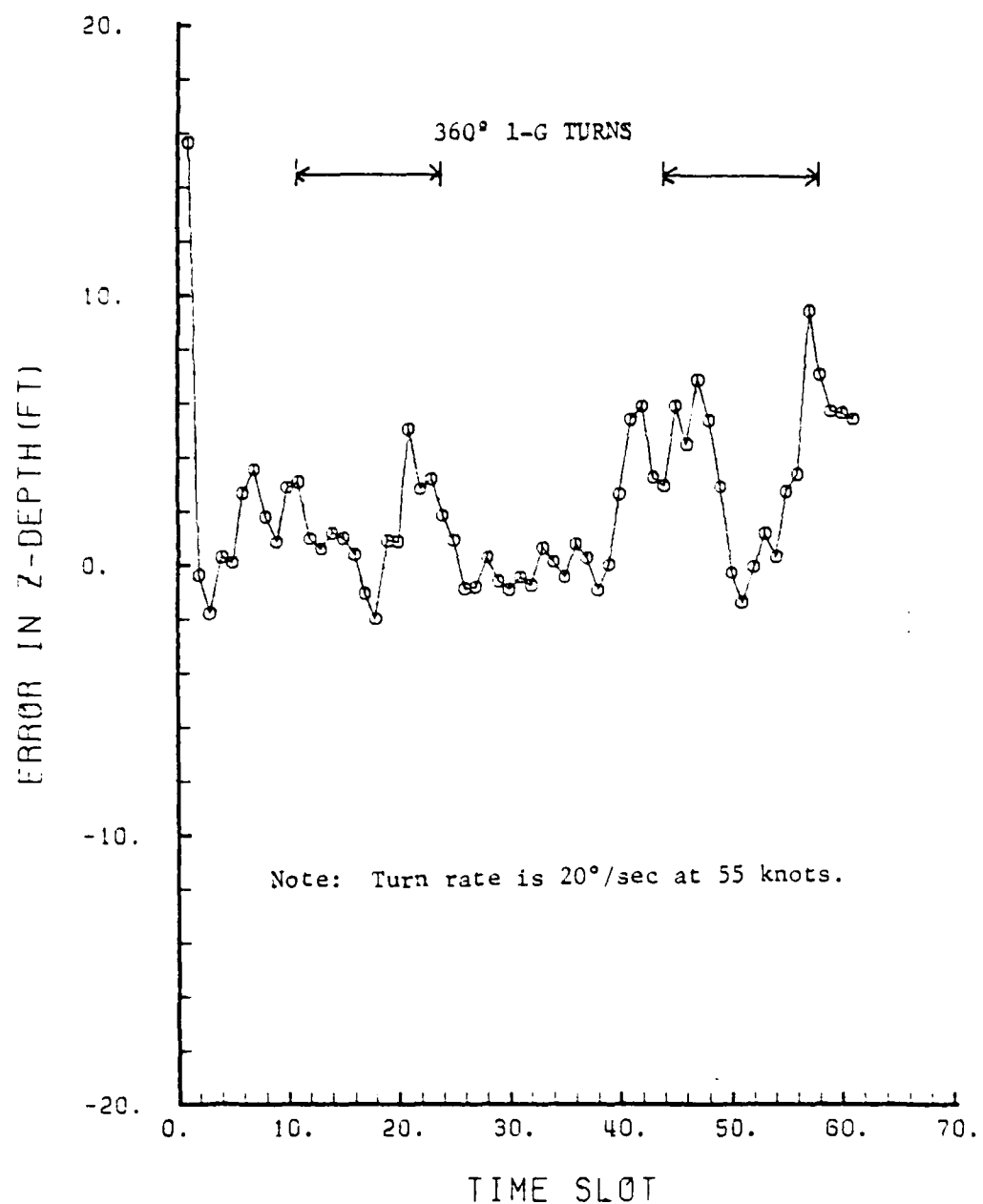


Figure 47. Error in Torpedo Depth During a Maneuvering Run in the Area of a Single Array

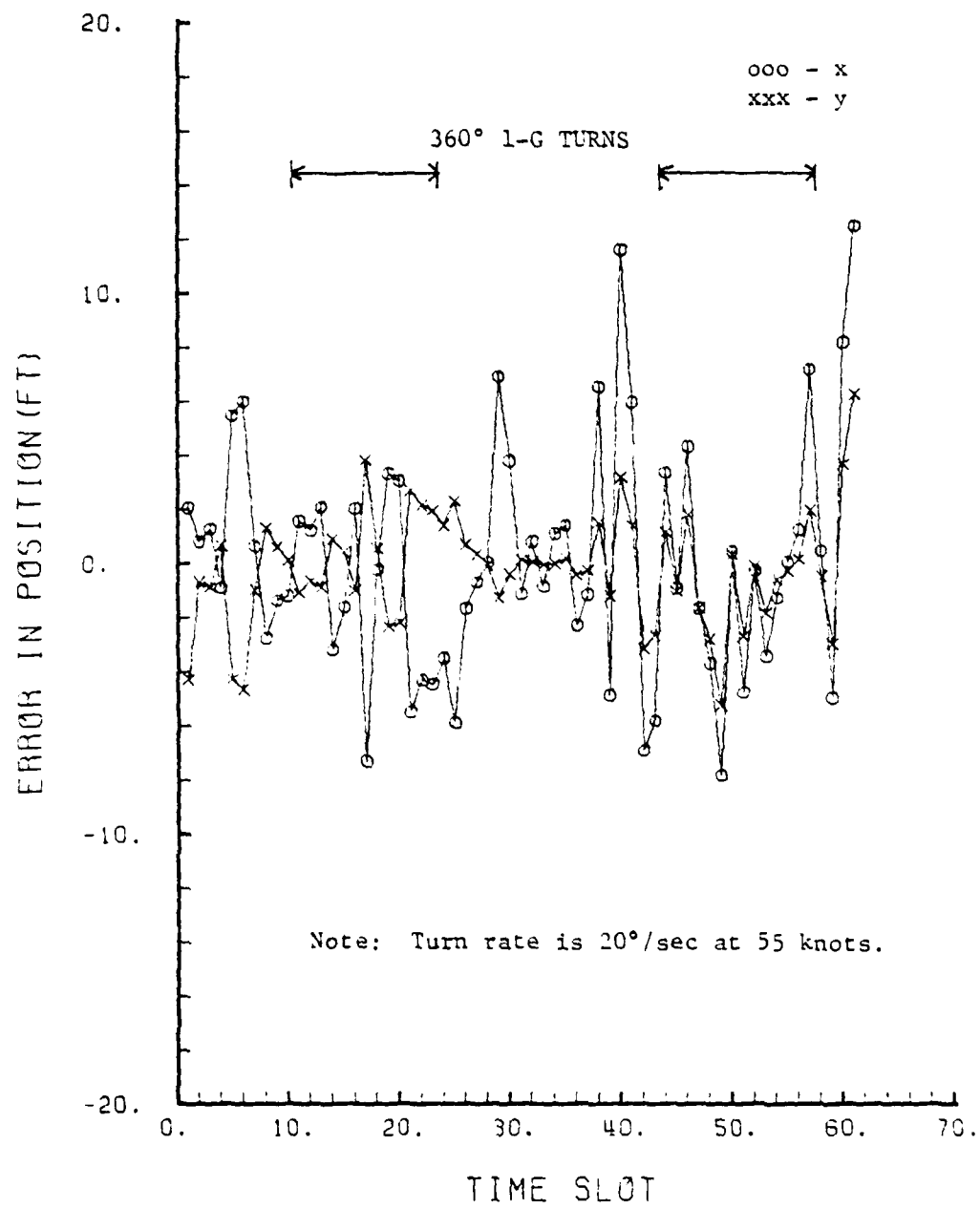


Figure 48. Error in Torpedo Position During a Maneuvering Run in the Area of a Single Array

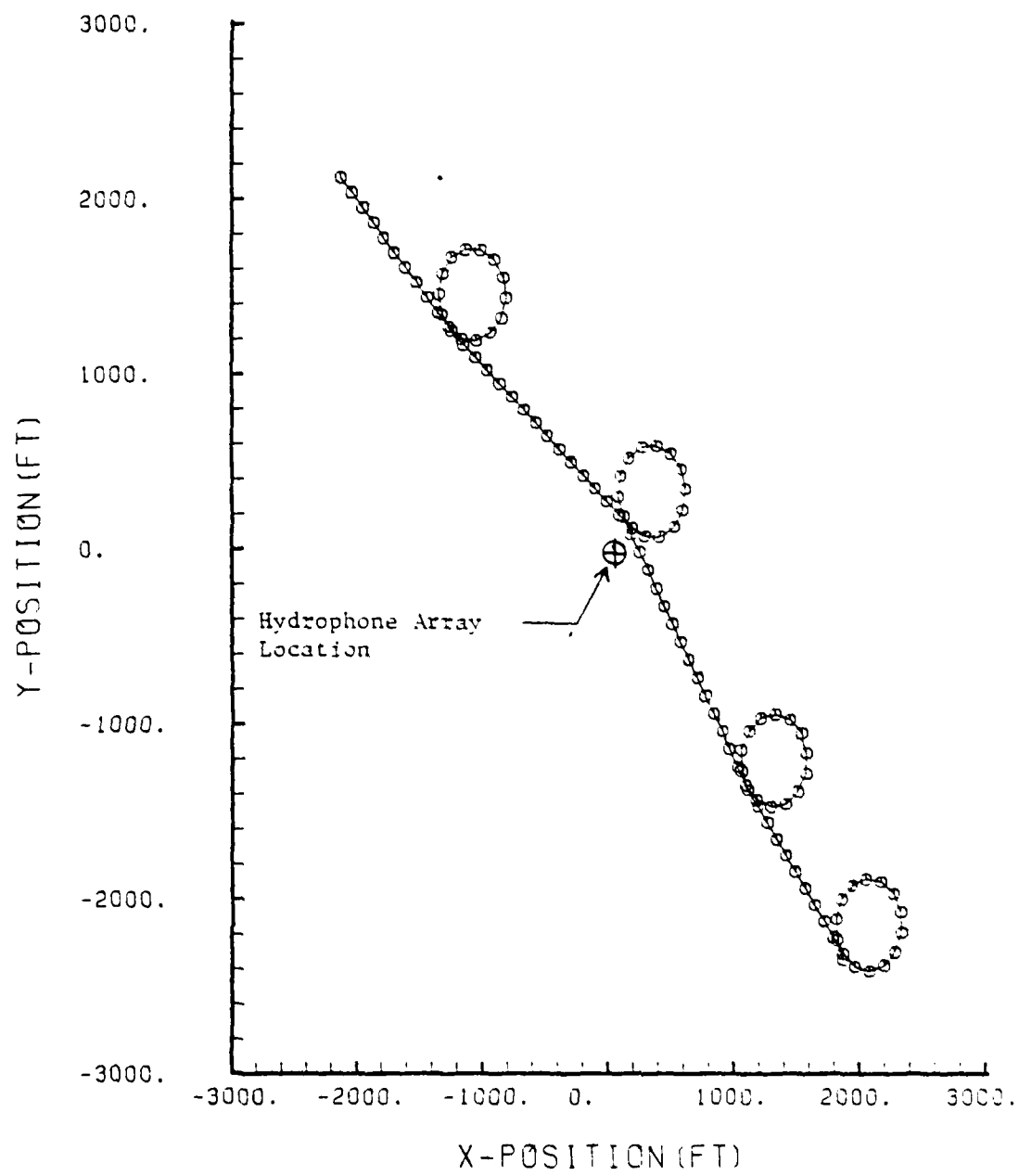


Figure 49. True Trajectory of the Torpedo During a Maneuvering Run in the Area of a Single Array

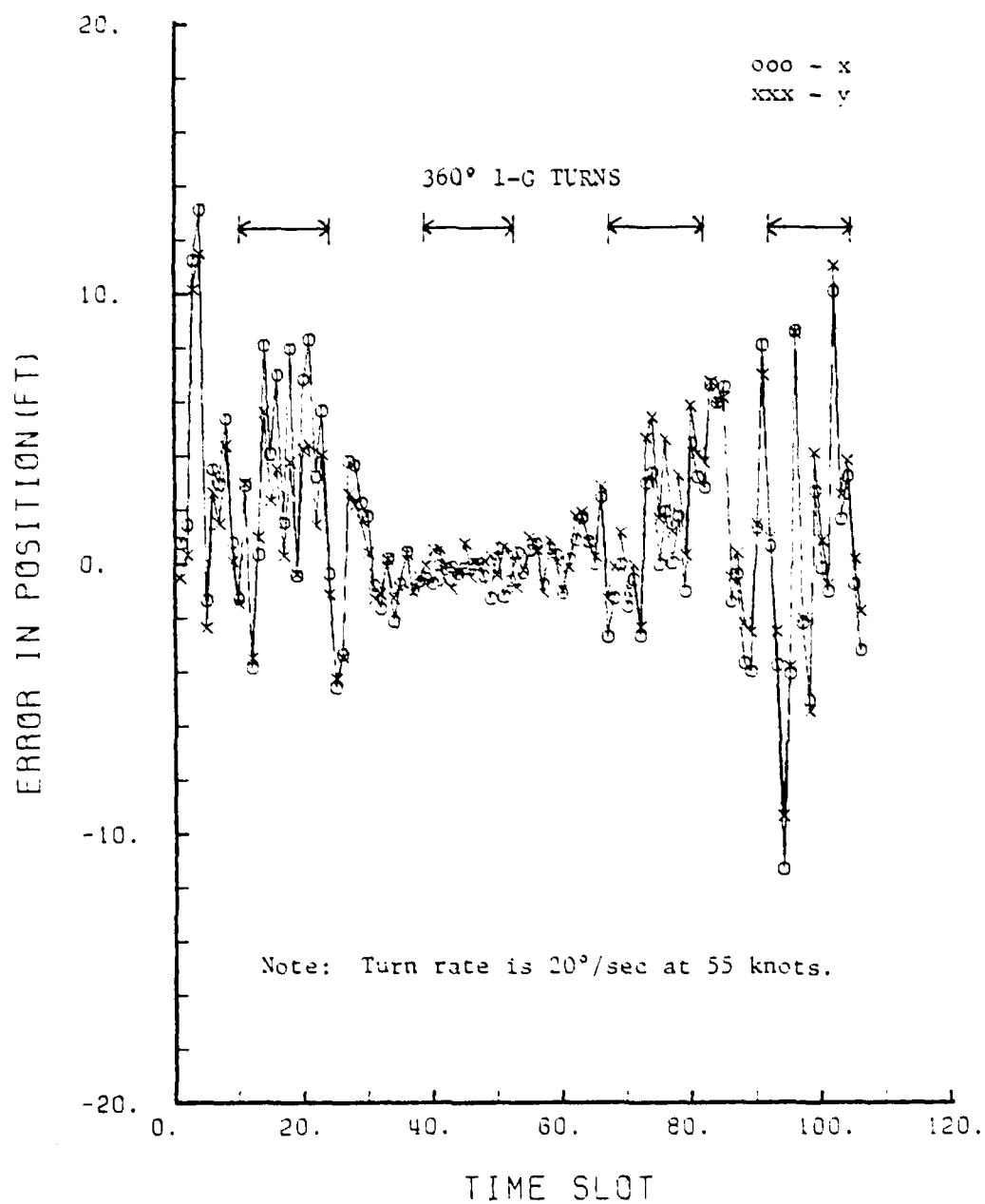


Figure 50. Error in Torpedo Position During a Maneuvering Run in the Area of a Single Array

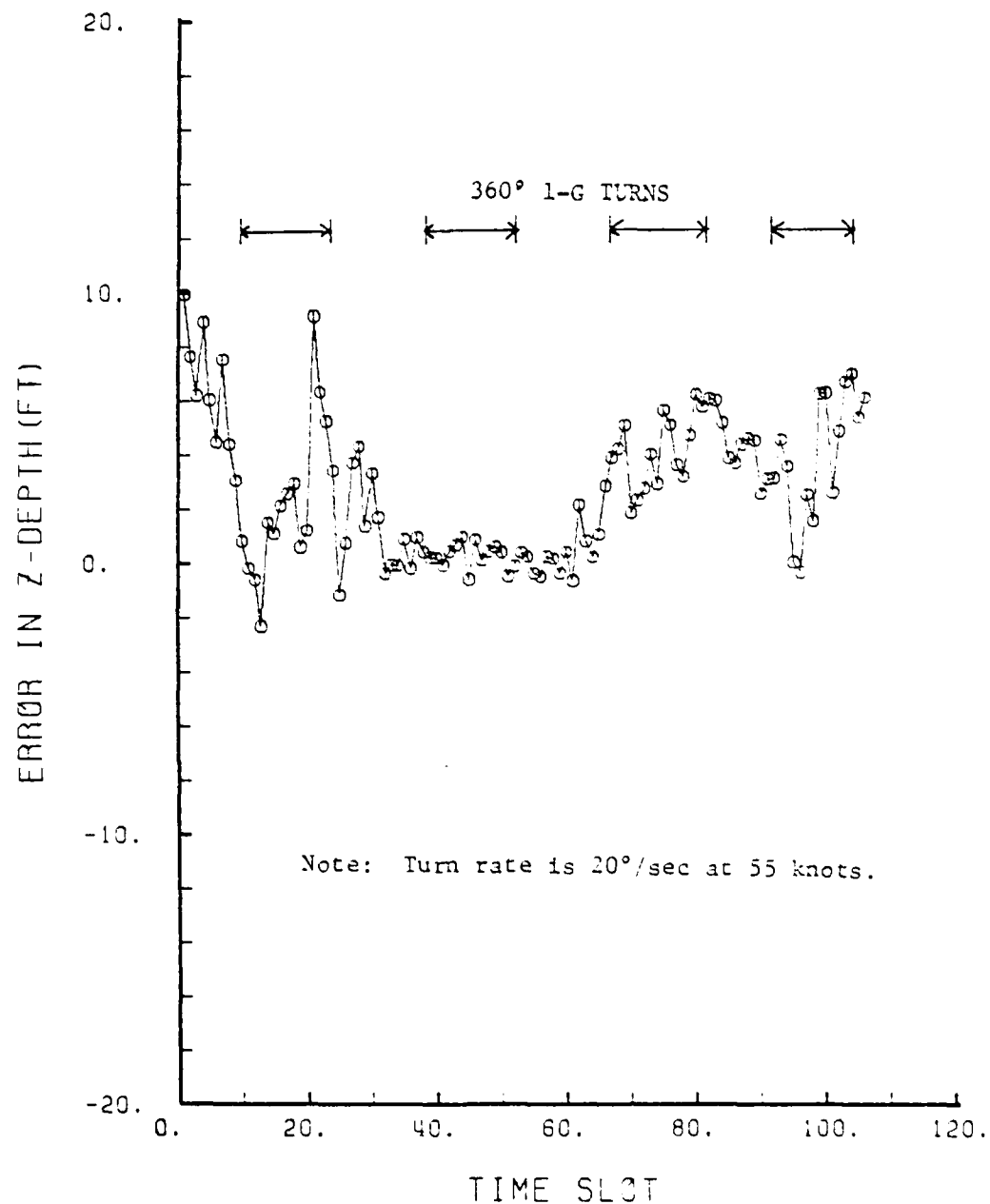


Figure 51. Error in Torpedo Depth During a Maneuvering Run in the Area of a Single Array

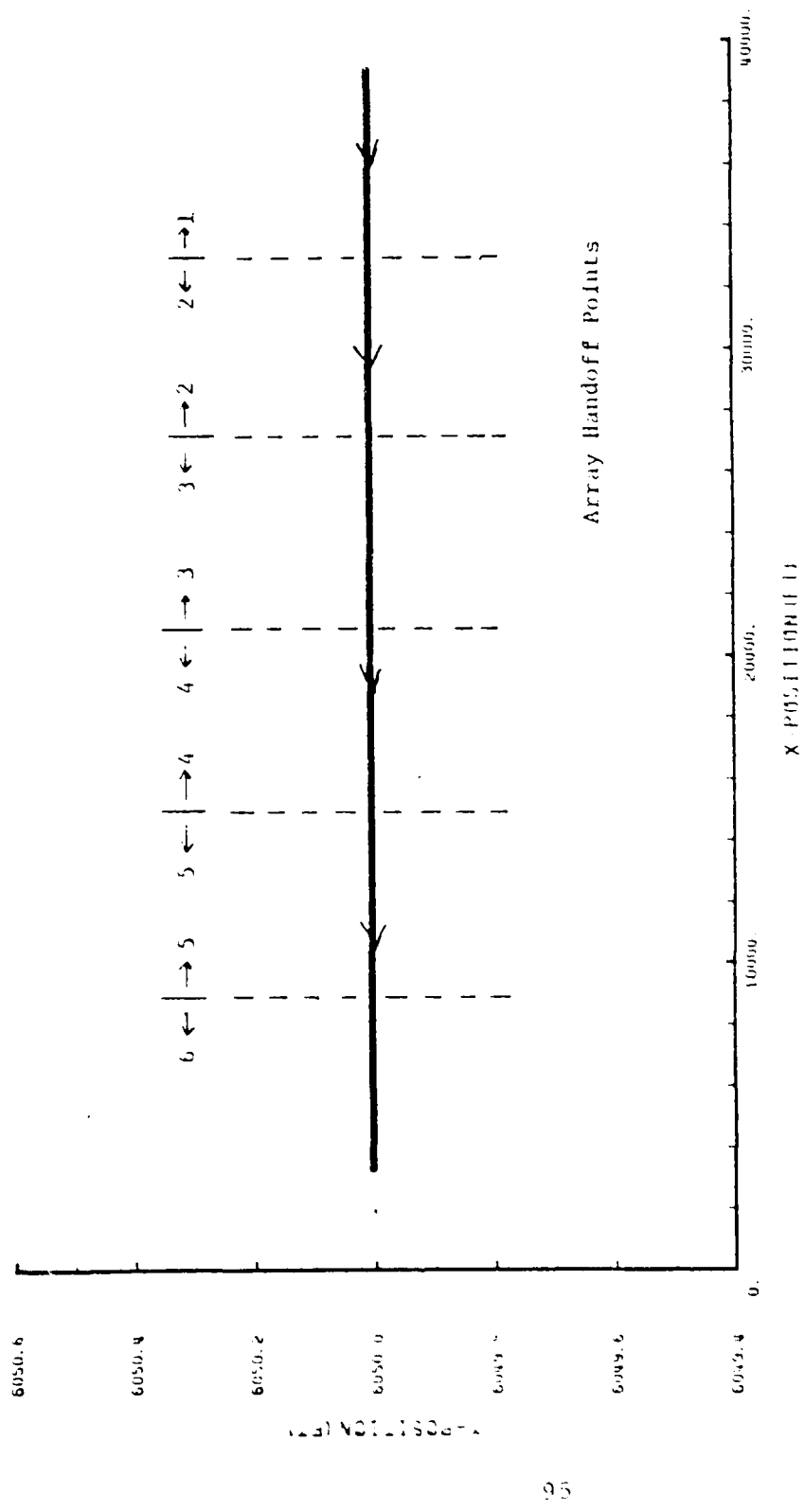


Figure 52. True trajectory of the torpedo during a straight run through multiple arrays.

AD-A092 303

NAVAL POSTGRADUATE SCHOOL MONTEREY CA
AN APPLICATION OF KALMAN FILTERING TO TORPEDO TRACKING.(U)
SEP 80 P A O'BRIEN

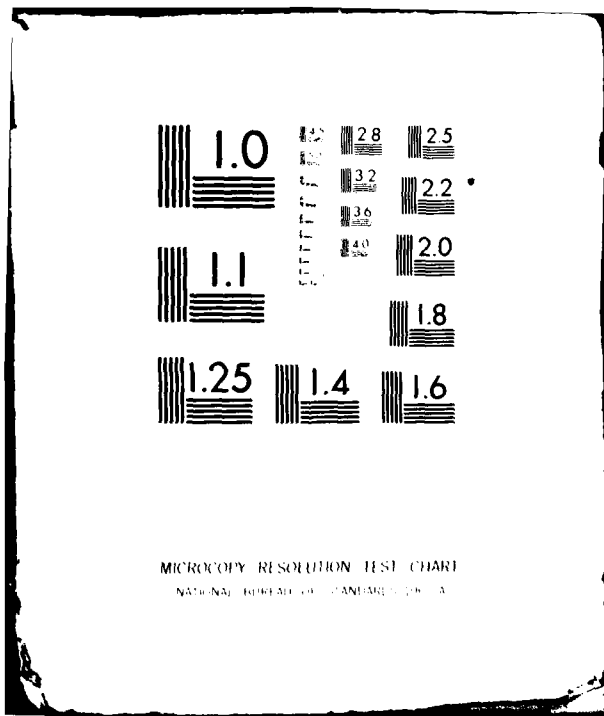
F/G 17/1

UNCLASSIFIED

2 1 2
AL
SACRISTY

NL

END
DATE
REMOVED
1 81
DTIC



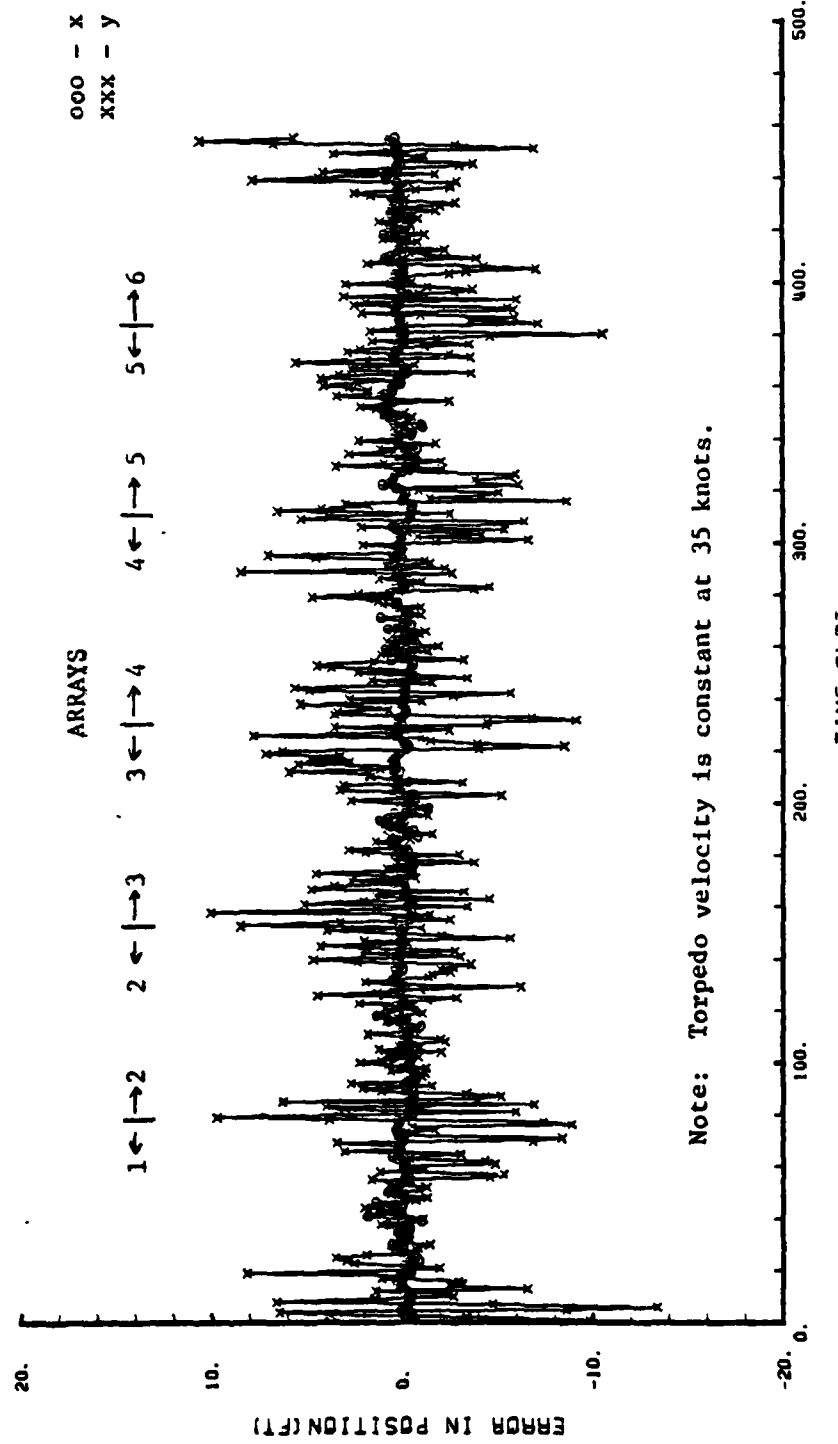


Figure 53. Error in Torpedo Position During a Straight Run Through Multiple Arrays

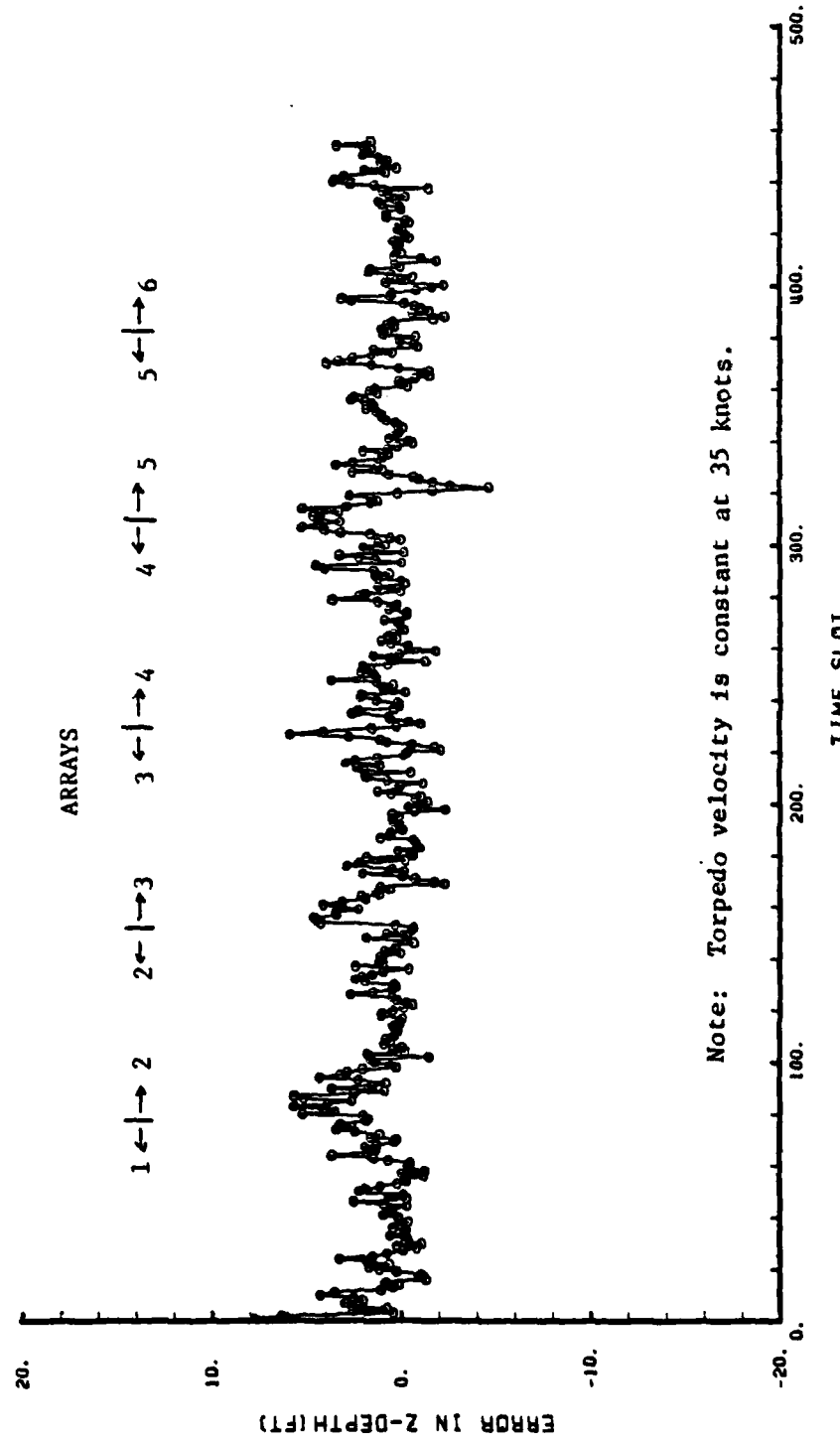


Figure 54. Error in Torpedo Depth During a Straight Run Through Multiple Arrays

APPENDIX A

PROGRAM DESCRIPTION AND FEATURES

The sequential Extended Kalman Filter routine used for torpedo tracking is modularized for ease of implementation. The program is general in nature and many of the parameters of the filter are variable including:

- a. The number of states in the filter--N
- b. The number of random forcing functions--M
- c. The number of measurements--JS
- d. Number of time slots--JTIME

The constant matrices PHI, R, COVW, and GAMMA are initialized in the beginning of the program using data statements. The filter is initialized with P(1/0) and X(1/0) (initial covariance of estimation error and states) using subroutine INIT. The first estimate is at time 1 and continues until ITIME = JTIME+1. True measurement times (ZI) are computed using either subroutines TRAJEC or TRAJC3, depending on whether single array or multiple array tracking is implemented. Either subroutine will compute four measurement times (T_C , T_X , T_Y , T_Z) for each time slot. The measurement times are corrupted by zero-mean, white Gaussian noise using the IBM-360 subroutine SNORM. For each of the four time measurements the corresponding row of the linearizing H matrix is calculated using either subroutine CHROW or CHROW3, depending on whether single array

or multiple array tracking is used. The corresponding gain matrix column GI is then found. These row and column values are utilized in forming the covariance of estimation error, PI, for that particular time measurement. Next the estimate of the observation time ZHAT from that particular hydrophone is formed using the subroutine CZHAT or CZHAT3, depending on whether single or multiple array tracking is implemented. The residual ZDIFF(I) = ZIC(I) - ZHAT, is then calcualated. Finally the estimate of the states XI based on one time measurement is calculated and the process is repeated for the next measurement. After the four iterations, four transit time measures are formed using the last estimate of the states, X4, in either subroutine CZHAT or CZHAT3. The corresponding four transit time residuals are then calculated. The average of the absolute value of the time residuals is formed (ZDIFAV) and compared to a preset threshold value in the software. If ZDIFAV is above the threshold, subroutine QFIND is used to calcuate a new Q which is then added to the last covariance of error estimate, P4. The software then reprocesses the transit time measurements for the same time slot. This procedure continues until the ZDIFAV measurement is equal or below the threshold value, at which time the last estimate of the state vector and covariance matrix become the XKK and PKK values for the time slot. Finally, the predictions XKKMI and PKKMI are formed before the process is repeated for the next time slot. PTLOP is used to generate line printer plots and PLOTG is used to generate VERSATEC plots.

A. PROGRAM SUBROUTINES

A brief description of the subroutines that are used with the filter are described below:

1. TRAJEC--This subroutine develops the torpedo trajectory which is used as truth data for the filter. The subroutine generates constant velocity and heading tracks. turns of any desired turn rate and G force can be performed at any time along the torpedo track. The subroutine outputs true transit times, ZI(I), and the X, Y, Z positions, TD(I), of the torpedo for each time slot. The subroutine is used during single array tracking.

2. TRAJC3--This subroutine performs the same function as TRAJEC but is used only during multiple array tracking.

3. INIT--This subroutine generates the initial state vector ($X_0/-1$) and initial covariance matrix ($P_0/-1$).

4. CHROW--This subroutine computes the appropriate row of the linearizing H matrix. Each row corresponds to one of the four transit time measurements, T_C , T_X , T_Y , T_Z . This subroutine is used during single state array tracking.

5. CHROW3--THIS subroutine performs the same functions as CHROW and used during multiple array tracking.

6. CZHAT--This subroutine computes the estimated transit times for the filter. Four time estimates, ZHAT, are calculated corresponding to each of the four true transit times ZI(I). This subroutine is used during single array tracking.

7. CZHAT3--Subroutine performs same functions as CZHAT however it is used only during multiple array tracking.

8. QFIND--This subroutine develops an adaptive Q matrix which is a function of the torpedo velocity. Three input variables defined in a data statement at the beginning of the program can be adjusted:

aa. SIGACC--Maximum expected horizontal acceleration of the torpedo.

bb. SIGDIV--Maximum expected change in vertical velocity.

cc. SIGCC--Maximum expected turn rate of the torpedo in the horizontal plane.

The values listed in the program were used and kept constant during the simulation tests. If the user desires not to use the adaptive Q subroutine software code is provided at the beginning of the program to calculate a constant Q matrix.

9. SNORM--This is an IBM-360 subroutine contained in the IMSL library. The routine generates zero mean white Gaussian noise with an RMS value normalized to 1. The main program scales the noise and adds it to the transit times measurements.

10. PLOTP--This is an IBM-360 subroutine used to generate the line printer plots. Information on this subroutine can be obtained from the IMSL library.

11. PLOTG--This is an IBM-360 subroutine used to generate the VERSATEC plots. Information on this subroutine can be obtained from the IMSL library.

B. UTILITY PROGRAMS

These subroutines were designed to be used for repetitive matrix and vector manipulations:

1. PROD--multiplying two matrices
2. MMULT--multiplying a matrix and a vector
3. VMULT--multiplying two vectors
4. TRANS--transposing a matrix
5. ADD--adding two matrices

APPENDIX B
SEQUENTIAL EXTENDED KALMAN FILTER PROGRAM LISTING

ପିପିପି ପିପିପି ପିପିପି ପିପିପି ପିପିପି

3

```

163  FORMAT ('0','R MATRIX')
      DO 264 I=1,4
264  WRITE(6,136)(R(I,J),J=1,4)
136  FORMAT(4F14.11)
      WRITE(6,125)
136  FORMAT(4F14.11)
      WRITE(6,105,'COV W MATRIX')
C265  FORMAT(10*,'COV W MATRIX')
      DO 266 I=1,3
C266  WRITE(6,126){COVW(I,J),J=1,3}
C267  FORMAT(3F11.6)

C CALCULATE THE Q MATRIX
      CALL PROD(GAMMA,COVM,N,M,M,QTEMP)
      CALL PROD(QTEMP,GAMMAT,N,N,N,Q)
      WRITE(6,100,'Q MATRIX')
100   FORMAT(10*,1N)
      DO 101 LI=1,N
C101  WRITE(6,102){Q(LI,LJ),LJ=1,N}
C102  FORMAT(1X,5F15.4)

C START THE TIME SLOT LOOP AND SET ARRAY HANDOFF POINT
      ITIME=JTIME+1
      XT=36000.0
      SW=XT-3000.0
      DO 99 KK=1,ITIME
99    WRITE(6,11) KK
      FORMAT(1X,100('**'),'TIME=',I4//)

C6   GET HYDROPHONE ARRAY COORDINATES
      DO 600 I3=1,4
          XB(I3)=HYDRO(18,3*I3-2)
          YB(I3)=HYDRO(18,3*I3-1)
600   ZB(I3)=HYDRO(18,3*I3)
      IF(XKKM1(1).GT.SW)GO TO 610
      I8=I8+1
      WRITE(6,1759)I8,KK
      FORMAT(10.,15{,*},15{,*},15{,*},1/)

759   FORMAT(10.,15{,*},15{,*},15{,*},1/)

      SW=SW-6000.
      XT=XT-6000.
      WRITE(6,167)
      FORMAT(10,'XKKM1')
      DO 51 LA=1,N
C51   WRITE(6,150){XKKM1(LA)}
      FORMAT(1X,5F14.4)
C

```

```

C COMPUTE THE TRUE TIMES AND TRUE POSITIONS
C   610 CALL TRAJC3(KK,DATA,ZI,TD,XB,YB,ZB)
C   610 CALL TRAJEC(KK,DATA,ZI,TD)
A14=PHI(1,2)
TRUX(KK)=TD(1)
TRY(KK)=TD(2)
TRUZ(KK)=TD(3)

C FIRST GET HROW-CALCULATE GAIN,ESTIMATE,COVARIANCE OF
C ERROR BASED IN ONE TIME MEASUREMENT-TC,TX,TY,TZ/
C
C DO 97 I=1,1,JS
C     CALL HROW3(I,HROW,XB,YB,ZB)
C     CALL HROW(I,HROW)
C     CALL MMULT(PKKM1,HROW,N,N,NUM)
C     CALL VMULT(HROW,GNUM,N,GTEMP)
C     GDENOM=GTEMP+R(I,I)
C     DO 16 IX=1,N
C        GI(IX)=GNUM(IX)/GDENOM
C
C THIS IS THE FIRST GAIN COLUMN
C CALCULATE THE COVARIANCE OF ERROR PI
C
C DO 77 IP=1,N
C     DO 79 JP=1,N
C        PDUM(IP,JP)={-1.*GI(IP))*HROW(JP)}
C        IF(IP.EQ.JP)PDUM(IP,JP)=1.+PDUM(IP,JP)
C        CONTINUE
C    CONTINUE
C    CALL PROD(PDUM,PKKM1,N,N,N,PI)
C
C CALCULATE FIRST MEASUREMENT PREDICTION
C
C CALL CZHAT(I,ZHAT)
C CALL CZHAT3(I,ZHAT,XB,YB,ZB)
C
C GET WHITE NOISE,SCALE AND ADD TO TRUE MEASUREMENT TIME
C
C CALL SNORM(19,ZC,4)
ZCS=ZC(1)*00001
ZIC(1)=ZCS+ZI(1)
ZDIFF(1)=ZIC(1)-ZHAT
C
C THESE STATEMENTS ARE FOR ADDITIONAL PLOTTING
C
C GX(KK,I)=GI(1)
C GY(KK,I)=GI(3)

```

```

ZDIFF(1)=ZK(1)=ZDIFF(1)
IF (K<=GT) ZR=1
ZDM(1)=ZDIFF(1)
ZDM(2)=ZDIFF(1)
GXN(1)=GI(1)
GXN(2)=GI(1)
GYN(1)=GI(3)
GYN(2)=GI(3)
GO TO 74
CONTINUE
IF (ZDIFF(1)*GT*ZDM(1)) ZDM(1)=ZDIFF(1)
IF (ZDIFF(1)*LT*ZDM(2)) ZDM(2)=ZDIFF(1)
IF (GI(1)*LT*GXN(1)) GXN(1)=GI(1)
IF (GI(1)*LT*GXN(2)) GXN(2)=GI(1)
IF (GI(3)*LT*GYN(1)) GYN(1)=GI(3)
IF (GI(3)*LT*GYN(2)) GYN(2)=GI(3)
CONTINUE
73   COMPUTE THE GATE FOR ERRONEOUS TIME MEASUREMENTS
      PK1=DABS(P1(1,1))
      PK2=DABS(P1(3,3))
      PK3=DABS(P1(5,5))
      IF ((PK1*GE*PK3)*AND.(PK1*GE*PK5)) P=PK1
      IF ((PK3*GE*PK1)*AND.(PK3*GE*PK5)) P=PK3
      IF ((PK5*GE*PK1)*AND.(PK5*GE*PK3)) P=PK5
      PGATE=SQRT(P)/4860
      RGATE=DSQRT(DABS(R(1,1)))
      GATE=3.*((PGATE+RGATE)
C       EDIT INVALID TIME MEASUREMENTS
      IF (ZDIFF(1)*LT*GATE) GO TO 500
      WRITE(6,501)KK
      FORMAT(100,'GATE HAS BEEN EXCEEDED TIME',14)
      DO 502 LC=1,N
      GI(LG)=0.0
      C       TAG INVALID TIME MEASUREMENT
      ZDIFF(1)=999.
      C       CALCULATE THE ESTIMATE BASED ON ONE MEASUREMENT
      500
      17   DO 17 IZ=1,N
            X1(IZ)=XKKM(IZ)+GI(IZ)*ZDIFF(1)
            IF (I.EQ.4) GO TO 56
            DO 19 IQ=1,N

```

```

19      XKKM1(IQ)=XI(IQ)
      DO 23 IQ=1,N
      DO 18 JQ=1,N
      PKKM1(IQ,JQ)=PI(IQ,JQ)
      CONTINUE
18      WRITE(6,31)
31      FORMAT(0.0)
      CONTINUE
C      NOTE-CALLED ORIGINAL X(0/-1). XKKM1. UPDATED AFTER 1
C      MEASUREMENT CALLED IT XI. THEN MADE XKKM1=XI AND WENT
C      THRU ITERATION AGAIN. AFTER YOU HAVE UPDATED XKKM1 FOR
C      EACH MEASUREMENT XKK=XI AND PKK=PI
C
C      DO 57 ID=1,N
      XKK(ID)=XI(ID)
      XKKM1(ID)=XI(ID)
      DO 58 JD=1,N
      PKK(ID,JD)=PI(ID,JD)
      PKKM1(ID,JD)=PI(ID,JD)
      CONTINUE
57
56      RECALCULATE TIME MEASUREMENTS, FORM ABSOLUTE VALUE OF RESIDUALS
      DO 81 I=1,4
      EDIT INVALID TIME MEASUREMENTS FOR ADAPTIVE MANEUVER ROUTINE
      IF (ZDIFF(I).GE.999.) GO TO 82
      CALL CZHAT(I,ZHAT)
      CALL CZHAT(I,ZHAT,XB,YB,ZB)
      ZDIFF(I)=DABS(ZIC(I)-ZHAT)
      GO TO 81
      ZDIFF(I)=0.0
      NZDIFF = NZDIFF - 1
      CONTINUE
81
82      IF ALL TIME MEASUREMENTS EXCEED GATE BYPASS ADAPTIVE
      MANEUVER ROUTINE
      IF (NZDIFF.EQ.0) GO TO 80
      ZDIFAV=(ZDIFF(1)+ZDIFF(2)+ZDIFF(3)+ZDIFF(4))/NZDIFF
      DC NOT PERFORM ADAPTIVE MANEUVERING
      IF FILTER HAS NOT ACHIEVED STEADY STATE
      IF (KK.LE.4) GO TO 80
      THE00960
      THE00965
      THE00970
      THE00975
      THE00980
      THE00985
      THE00990
      THE00995
      THE01000
      THE01005
      THE01010
      THE01015
      THE01020
      THE01025
      THE01030
      THE01035
      THE01040
      THE01045
      THE01050
      THE01055
      THE01060
      THE01065
      THE01070
      THE01075
      THE01080
      THE01085
      THE01090
      THE01095
      THE01100
      THE01105
      THE01110
      THE01115
      THE01120
      THE01125
      THE01130
      THE01135
      THE01140
      THE01145
      THE01150
      THE01155
      THE01160
      THE01165
      THE01170
      THE01175
      THE01180
      THE01185
      THE01190
      THE01195

```

```

C IF ZDIFAV MEETS CRITERIA TRANSFER OUT OF
C ADAPTIVE MANEUVER ROUTINE
C IF(ZDIFAV.LE..100000-04)GO TO 80
C
C INCREASE THE GAIN
C CALL QFIND(KK,SIGACC,SIGDIV,SIGCC,A14,Q)
C CALL ADD(PKK,Q,N,N,PKKM1)
C
C PERFORM ADAPTIVE MANEUVERING BY REITERATING SAME TIME SLOT
C GO TO 711
C
C
C 80 NZDIFF=4
C XDIFF1(KK)=XKK(1)-TRUX(KK)
C XDIFF3(KK)=XKK(3)-TRUY(KK)
C
C CALCULATE THE PREDICTIONS FOR PKKM1
C CALL QFIND(KK,SIGACC,SIGDIV,SIGCC,A14,Q)
C WRITE(6,100)
C DO 765 I=1,N
C      WRITE(6,766)(Z(I,J),J=1,N)
C      FORMAT(1X,5F10.4)
C      WRITE(6,767)
C      FORMAT(1X,5F10.4)
C
C 766 CALL PROD(PHI1,PKK,N,N,PHIPKK)
C CALL PROD(PHI1,PKK,PHIT,N,N,PKTEMP)
C CALL ADD(PKTEMP,Q,N,N,PKKM1)
C
C CALCULATE NEW XKKM1
C CALL MMULT(PHI,XKK,N,N,XKKM1)
C DO 41 IG=1,N
C      XP(IG,KK)=XKK(IG)
C DO 38 II=1,N
C      DO 39 JJ=1,N
C          PI(II,II,JJ)=PKK(II,JJ)
C 38 CONTINUE
C 41 CONTINUE
C 99 WRITE(6,909)ZDM(1),ZDM(2),GXM(1),GXM(2)
C 909 FORMAT(16E14.5)
C
C SET UP ARRAYS AND SCALE FACTORS FOR PLOTP AND PLOTG

```

```

C C1(1)=285.
C C1(2)=330.
C C3(1)=0.
C C3(2)=500.
C C4(1)=0.
C C5(2)=40000.
C C5(1)=100000.
DO 91 KK=1,ITIME
X1(KK)=XP(1,KK)
X3(KK)=XP(3,KK)
X5(KK)=XP(5,KK)
DO 92 KK=1,ITIME
KOUNT(IK)=IK
DO 113 IF=1,ITIME
AKOUNT(IF)=FLOAT(KOUNT(IF))

C GENERATE LINE PRINTER PLOTS
DO 238 II=1,N
JJ=II
 239 KK=1,ITIME
PVEC(KK)=SQR(T(P1(KK,II,JJ)))
WRITE(6,900)
CALL PLOTP(AKOUNT,PVEC,ITIME,0)
WRITE(6,800)II,JJ
FORMAT(23X,PKK(.,II,.,.,.,VS TIME))
FORMAT(23X,PKK(.,II,.,.,.,VS TIME))
FORMAT(6,900)
WRITE(6,900)
CALL PLOTP(AKOUNT,X1,ITIME,2)
CALL PLOTP(AKOUNT,TRUX,ITIME,3)
FORMAT(25X,XPOSIT VS TIME)
FORMAT(25X,YPOSIT VS TIME)
CALL PLOTP(AKOUNT,XDIFF1,ITIME,0)
WRITE(6,805)
FORMAT(25X,DEVIATION FROM TRUE X)
FORMAT(6,900)
CALL PLOTP(C3,C5,2,1)
CALL PLOTP(AKOUNT,X3,ITIME,2)
FORMAT(6,802)
FORMAT(25X,YPOSIT VS TIME)
WRITE(6,900)
CALL PLOTP(AKOUNT,XDIFF3,ITIME,0)
WRITE(6,806)

```

```

806 FORMAT(25X,'DEVIATION FROM TRUE Y')
     WRITE(6,900)
     CALL PLOT(C3,C1,2,1)
     CALL PLOT(AKOUNT,X5,ITIME,2)
     CALL PLOT(AKOUNT,TRUZ,ITIME,3)
     WRITE(6,803)
     FORMAT(25X,'Z DEPTH VS TIME')
     WRITE(6,900)
     CALL PLOT(C4,C5,2,1)
     CALL PLOT(X1,X3,ITIME,2)
     CALL PLOT(TRUX,TRUY,ITIME,3)
     WRITE(6,804)
     FORMAT(25X,'GEOGRAPHIC Y VS X')
     WRITE(6,900)
     THIS IS THE BLOCK TO DO THE EXTRA PLOTS
     CALL PLOT(C3,ZDM,2,1)
     CALL PLOT(AKOUNT,ZDIFF1(1,1),ITIME,2)
     CALL PLOT(AKOUNT,ZDIFF1(1,2),ITIME,2)
     CALL PLOT(AKOUNT,ZDIFF1(1,3),ITIME,2)
     CALL PLOT(AKOUNT,ZDIFF1(1,4),ITIME,3)
     WRITE(6,70)
     WRITE(6,75)
     WRITE(6,900)
     CALL PLOT(C3,GXM,2,1)
     CALL PLOT(AKOUNT,GX(1,1),ITIME,2)
     CALL PLOT(AKOUNT,GX(1,2),ITIME,2)
     CALL PLOT(AKOUNT,GX(1,3),ITIME,2)
     CALL PLOT(AKOUNT,GX(1,4),ITIME,3)
     WRITE(6,76)
     WRITE(6,75)
     WRITE(6,900)
     CALL PLOT(C3,GYM,2,1)
     CALL PLOT(AKOUNT,GY(1,1),ITIME,2)
     CALL PLOT(AKOUNT,GY(1,2),ITIME,2)
     CALL PLOT(AKOUNT,GY(1,3),ITIME,2)
     CALL PLOT(AKOUNT,GY(1,4),ITIME,3)
     WRITE(6,78)
     WRITE(6,75)
     WRITE(6,900)
     FORMAT(20X,'ZDIFF VS TIME')
     TX=*,TY=X,TZ=.  .
     FORMAT(20X,'GAIN IN X VS TIME')
     FORMAT(20X,'GAIN IN Y VS TIME')
     END OF BLOCK FOR EXTRA PLOTS
     STOP
     END
C GENERATE PLOTG CURVES

```

C

```

111
      DO 240 KK=1 ITIME
      PVEC(KK)=PI(KK)VEC(KK)
240    CALL PLOTG(AKOUNT,PVEC,ITIME,1,1,'TIME SLOT', 9,'RMS ESTIMATE OF THE01920
1 POSITION ERROR(FT), 34,0.,0.,0.,15.,12.,7.) THE01925
1 IT=3 THE01930
      DO 242 KK=1 ITIME
      PVEC(KK)=PI(KK)VEC(KK)
242    PVEC(KK)=SQRT(PVEC(KK))
1 CALL PLOTG(AKOUNT,PVEC,ITIME,2,1,4,'TIME SLOT', 9,'RMS ESTIMATE OF THE01940
1 POSITION ERROR(FT), 34,0.,0.,0.,15.,12.,7.) THE01945
1 IT=2 THE01950
      DO 241 KK=1 ITIME
      PVEC(KK)=PI(KK)VEC(KK)
241    PVEC(KK)=SQRT(PVEC(KK))
1 CALL PLOTG(AKOUNT,PVEC,ITIME,1,1,'TIME SLOT', 9,'RMS ESTIMATE OF THE01955
1 VELOCITY ERROR(FT/SEC), 38,0.,0.,0.,0.,0.,12.,7.) THE01960
1 IT=2 THE01965
      DO 243 KK=1 ITIME
      PVEC(KK)=PI(KK)VEC(KK)
243    PVEC(KK)=SQRT(PVEC(KK))
1 CALL PLOTG(AKOUNT,PVEC,ITIME,2,1,4,'TIME SLOT', 9,'RMS ESTIMATE OF THE01970
1 VELOCITY ERROR(FT/SEC), 38,0.,0.,0.,0.,0.,12.,7.) THE01975
1 IT=4 THE01980
      DO 244 KK=1 ITIME
      PVEC(KK)=PI(KK)VEC(KK)
244    CALL PLOTG(AKOUNT,TRUX,ITIME,1,1,'TIME SLOT', 9,'X-POSITION(FT)' THE01985
1 DEPTH ERROR(FT), 31,0.,0.,0.,15.,12.,7.) THE01990
1 CALL PLOTG(AKOUNT,X1,ITIME,1,1,1,1,'TIME SLOT', 9,'X-POSITION(FT)', THE02000
1 IT=5 THE02005
      DO 245 KK=1 ITIME
      PVEC(KK)=PI(KK)VEC(KK)
245    CALL PLOTG(AKOUNT,ITIME,1,1,1,1,'TIME SLOT', 9,'X-POSITION(FT)' THE02010
1 DEPTH ERROR(FT), 31,0.,0.,0.,15.,12.,7.) THE02015
1 CALL PLOTG(AKOUNT,X1,ITIME,1,1,1,1,'TIME SLOT', 9,'X-POSITION(FT)', THE02020
1 IT=4 THE02025
      DO 246 KK=1 ITIME
      PVEC(KK)=PI(KK)VEC(KK)
246    CALL PLOTG(AKOUNT,XDIFF1,ITIME,1,1,1,1,'TIME SLOT', 9,'X-POSITION(FT)' THE02030
1 DEPTH ERROR(FT), 31,0.,0.,0.,15.,12.,7.) THE02035
1 CALL PLOTG(AKOUNT,X1,ITIME,1,1,1,1,'TIME SLOT', 9,'X-POSITION(FT)', THE02040
1 IT=3 THE02045
      DO 247 KK=1 ITIME
      PVEC(KK)=PI(KK)VEC(KK)
247    PVEC(KK)=SQRT(PVEC(KK))
1 CALL PLOTG(AKOUNT,PVEC,ITIME,2,1,4,'TIME SLOT', 9,'Y-POSITION(FT)', THE02050
1 VELOCITY ERROR(FT/SEC), 38,0.,0.,0.,0.,0.,12.,7.) THE02055
1 IT=2 THE02060
      DO 248 KK=1 ITIME
      PVEC(KK)=PI(KK)VEC(KK)
248    CALL PLOTG(AKOUNT,XDIFF2,ITIME,2,1,4,'TIME SLOT', 9,'X-POSITION(FT)' THE02065
1 DEPTH ERROR(FT), 31,0.,0.,0.,15.,12.,7.) THE02070
1 CALL PLOTG(AKOUNT,X1,ITIME,2,1,4,4,'TIME SLOT', 9,'X-POSITION(FT)', THE02075
1 IT=1 THE02080
      DO 249 KK=1 ITIME
      PVEC(KK)=PI(KK)VEC(KK)
249    CALL PLOTG(AKOUNT,XDIFF3,ITIME,2,1,4,'TIME SLOT', 9,'X-POSITION(FT)' THE02085
1 DEPTH ERROR(FT), 31,0.,0.,0.,15.,12.,7.) THE02090
1 CALL PLOTG(AKOUNT,X1,ITIME,2,1,4,4,'TIME SLOT', 9,'X-POSITION(FT)', THE02095
1 IT=0 THE02100
      DO 250 KK=1 ITIME
      PVEC(KK)=PI(KK)VEC(KK)
250    CALL PLOTG(AKOUNT,XDIFF4,ITIME,2,1,4,'TIME SLOT', 9,'X-POSITION(FT)' THE02105
1 DEPTH ERROR(FT), 31,0.,0.,0.,15.,12.,7.) THE02110
1 CALL PLOTG(AKOUNT,X1,ITIME,2,1,4,4,'TIME SLOT', 9,'X-POSITION(FT)', THE02115
1 IT=1 THE02120
      DO 251 KK=1 ITIME
      PVEC(KK)=PI(KK)VEC(KK)
251    CALL PLOTG(AKOUNT,XDIFF5,ITIME,2,1,4,'TIME SLOT', 9,'X-POSITION(FT)' THE02125
1 DEPTH ERROR(FT), 31,0.,0.,0.,15.,12.,7.) THE02130
1 CALL PLOTG(AKOUNT,X1,ITIME,2,1,4,4,'TIME SLOT', 9,'X-POSITION(FT)', THE02135
1 IT=2 THE02140
      DO 252 KK=1 ITIME
      PVEC(KK)=PI(KK)VEC(KK)
252    CALL PLOTG(AKOUNT,X3,ITIME,1,1,1,1,'TIME SLOT', 9,'Y-POSITION(FT)', 141 THE02145
1 DEPTH ERROR(FT), 31,0.,0.,0.,15.,12.,7.) THE02150
1 CALL PLOTG(AKOUNT,X1,ITIME,2,1,4,'TIME SLOT', 9,'Y-POSITION(FT)', THE02155
1 IT=0 THE02155

```



```

SUBROUTINE TRAJECIK, DATA, ZI, TD)
  SUBROUTINE COMPUTES TRUE TRAJECTORY OF TORPEDO
  DATA(1)=TRUE X POSITION, DATA(2)=TRUE Y POSITION
  DATA(3)=TRUE Z POSITION, DATA(4)=TRUE X VELOCITY
  DATA(5)=TRUE Y VELOCITY, DATA(6)=0., DATA(7)=0., DATA(8)=0.
  DATA(9)=0., DATA(10)=0., DATA(11)=0.
  DATA(12)=ACCELERATION ANGLE (RADIAN'S) DATA(13)=TURN RATE (RAD./SEC)
  DATA(14)=SAMPLE TIME DATA(15)=HORIZONTAL ACCELERATION (FT./SEC.)
  DATA(16)=TIME SLOT INTERVAL DURING WHICH MANEUVER
  TAKES PLACE, DATA(17)=TRUE TIMES, TD=TRUE POSITION
  DOUBLE PRECISION DATA(23), ZI(4), TD(3)
  DIMENSION DATA(23), ZI(4), TD(3)
  T=0.0
  VEL=486.0
  RANGE=DSQRT((DATA(11)*DATA(11)+DATA(12)*DATA(12)+DATA(13)*DATA(13)))
  I=1
  ZI(1)=ZI(1)/VEL*((DATA(11)+15.)*2)+((DATA(12)+15.)*2)+((DATA(13)
  1+15.)*2)*.5
  I=2
  ZI(1)=ZI(1)/VEL*((DATA(11)-15.)*2)+((DATA(12)+15.)*2)+((DATA(13)
  1+15.)*2)*.5
  I=3
  ZI(1)=ZI(1)/VEL*((DATA(11)+15.)*2)+((DATA(12)-15.)*2)+((DATA(13)
  1+15.)*2)*.5
  I=4
  ZI(1)=ZI(1)/VEL*((DATA(11)+15.)*2)+((DATA(12)+15.)*2)+((DATA(13)
  1-15.)*2)*.5
  DO 9 I=1,3
  TD(I)=DATA(11)
  CONTINUE
  IF((K'LE.DATA(17)).AND.(K.GT. DATA(16))) GO TO 11
  DATA(7)=0.0
  DATA(8)=0.0
  DATA(14)=1.31
  GO TO 12
  DATA(14)=.005
  DATA(12)=DATA(12)+DATA(13)*DATA(14)
  DATA(7)=DATA(15)*DCOS(DATA(12))
  DATA(8)=DATA(15)*DSIN(DATA(12))
  DO 10 I=1,5
  DATA(I)=DATA(I)+DATA(I+3)*DATA(14)+((DATA(14)+((DATA(14)+((DATA(14)
  11 CONTINUE
  T=T+DATA(14)
  IF(ABS(T-1.31).LE.0.0001) RETURN
  GO TO 13
  END

```

```

SUBROUTINE TRAJC3IK, DATA, ZI, TD, XB, YB, ZB)
C
C SUBROUTINE COMPUTES TRUE TRAJECTORY OF TORPEDO
C
DATA(1)=TRUE X POSITION, DATA(2)=TRUE Y POSITION
DATA(3)=TRUE Z POSITION, DATA(4)=TRUE X VELOCITY
DATA(5)=TRUE Y VELOCITY, DATA(6)=0., DATA(7)=0., DATA(8)=0.
DATA(9)=0., DATA(10)=0., DATA(11)=0.
DATA(12)=ACCELERATION ANGLE (RADIAN), DATA(13)=TURN RATE (RAD./SEC)
DATA(14)=TIME, DATA(15)=HORIZONTAL ACCELERATION (F/SEC)
DATA(16)=SAMPLE TIME SLOP, INTERVAL DURING WHICH MANEUVER
TAKES PLACE, ZI=TRUE TIMES, TD=TRUE POSITION
C
DOUBLE PRECISION DATA(2), ZI(4), TD(3), XB(4), YB(4), ZB(4)
DIMENSION DATA(2), ZI(4), TD(3), XB(4), YB(4), ZB(4)
T=0.0
VEL=486.0
RANGE=DSQRT((DATA(1)+DATA(2)*DATA(3)+DATA(4)*DATA(5))
DO 5 I=1,4
      ZI(I)=1.0
      VEL=((DATA(1)-XB(I))*2)+((DATA(2)-YB(I))*2)
      +(DATA(3)-ZB(I))*0.5
      5 CONTINUE
      DO 9 I=1,3
          TD(I)=DATA(I)
          9 CONTINUE
          IF((K.LT.DATA(17)).AND.(K.GT. DATA(16))) GO TO 11
          DATA(7)=0.0
          DATA(8)=0.0
          DATA(14)=1.31
          GO TO 12
          DATA(14)=0.05
          DATA(12)=DATA(12)+DATA(13)*DATA(14)
          DATA(7)=DATA(15)*DCOS(DATA(12))
          DATA(8)=DATA(15)*DSIN(DATA(12))
          DO 10 I=1,2
              DATA(I)=DATA(I)+DATA(I+3)*DATA(I+2)/2)*DATA(I+6)
              10 CONTINUE
              T=T+DATA(14)
              IF(ABS(T-1.31).LE.0.0001) RETURN
              GO TO 13
          END
THE02605
THE02615
THE02620
THE02625
THE02630
THE02635
THE02640
THE02645
THE02650
THE02655
THE02660
THE02665
THE02670
THE02675
THE02680
THE02685
THE02690
THE02695
THE02700
THE02705
THE02710
THE02715
THE02720
THE02725
THE02730
THE02735
THE02740
THE02745
THE02750
THE02755
THE02760
THE02765
THE02770
THE02775
THE02780
THE02785
THE02790
THE02795
THE02800
THE02805

```

```

SUBROUTINE INIT (XKKM1,PKKM1)
C THIS ROUTINE IS TO INITIALIZE THE ARRAYS XKKM1 AND PKKM1.
C THESE VARIABLES ARE PART OF A COMMON BLOCK.
      DOUBLE PRECISION XKKM1,PKKM1
      DIMENSION XKKM1(5),PKKM1(5,5)
      DO 20 J=1,5
      DO 10 I=1,5
      PKKM1(I,J)=0.0
10    CONTINUE
      XKKM1(1)=38.975.
      XKKM1(2)=-50.5.
      XKKM1(3)=60.5.
      XKKM1(4)=-10.
      XKKM1(5)=300.
20    CONTINUE
      DO 30 I=1,5
      PKKM1(I,I)=1000.
30    CONTINUE
      RETURN
      END

```

C
C C C C
SUBROUTINE CZHAT(I,ZHAT)
THIS SUBROUTINE COMPUTES ESTIMATES OF TRANSIT TIME MEASUREMENTS
FOR SINGLE ARRAY TRACKING

DOUBLE PRECISION XKKM1,ZHAT
COMMON XKKM1(5)
VEL=4860.
IF(I.EQ.1)ZHAT=1./VEL*((XKKM1(1)+15.)**2)+(XKKM1(3)+15.)**2)
1+((XKKM1(5)+15.)**2)**0.5
IF(I.EQ.2)ZHAT=1./VEL*((XKKM1(1)-15.)**2)+(XKKM1(3)+15.)**2)
1+((XKKM1(5)+15.)**2)**0.5
IF(I.EQ.3)ZHAT=1./VEL*((XKKM1(1)+15.)**2)+(XKKM1(3)-15.)**2)
1+((XKKM1(5)+15.)**2)**0.5
IF(I.EQ.4)ZHAT=1./VEL*((XKKM1(1)+15.)**2)+(XKKM1(3)+15.)**2)
1+((XKKM1(5)-15.)**2)**0.5
RETURN
END

THE02920
THE02925
THE02930
THE02935
THE02940
THE02945
THE02950
THE02955
THE02960
THE02965
THE02970
THE02975
THE02980
THE02985
THE02990
THE02995
THE03000
THE03005

```

SUBROUTINE CZHAT3 ( I , ZHAT , XB , YB , ZB )
C THIS SUBROUTINE COMPUTES ESTIMATES OF TRANSIT TIME MEASUREMENTS
C FOR MULTIPLE ARRAY TRACKING
C
DOUBLE PRECISION XKMK1,ZHAT
COMMON XKMK1(5)
DIMENSION XB(4) , YB(4) , ZB(4)
VEL=4860.
X0=XB(1)
Y0=YB(1)
Z0=ZB(1)
ZHAT=(1./VEL)*(((XKMK1(1)-X0)**2)+((XKMK1(3)-Y0)**2)+((XKMK1(5)
1-Z0)**2)**0.5
RETURN
END

```

```

SUBROUTINE CHROW(I,HROW)
C THIS SUBROUTINE USED FOR SINGLE ARRAY TRACKING
C DOUBLE PRECISION XKKM1,DENOM1,DENOM2,DENOM3,DENOM4,DENOM5,HROW,
1H1,H3,H5
COMMON XKKM1(5)
DIMENSION HROW(5)
VEL=4860.
DENOM1=((XKKM1(1)+15.)*#2)+(XKKM1(3)+15.)*#2)+(XKKM1
1(5)+15.*#*2)*#0.5
DENOM2=((XKKM1(i)-15.)*#2)+((XKKM1(3)+15.*#2)+(XKKM1
1(5)+15.*#*2)*#0.5
DENOM3=((XKKM1(i)+15.)*#2)+((XKKM1(3)-15.)*#2)+(XKKM1
1(5)+15.*#*2)*#0.5
DENOM4=((XKKM1(i)+15.)*#2)+(XKKM1(3)+15.)*#2)+(XKKM1
1(5)-15.)*#2)*#0.5
A1=1.
A2=1.
A3=1.
DENOM4=DENOM1
IF(I1.EQ.2)DENOM4=DENOM2
IF(I1.EQ.3)DENOM4=DENOM3
IF(I1.EQ.4)DENOM4=DENOM4
IF(I1.EQ.2)A1=-1
I1=(1.0/VEL)*(XKKM1(1)+A1*15.)/DENOM1
I2=(1.0/VEL)*((XKKM1(3)+A2*15.)/DENOM2)
I3=(1.0/VEL)*(XKKM1(3)+A2*15.)/DENOM3
IF(I1.EQ.4)A3=-1
H5=(1.0/VEL)*(XKKM1(5)+A3*15.)/DENOM4
HROW(1)=H1
HROW(3)=H3
HROW(5)=H5
DO 27 J=2,4,2
HROW(J)=0.
27 RETURN
END

```

```

SUBROUTINE CHROW3 (I, HROW, XB, YB, ZB)
C THIS SUBROUTINE USED FOR MULTIPLE ARRAY TRACKING
C
DOUBLE PRECISION XKKM1,HROW,DENOM
COMMON XKKM1(5)
DIMENSION HROW(5),XB(4),YB(4),ZB(4)
VEL=4860.
XB(1)=X0
YB(1)=Y0
ZB(1)=Z0
DENOM=((XKKM1(1)-X0)**2)+((XKKM1(3)-Y0)**2)+((XKKM1(5)-Z0)
1**2)*0.5
HROW(1)=(1./VEL)*( (XKKM1(1)-X0)/DENOM)
HROW(3)=(1./VEL)*( (XKKM1(3)-Y0)/DENOM)
HROW(5)=(1./VEL)*( (XKKM1(5)-Z0)/DENOM)
DO 27 J=2,4,2
HROW(J)=0.
27
RETURN
END

```

```

C SUBROUTINE QFIND(K,SIGACC,SIGDIV,SIGCC,A,Q)
C THIS SUBROUTINE COMPUTES THE ADAPTIVE Q MATRIX
C
C DOUBLE PRECISION XHKKM1,PKKM1(5,5),PKK,XHKK,K,Q
C COMMON XHKKM1(5,5),PKKM1(5,5),PKK(5,5),XHKK(5)
C DIMENSION Q(5,5)
C IF(K.NE.1) GO TO 15
DO 10 I=1,5
DO 10 J=1,5
 10  Q(I,J)=0.0
      SIGACC=SIGACC**2
      SIGDIV=A)**2
      SIGCC=SIGCC**2
      G1=(A**2)/2.0
      G2=G1**2
      G3=A*G1
      A2=A**2
      A1=XHKK(2)/SQRT(A1)
 15  A3=XHKK(4)
      B=XHKK(4)/SQRT(A1)
      C=XHKK(4)/SQRT(A1)
      D=XHKK(2)
      E1=(A3**2)*SIGACC+(B**2)*SIGCC
      E2=(C**2)*SIGCC-B*D*SIGCC+(D**2)*SIGCC
      Q(1,1)=E1*G2
      Q(1,2)=E3*E1
      Q(1,3)=E12*G2
      Q(1,4)=G3*E12
      Q(2,2)=A2*E12
      Q(2,3)=G3*E12
      Q(2,4)=A2*E12
      Q(3,3)=G2*E2
      Q(3,4)=G3*E2
      Q(4,4)=A2*E2
DO 27 I=1,4
      DO 27 J=1,1
        Q(I,J)=Q(J,I)
 27  RETURN
END

```

THE03580
THE03585
THE03590
THE03595
THE03600
THE03605
THE03610
THE03615
THE03620
THE03625
THE03630
THE03635

SUBROUTINE PROD(A,B,N,M,L,C)
DOUBLE PRECISION A,B,C
DIMENSION A(N,M),B(M,L),C(N,L)
DO 1 I=1,N
DO 1 J=1,L
C(I,J)=0.
DO 2 I=1,N
DO 2 J=1,L
DO 2 K=1,M
C(I,J)=C(I,J)+A(I,K)*B(K,J)
1 RETURN
2 END

1

2

THE03640
THE03645
THE03650
THE03655
THE03660
THE03665
THE03670
THE03675
THE03680
THE03685

```
SUBROUTINE MMULT(A,B,N,M,C)
DOUBLE PRECISION A,B;C
DIMENSION A(N,M),B(M),C(N)
DO 3 I=1,N
C(I)=0.
DO 4 J=1,M
C(I)=C(I)+A(I,J)*B(J)
CONTINUE
RETURN
END
```

```
SUBROUTINE VMJLT(A,B,N,C)
DOUBLE PRECISION A,B
DIMENSION A(N),B(N)
C=0.
DO 6 I=1,N
  C=C+A(I)*B(I)
RETURN
END
```

```
THE03690
THE03695
THE03700
THE03705
THE03710
THE03715
THE03720
THE03725
```

```
SUBROUTINE TRANS(A,N,M,B)
DOUBLE PRECISION A,B
DIMENSION A(N,M),B(M,N)
DO 13 I=1,N
DO 13 J=1,M
B(J,I)=A(I,J)
13      RETURN
END
```

13

```
THE03730
THE03735
THE03740
THE03745
THE03750
THE03755
THE03760
THE03765
```

```
SUBROUTINE ADD (A,B,N,M,C)
DOUBLE PRECISION A,B,C
DIMENSION A(N,M),B(N,M),C(N,M)
DO 15 I=1,N
DO 15 J=1,M
C(I,J)=A(I,J)+B(I,J)
15 RETURN
END
```

15

```
THE03770
THE03775
THE03780
THE03785
THE03790
THE03795
THE03800
THE03805
```

LIST OF REFERENCES

1. Benson, Eric J. An Application of Kalman Filtering to Underwater Tracking, Master's Thesis, Naval Postgraduate School, December 1976.
2. Dwyer, Dennis M. Real Time Kalman Filtering For Torpedo Range Tracking, Master's Thesis, Naval Postgraduate School, December 1978.
3. Technical Manual, NAVORD OD 41964, NAVTOPRSTA Keyport Range Complex and Associated Data, May 1970.
4. Kirk, Donald E., EE4413 Optimal Control Systems Class Notes, Unpublished.
5. Mitschang, George W. An Application of Nonlinear Filtering Theory to Passive Target Location and Tracking. Ph.D. Thesis, Naval Postgraduate School, 1975.

INITIAL DISTRIBUTION LIST

	No. Copies
1. Defense Technical Information Center Cameron Station Alexandria, Virginia 22314	2
2. Library, Code 0142 Naval Postgraduate School Monterey, California 93940	2
3. Department Chairman, Code 62 Department of Electrical Engineering Naval Postgraduate School Monterey, California 93940	1
4. Professor H. A. Titus, Code 62Ts Department of Electrical Engineering Naval Postgraduate School Monterey, California 93940	5
5. Associate Professor Alex Gerba, Code 62Gz Department of Electrical Engineering Naval Postgraduate School Monterey, California 93940	1
6. Commanding Officer Naval Torpedo Station Keyport, Washington 98345	5
7. Paul A. O'Brien ASATD-AT-51 Naval Air Test Center Patuxent River, Maryland 20670	2

**DATE
FILMED**

-8